



Brigham Young University  
BYU ScholarsArchive

---

Theses and Dissertations

---

2024-12-13

## Applications of Phosphorus Geochemistry to Utah Lake

Jacob Barry Taggart  
*Brigham Young University*

Follow this and additional works at: <https://scholarsarchive.byu.edu/etd>



Part of the [Engineering Commons](#)

---

### BYU ScholarsArchive Citation

Taggart, Jacob Barry, "Applications of Phosphorus Geochemistry to Utah Lake" (2024). *Theses and Dissertations*. 11108.

<https://scholarsarchive.byu.edu/etd/11108>

This Dissertation is brought to you for free and open access by BYU ScholarsArchive. It has been accepted for inclusion in Theses and Dissertations by an authorized administrator of BYU ScholarsArchive. For more information, please contact [ellen\\_amatangelo@byu.edu](mailto:ellen_amatangelo@byu.edu).

Applications of Phosphorus Geochemistry to Utah Lake

Jacob B. Taggart

A dissertation submitted to the faculty of  
Brigham Young University  
in partial fulfillment of the requirements for the degree of  
Doctor of Philosophy

Gustavious P. Williams, Chair  
Gregory T. Carling  
A. Woodruff Miller  
Theron G. Miller

Department of Civil and Construction Engineering

Brigham Young University

Copyright © 2024 Jacob B. Taggart

All Rights Reserved

# *Applications of Phosphorus Geochemistry to Utah Lake*

Jacob B. Taggart  
Department of Civil and Construction Engineering  
Doctor of Philosophy

**BYU ENGINEERING**

## ABSTRACT

### Applications of Phosphorus Geochemistry to Utah Lake

Jacob B. Taggart

Department of Civil and Construction Engineering, BYU

Doctor of Philosophy

This compilation of studies provides an examination of phosphorus dynamics in the suspended solids, water column, and lakebed sediments of Utah Lake, a large, shallow, and phosphorus-rich water body. The first study introduces a novel phosphorus microfractionation (P-MF) method designed for small samples of suspended solids and sediments. This method reveals that suspended solids in Utah Lake can have a significantly higher phosphorus content across most fractions compared to lakebed sediments, highlighting the importance of considering suspended solids in nutrient management strategies. The second study analyzes historical phosphorus mass and concentrations, demonstrating that water column phosphorus levels have remained stable over time despite significant changes in lake volume and internal phosphorus mass. This stability is attributed to sorption processes, suggesting that external phosphorus load reductions may have a limited impact on the lake's phosphorus concentrations. The third study offers a detailed geochemical analysis of near-shore sediment cores, uncovering significant chemostratigraphic variability across the lake and complex interactions between phosphorus and other ICP-detectable elements. Together, these studies provide valuable insights into the internal processes and unique characteristics of Utah Lake, thereby informing future strategies for managing phosphorus levels and improving water quality in Utah Lake and similar shallow lakes.

Keywords: calcium carbonate; historical data; ICP-detectible elements; lakebed sediment; mass balance; microfractionation; organic matter; phosphorus; P-MF method; sediment cores; sequential extraction; sorption; suspended solids; Utah Lake

## Acknowledgments

First and foremost, I would like to give special thanks to my advisor, Gus Williams, for his unwavering guidance and support throughout my PhD program. His mentorship and encouragement were invaluable during the many highs and lows of being a graduate student. I am very appreciative of his help in securing scholarships, connecting me with resources and lab space, facilitating attendance at research conferences, and navigating the ever-evolving terrain of research projects.

I am also deeply grateful to my committee member, Theron Miller, for coordinating the financial support for my research through the Wasatch Front Water Quality Council and South Davis Sewer District. A phone call with him nearly seven years ago set me on the path to researching Utah Lake for both my master's and doctorate degrees. His guidance has been particularly pivotal in my academic journey.

I would also like to express my gratitude to my committee members, Greg Carling and Wood Miller, for their invaluable support and guidance. Their insights were especially beneficial during the initial stages of the sediment cores and historical phosphorus mass projects, respectively.

I am thankful for the support and assistance of my fellow students, Justin Telfer, Mitch Brown, Kaylee Tanner, Anna Cardall, Rebecca Ryan, Rachel Valek, Lauren Woodland, Paige Blocker, Madeline Oxborrow, and Marisa Woodland, who helped with various aspects of my research, from fieldwork and lab work to writing. I would like to give a special shoutout to Kaylee for rescuing me on the lake when the boat ran out of gas, and to Paige and Lauren for their above-and-beyond dedication when core sampling caused them to get completely soaked from head to toe.

I am grateful to Erin Jones from BYU's Environmental Analytical Laboratory for her guidance on various lab procedures and for her never-ending positivity and patience with me whenever I encountered issues or unintentionally damaged or destroyed lab equipment.

I would like to thank Janice Kapp Perry for generously allowing me to live in her home while I worked on my doctorate degree. Not only did this arrangement allow me to live close to campus, but it also allowed me to build an unexpected yet rewarding friendship with one of the Church's most talented and prolific songwriters. She's a saint for putting up with me and my many quirks, pranks, and overly strong opinions.

And last of all, I'd like to thank my parents, siblings, and extended family members for their endless love and support as I've pursued various forms of higher education. Their ability to see my potential has motivated me to remain diligent when I have found myself out of my element, and they have inspired me to continually strive toward becoming the best version of myself.

## Table of Contents

Abstract .....	iii
Acknowledgements.....	iv
List of Figures.....	viii
List of Tables.....	xii
<b>1 Introduction .....</b>	<b>1</b>
<b>2 Development of a Phosphorus Microfractionation (P-MF) Method for Measuring Phosphorus Fractions in Small Quantities of Suspended Solids and Sediments .....</b>	<b>4</b>
2.1 Introduction .....	5
2.1.1 <i>Preliminary Background</i> .....	5
2.1.2 <i>P-Fractionation of Suspended Solids</i> .....	5
2.1.3 <i>Utah Lake Target Study</i> .....	7
2.1.4 <i>Research Overview</i> .....	7
2.2 Methods.....	9
2.2.1 <i>Fraction Descriptions</i> .....	9
2.2.2 <i>Study Materials</i> .....	11
2.2.3 <i>Method Development</i> .....	11
2.2.4 <i>Method Description</i> .....	12
2.3 Results and Discussion.....	14
2.3.1 <i>Baseline Results</i> .....	14
2.3.2 <i>One-way ANOVAs</i> .....	17
2.3.3 <i>Post-hoc Tests</i> .....	20
2.4 Conclusion .....	23
2.4.1 <i>Study Limitations and Suggestions for Future Research</i> ....	23
2.5 Supplemental Information.....	24
<b>3 Historical Phosphorus Mass and Concentrations in Utah Lake: A Case Study with Implications for Nutrient Load Management in a Sorption-Dominated Shallow Lake .....</b>	<b>32</b>
3.1 Introduction .....	33
3.1.1 <i>Study Motivation</i> .....	33

3.1.2 Utah Lake Background.....	34
3.1.3 Phosphorous-Rich Sediments.....	35
3.1.4 Nutrient Mass Balance Models .....	35
3.1.5 Sorption .....	37
3.1.6 Research Overview .....	38
3.1.7 Hypothesis.....	39
3.2 Data and Methods.....	39
3.2.1 Data Sources and Descriptions.....	39
3.2.2 Analysis Methods .....	44
3.3 Results.....	48
3.3.1 Lake Volume Variability .....	48
3.3.2 Phosphorus Concentration Variability .....	50
3.3.3 Phosphorous Outflow—Jordan River .....	55
3.3.4 Phosphorus Mass Variability.....	57
3.3.5 Sorption Calculations .....	59
3.4 Discussion .....	63
3.4.1 Variability .....	63
3.4.2 Isotherm Calculations Implications .....	64
3.4.3 Sorption Lines of Evidence.....	65
3.5 Conclusions.....	67
3.6 Afterword.....	69
<b>4 A Geochemical Study of Near-Shore Sediment Cores from Utah Lake, Utah, USA.....</b>	<b>70</b>
4.1 Introduction .....	71
4.1.1 Study Motivation.....	71
4.1.2 Background on Utah Lake.....	72
4.1.3 Core Collection Sites .....	73
4.2 Materials and Methods.....	73
4.2.1 Sample Collection and Preparation .....	73
4.2.2 Microwave Digestion and ICP-OES .....	76
4.2.3 Fractional Calcium Carbonate .....	76
4.2.4 Fractional Organic Matter .....	77
4.2.5 Color and Texture .....	77
4.2.6 Core Shortening .....	77
4.2.7 Methods of Analysis .....	79
4.3 Results and Discussion.....	80
4.3.1 Core Depth, Color, and Texture.....	80
4.3.2 Elemental Concentrations.....	83

4.3.3 <i>Fractional Calcium Carbonate</i> .....	91
4.3.4 <i>Fractional Organic Matter</i> .....	93
4.3.5 <i>Sediment Phosphorus</i> .....	94
4.4 Conclusion .....	101
4.4.1 <i>Key Findings</i> .....	101
4.4.2 <i>Study Limitations and Suggestions for Future Research</i> ..	102
4.5 Appendix.....	104
<b>5 Conclusions</b> .....	109
<b>6 References</b> .....	111

## List of Figures

2.1	Utah Lake total suspended solids from the Ambient Water Quality Management System (AWQMS) database provided by the Utah Department of Environmental Quality, depicting 936 lake water samples from 1989-2019.....	8
2.2	Results for both actual (raw) and estimated total P .....	16
2.3	Results for water-soluble P.....	18
2.4	Results for loosely-sorbed P .....	18
2.5	Results for Fe- & Al-bound P .....	19
2.6	Results for Ca-bound P .....	19
2.7	Results for residual P .....	20
2.8	Stepwise P-MF procedure .....	31
3.1	Geologic phosphate sources in the Utah Lake Watershed .....	36
3.2	Daily Utah Lake volumes in cubic meters ( $m^3$ ) from 13 July 1989 to 4 August 2023.....	40
3.3	Jordan River outflow volumes in cubic meters ( $m^3$ ) reported as cumulative monthly volumes from 1 January 1989 to 1 July 2023 .....	41
3.4	Distribution of Jordan River outflow volumes by month in cubic meters ( $m^3$ ) from 1 January 1989 to 1 July 2023.....	41
3.5	Locations and number of phosphate samples available from the AWQMS database .....	42
3.6	Dissolved P (DP) concentrations in Utah Lake from 1989 to 2022 .....	44

3.7	Interpolated dissolved P (DP) concentrations in Utah Lake based on either the mean or median values measured on the same day .....	46
3.8	Dissolved P (DP) concentrations in Utah Lake from 1989 to 2022 grouped by year.....	47
3.9	Annual distributions of Utah Lake volume ( $m^3$ ) from 13 July 1989 to 4 August 2023.....	49
3.10	Analysis of means (ANOM) results of Utah Lake volume data grouped by year.....	49
3.11	Monthly distributions of Utah Lake volumes in cubic meters.....	50
3.12	Analysis of means (ANOM) results on Utah Lake dissolved P (DP) concentration data grouped by year .....	51
3.13	Distribution of Utah Lake dissolved P (DP) concentration by month .....	52
3.14	ANOM analysis of Utah Lake monthly dissolved P (DP) mean values.....	53
3.15	Utah Lake dissolved P (DP) concentrations sorted by measurement location ID.....	55
3.16	Analysis of means (ANOM) report for the 22 different Utah Lake sampling sites.....	56
3.17	Monthly mass outflow (Mg or t) of Utah Lake dissolved P (DP) in the Jordan River for months in which we have measured data .....	56
3.18	Monthly mass outflow (Mg or t) of Utah Lake dissolved P (DP) .....	57
3.19	Monthly values of the mass (Mg or t) of Utah Lake dissolved P (DP) .....	57
3.20	Panel (A) is a detail of Figure 3.19, which shows the total mass (Mg or t) of dissolved P (DP) in Utah Lake, while panel (B) shows monthly DP total mass inflows (Mg or t) from all sources including sorption into Utah Lake .....	59

3.21 Example data that represent P adsorption to a sandy clay loam soil fit with a Freundlich isotherm .....	60
4.1 Core sampling locations throughout Utah Lake .....	75
4.2 Photograph of a core catcher.....	76
4.3 Side view of core shortening mechanisms within an open-barrel core sampler .....	77
4.4 Depth comparison between a compacted and uncompacted sediment core sample.....	79
4.5 Comparison of core depths and colors.....	81
4.6 Strongly correlated ICP-detectable elements ( $r > 0.5$ ) from all 10 sediment cores.....	84
4.7 Min-max normalized distribution of elemental concentrations across all 10 core samples .....	85
4.8 Multidimensional scaling results for ICP-detectible elements from all 10 sediment cores.....	86
4.9 Min-max normalized elemental concentrations for the Benjamin (A) and Provo Bay (B) cores .....	89
4.10 Multidimensional scaling results for sample depths 0-140 cm from all 10 sediment cores.....	90
4.11 Multidimensional scaling results for all 10 sample locations.....	91
4.12 Fractional $\text{CaCO}_3$ from near-shore core samples from Utah Lake .....	92
4.13 Fractional OM from near-shore core samples from Utah Lake.....	93
4.14 Interpolated P concentrations across all 10 sediment core samples .....	96
4.15 Distribution of sediment P down to 140 cm deep from all 10 core samples (panel A) and the non-bay core samples (excluding Goshen North, Goshen South, and Provo Bay; panel B).....	97
4.16 P concentrations for each of the 10 sediment cores .....	98

4.17 Median normalized concentration for P, Ca, and Fe across all 10 core samples. ....	99
4.18 Median normalized concentrations for P and strong to moderately correlated immobile pollutants, including Zn, Cu, Pb, Cd, and Ni .....	100

## *List of Tables*

2.1	P-MF results for total phosphorus ( $\text{mg kg}^{-1}$ ) with each sample size including three replicates.....	16
2.2	P-MF results for individual fractions ( $\text{mg kg}^{-1}$ ) with each sample size including three replicates.....	21
2.3	Post-hoc connected letters report for P-MF samples .....	22
3.1	A list of sampling locations and IDs for Utah Lake P data from the AWQMS database .....	43
3.2	Tukey–Kramer pair-wise connecting letter report for annual means.....	52
3.3	Tukey–Kramer pair-wise connecting letter report for monthly means.....	54
3.4	Equilibrium concentrations, mass, and dissolved P (DP) mass added to a column of water that is 3 m deep, has a cross-sectional area of $10 \text{ cm}^2$ , and interacts with sediment that is 10 cm deep.....	61
4.1	Sediment core sample information .....	74
4.2	Texture and color of the Airport core sample.....	82
4.3	Summary statistics for elemental concentrations across all sediment cores.....	83
4.4	Airport Core Sample Results .....	104
4.5	Benjamin Core Sample Results .....	104
4.6	Goshen North Core Sample Results.....	105
4.7	Goshen South Core Sample Results .....	105
4.8	Lindon Marina Core Sample Results .....	106
4.9	Mosida Core Sample Results .....	106

4.10	North Shore Core Sample Results .....	107
4.11	Powell Slough Core Sample Results .....	107
4.12	Provo Bay Core Sample Results .....	108
4.13	Saratoga Springs Core Sample Results.....	108

## 1 Introduction

Utah Lake is a critical natural and economic asset for north-central Utah, playing a central role in the Great Salt Lake watershed. It supports the region's ecosystems and serves as an essential water source for both human communities and a diverse array of wildlife. Despite its significance, Utah Lake's murky waters, muddy sediments, and recurring harmful algal blooms cause the lake to be perceived as a great disappointment—a neglected resource falling short of its true potential as a vibrant natural asset.

Over the years, many efforts have been made to address the lake's water quality, with much attention having been drawn to phosphorus and its role in fueling harmful algal blooms. In the mid-2000s, the Utah Division of Water Quality tasked PSOMAS with conducting a detailed study of Utah Lake's water quality with the intention of establishing a Total Maximum Daily Load (TMDL) on phosphorus entering the lake. The final report from PSOMAS includes the following statement:

**"Research has shown that limiting the introduction of nutrients to a system influences overall productivity of a system but the individual lake system must be understood to comprehend the internal processes that may influence the cycling of TP [total phosphorus] and to identify the appropriate mechanisms for limiting TP in a watershed."**

This statement refers to restoration work on water bodies worldwide which have found success reducing algal blooms by limiting the introduction of human-derived sources of phosphorus. While it might seem logical to apply a general strategy to manage Utah Lake's phosphorus levels, PSOMAS recommends adopting an approach tailored to the lake's unique characteristics in order to achieve the most effective outcome.

Efforts are underway to upgrade wastewater treatment facilities around Utah Lake to reduce phosphorus contributions from effluent. Additionally, ongoing carp removal aims to minimize sediment resuspension of phosphorus caused by the feeding habits of these invasive fish. However, these efforts compete directly with natural phosphorus

inputs, such as wind-driven sediment resuspension, wind-blown dust containing phosphorus, and erosion of nearby phosphorus-rich rock. It is unclear whether current efforts to limit phosphorus in Utah Lake will be enough to prevent harmful algal blooms.

The goal of my research is to deepen our understanding of Utah Lake's internal processes and unique characteristics, and thereby provide valuable knowledge to help others develop effective strategies for reducing phosphorus levels in Utah Lake. To do this, I focused my research on the following three aspects of the lake: 1) phosphorus associated with suspended sediments, 2) phosphorus associated with the water column, and 3) phosphorus associated with lakebed sediment.

My first study introduces a novel phosphorus microfractionation (P-MF) method adapted for small samples of suspended solids and sediments. Traditional methods for phosphorus fractionation are often impractical for small sample sizes, but the P-MF method described here addresses this gap by attempting an analysis of phosphorus fractions in small quantities. The study's findings indicate that suspended solids in Utah Lake have significantly higher phosphorus content across most fractions when compared to lakebed sediments, emphasizing the need to consider suspended solids in phosphorus management strategies.

My second study delves into the historical phosphorus mass and concentrations in Utah Lake, providing a comprehensive meta-analysis of how these parameters have changed over time. By utilizing state and federal records of lake volume, phosphorus content, and outflow, the study demonstrates that dissolved phosphorus concentrations in the lake have remained relatively stable despite significant changes in both lake volume and internal phosphorus mass. This stability is attributed to sorption processes, which dominate the phosphorus dynamics in the lake. The sorption model presented in this study aligns with historical data, showing that water column phosphorus concentrations are largely insensitive to external load reductions, a finding that has significant implications for nutrient load management in Utah Lake and other large shallow lakes.

My third study offers a detailed geochemical analysis of near-shore sediment cores from Utah Lake. By collecting and analyzing 10 sediment cores from various locations around the lake, this study provides a more comprehensive understanding of the geochemical variability in the lake's sediments. The core samples, which were a minimum of 140 cm deep, revealed noticeable chemostratigraphic variability, challenging the notion of homogeneity in lakebed sediments. The study found that elements with higher normalized mean concentrations tend to have stronger correlations with other elements, and identified depth trends that correlate with historical events, such as the onset of European settlement. The findings

highlight the complex interactions between phosphorus, calcium, iron, and trace metal pollutants, as well as the influence of both natural processes and human activities on elemental trends.

In summary, Utah Lake continues to be an essential but troubled natural resource. Despite its ecological and economic importance, the lake's persistent issues with water quality, particularly with elevated phosphorus levels and harmful algal blooms, have hindered its potential to support a healthy ecosystem, provide recreational opportunities, and sustain its economic ties. Efforts to improve the lake's condition have focused on reducing phosphorus inputs from wastewater effluent and carp behavior, but the lake's natural characteristics complicate these efforts. My research aims to enhance the understanding of Utah Lake's internal processes and unique characteristics to help inform future management strategies. Ultimately, this research contributes to the broader goal of restoring Utah Lake to a healthier state, ensuring it can continue to serve as a valuable natural asset for future generations.

## **2 Development of a Phosphorus Microfractionation (P-MF) Method for Measuring Phosphorus Fractions in Small Quantities of Suspended Solids and Sediments**

*Jacob B. Taggart, Rebecca L. Ryan, A. Wood Miller, Theron G. Miller, and Gustavious P. Williams*

**Abstract:** The standard methods for sediment phosphorus (P) fractionation are impractical for use with suspended solids due to the inherent difficulties associated with collecting sufficient sample quantities for analysis. To better accommodate fractionation when the analysis of small quantities of suspended solids or sediment is desired, we developed a P microfractionation method and sought to determine the threshold for the minimum sample size. The dry mass threshold is likely < 1.0 g for Utah Lake suspended solids and between 0.35–0.99 g for Utah Lake sediments, though we recommend further experimentation to refine these thresholds. We show that Utah Lake suspended solids have a significantly higher P content across most P-fractions compared Utah Lake sediments, emphasizing the importance of considering suspended solids when managing water nutrient levels in eutrophic water bodies. Despite the need for further research, P-microfractionation has the potential to enable researchers to use reasonably sized water samples to assess the P sorption behavior of suspended solids.

**Keywords:** lakebed sediment; microfractionation; phosphorus; P-MF method; sequential extraction; suspended solids; Utah Lake

---

## 2.1 Introduction

### 2.1.1 Background

Phosphorus (P) geochemistry is complex due to the wide variety of phases in which it occurs. For example, P can form mineral phases with calcium (Ca), iron (Fe), and aluminum (Al); it can also create organophosphorus salts through interactions with organic compounds or sorb onto solid surfaces through surface or cation exchange reactions [1, 2]. These solid phases, known as P-fractions, offer insight into the bioavailability of P as a nutrient to support growth and sustain life. Most work on P-fractionation has consequently been done to support agriculture [2-5], though applications have also been made for reservoir and lake sediments [2, 6-12].

A variety of fractionation procedures have been developed to quantify the P-fractions present in a given system, such as the methods by Kovar and Pierzynski [2], Petersen and Corey [13], and those summarized by Kleinman, et al. [3]. Although these methods use different processes and emphasize P storage across various fractions, they all follow a similar procedure: a soil or sediment sample is collected and then subjected to a series of physical or chemical treatments in a series of sequential extractions to isolate and measure P within the selected P-fractions.

Existing methods for assessing P-fractions in sediments and soils generally require a minimum of 1 to 2 g of a dried sample to perform an analysis, [2] with some methods requiring as little as 0.5 g [14]. Sample size is not typically an issue because soils and sediments are generally abundant and are easily sampled. However, this is not necessarily the case for suspended solids as most freshwater bodies have suspended solids concentrations on the order of a few tens to a few hundreds of mg L<sup>-1</sup>. This means that the number of liters needed to acquire a single gram of dry sediment from a typical water body could be in double and triple digits. This study presents an attempt to develop and implement a microfractionation method that uses significantly smaller sample sizes to improve the feasibility of measuring the P-fractional content of suspended solids in aquatic systems.

### 2.1.2 P-Fractionation of Suspended Solids

While sequential extraction is commonly used to measure P-fractions in soils and sediments, it is rarely applied to suspended solids, as the low concentration of these solids in surface waters would require impractically large water samples for analysis. Researchers have consequently resorted to conducting fractionation on bottom sediments as an analogue for describing the P-fractions of suspended solids [15]. Such estimates, however, are not necessarily representative of the actual composition and

behavior of suspended solids. This is because the biogeochemical and physical conditions between the bottom sediments and the water column can differ markedly, particularly in the photic zone, and because suspended solids generally have a smaller particle distribution than sediments [16]. Direct analysis of suspended solids is therefore preferable over proxy analysis of lakebed or riverbed sediments when suspended solids are the primary subject of interest.

Additional challenges arise when performing a sequential extraction on small samples. For example, sediment heterogeneity can be magnified by small samples, in which a few particles of a given mineral can significantly change the results. Another issue is the amount of the target element remaining in the fluids at the end of an extraction step, which in small samples can contain significant quantities compared to the quantities in the solid portion of the sample. Additionally, sample loss between fractionation steps can cause the extractions of already dilute extractants to become less accurate with each successive step and thereby produce skewed results that are unrepresentative of their true fractions [17].

In situations where a sequential extraction procedure causes undesirable sample loss or results in unwanted chemical reactions from its leaching reagents, parallel extraction procedures have been developed and used as an alternative method [18]. Parallel extraction uses the same leaching methods as sequential extraction, but the methods are applied to separate subsamples rather than using a consecutive series of extractions on a single sample. This approach requires an understanding of the aggressivity of each extraction step, as stronger leaching reagents often extract the target phases of weaker reagents in addition to their own phases, or they may not extract the weaker phase at all, making data analysis difficult. Once a hierarchy of aggressivity has been determined for the selected method of parallel extraction, a user can correct the results to quantify the extraction amounts of the more aggressive steps by considering the amounts likely extracted from the weaker phases or fractions [18].

Parallel extraction may appear to be a favorable method for evaluating suspended solids because of its ability to be applied to smaller samples. However, each parallel extraction step requires a separate subsample and therefore requires an initial sample that is multiple times larger than the amount required for sequential extraction. In addition to requiring significantly more material, parallel extraction is also undesirable because it generates results that are more difficult to interpret due to sample variation and the need for correction factors.

Researchers have published successful efforts to sequentially extract P from suspended solids by collecting between 2.5 and 5.0 L of sample water and then either centrifuging or settling the samples to obtain enough

material to perform extractions. These samples, however, were taken from rivers or streams immediately following a storm event, and consequently had very high levels of suspended solids to ensure that enough sample was collected for analysis [7, 8, 19]. Applying these approaches to typical lake and reservoir waters is difficult as they would require water volumes that are 10 to 100 times as large as the aforementioned river samples to collect the same amount of solid material.

#### 2.1.3 Utah Lake Target Study

Because traditional approaches for measuring P-fractions from suspended solids are impractical for most surface waters, our study developed a P-microfractionation (P-MF) method that requires less solid material for analysis that could be applied to relatively turbid water often encountered in freshwater lakes. We applied this method to Utah Lake, a large, shallow freshwater lake in north-central Utah with waters that are both eutrophic and turbid. Utah Lake's suspended solids typically fall between 30 and 75 mg L<sup>-1</sup> (Figure 2.1). While these levels are higher than is typically seen in most lakes and reservoirs, these levels are not unusual [20-22]. However, obtaining enough material for traditional sequential extraction methods (approximately 1-to-2-g samples at minimum) even at these concentrations would still require a very large water sample [9, 11].

For example, lake water with suspended solids concentrations of 75 to 30 mg L<sup>-1</sup>, like that of Utah Lake, would require about 13 to 33 L of water, respectively, to acquire a 1-g sample for analysis; double that, or 26 to 66 L, to acquire a 2-g sample. This means that it is impractical to perform P-fractionation on suspended solids from Utah Lake using traditional methods, as collecting ~20- to 50-L water samples is unrealistic for most assessment purposes. The majority of water bodies have even lower concentrations of suspended solids, making the collection of 1-to-2-g samples for those water bodies even more difficult [22]. The successful application of a P-MF method to Utah Lake would consequently serve as an ideal platform for adapting and applying P-MF to other surface waters.

#### 2.1.4 Research Overview

This study developed a P-MF method that accurately measures P-fractions from small quantities of suspended solids and sediment. P-fractionation methods are standardized and used extensively, particularly in agriculture. The method outlined in this study is based on previously published fractionation methods that are valid for inorganic solids under aerobic conditions, with the study focusing on the minimum sample size that can be reliably used for analysis.

In section 2.2.1, we define the P-fractions examined by our method, describe how those fractions are quantified, and explain why we selected

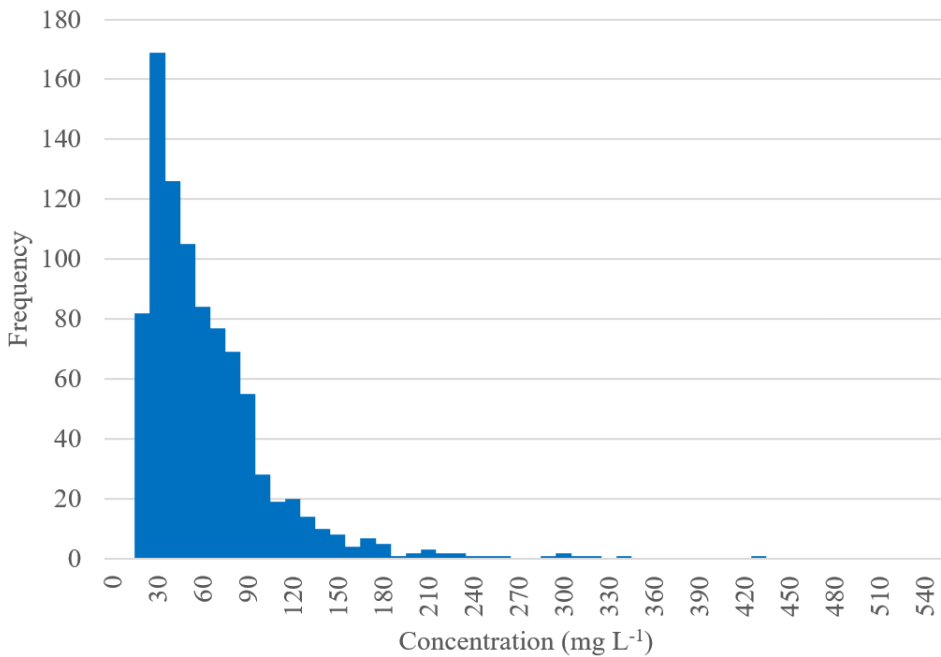


Figure 2.1. Utah Lake total suspended solids from the Ambient Water Quality Management System (AWQMS) database provided by the Utah Department of Environmental Quality, depicting 936 lake water samples from 1989-2019. Utah Lake's shallow depth combined with wind-induced waves and lakebed bioturbation cause the lake to experience high levels of suspended solids, falling mostly in the 30 to 75  $\text{mg L}^{-1}$  range.

those fractions for analysis. In section 2.2.2, we discuss the use of lakebed sediments and suspended solids from Utah Lake as the primary study material for our method development. In section 2.2.3, we explain how we adapted an existing P-fractionation method to assess a variety of small sample sizes, and in section 2.2.4, we summarize the steps of our P fractionation method along with the calculations required to convert the results into units of mass concentration.

In section 2.3.1, we present our baseline results from performing our fractionation method on different quantities of lakebed sediment and suspended solids from Utah Lake. This includes subsections on sample detection limits, the dry mass of our samples, sample controls, and the results for total P and the P-fractions. In section 2.3.2, we describe our use of one-way ANOVAs to determine if the observed differences in sample size were statistically significant. In section 2.3.3, we explain our use of post-hoc tests to determine which sample sizes produced anomalous results.

In section 2.4.1, we summarize the methods and results of this study and conclude by identifying some of this study's limitations along with suggestions for future research.

## 2.2 Methods

### 2.2.1 Fraction Descriptions

We based our microfractionation (P-MF) method on the method used by Casbeer, et al. [11] with additional details found in Casbeer [23]. We selected this method because it is designed for aerobic conditions (which should hold for suspended solids collected in most natural waters) and includes the assessment of the water-soluble fraction. This method does not separate Al-bound P from Fe- and manganese-bound P as separate fractions, but rather groups them into a single fraction. These fractions are typically released under anaerobic conditions and can generally be treated as one phase.

We quantify five fractions with this method: water-soluble P ( $P_{wat}$ ), loosely-sorbed P ( $P_{ion}$ ), Fe- & Al-bound P ( $P_{Fe}$ ), Ca-bound P ( $P_{Ca}$ ), and residual P ( $P_{res}$ ). The sum of these fractions is used to quantify total P ( $P_{tot}$ ). As a check, Casbeer suggests that duplicate samples be digested to determine  $P_{tot}$ , which can then be compared to the integrated value to quantify potential errors within sample variability and act as a quality assurance check.

The Casbeer, et al. [11] method uses a sample size of 10 g and performs a set of sequential extraction steps. In the first step, 20 mL of deionized (DI) water is mixed with the sediment sample, centrifuged, and then filtered to produce the supernatant for measuring  $P_{wat}$ . In the second step, 20 mL of 1 M KCl is mixed with the sediment and is shaken for 2 hours before being centrifuged and filtered to produce the supernatant for measuring  $P_{ion}$ . In the third step, 20 mL of 0.1 M NaOH is mixed with the sediment and is shaken for 17 hours before being centrifuged and filtered to produce the supernatant for measuring  $P_{Fe}$ . In the fourth step, 20 mL of 0.5 M HCl is mixed with the sediment and is shaken for 24 hours before being centrifuged and filtered to produce the supernatant for measuring  $P_{Ca}$ . And in the fifth step, the remaining sediment is subjected to persulfate digestion to produce the supernatant for measuring  $P_{res}$ .

The  $P_{wat}$  fraction, called water-soluble P, represents P sorbed to the solid surface as well as P contained in the pore water of the sample.  $P_{wat}$  is of significant interest to lake managers as P in this fraction is bioavailable, readily moves between solid and aquatic phases, and can strongly influence water column concentrations of dissolved P.

The  $P_{ion}$  fraction, while called “loosely-sorbed P”, represents the P that can be extracted by ion-exchange. This is P sorbed to the surface by electrostatic forces based on ion charge [24]. The  $P_{wat}$  and  $P_{ion}$  fractions are readily available to the water column and will release or sorb P easily with changing water chemistry and P concentrations. The concentration of P in the solids is a function of P concentration in the water column when

sorption is at equilibrium [24]. For natural waters, this phenomenon can be called a sorption-dominated system as well as a buffered system, where water column P concentrations are relatively insensitive to P inflows when sediments act as a large reservoir for both the uptake and release of P. This effect can be strengthened if sediments are continually mixed and suspended in the water column. The sediments act as a reservoir as the ratio of the solid phase to aquatic phase concentrations is generally on the order of several hundred times [25].

The  $P_{Fe}$  fraction represents P that is co-precipitated with Fe and Al minerals. These minerals are relatively insoluble under oxic conditions but are significantly more soluble under anoxic conditions, such as those found within lakebed sediments. For example, the stability constant for  $Fe(OH)_2$ , which is the dominant species under anoxic conditions, is several orders of magnitude higher than that of  $Fe(OH)_3$ , which is the dominant species under aerobic conditions [26]. This higher solubility of iron hydroxide in anoxic conditions means that the  $P_{Fe}$  fraction can be released to the water column if anoxic sediments are disturbed. If the aerobic water column is saturated with respect to Fe and Al minerals or other similar minerals, then these minerals will re-precipitate and potentially co-precipitate the P [27]. This P-fraction in the sediment can act as a P source for the water column if the water column is not saturated with respect to Fe or Al as most sediments are anoxic and P in the pore water can diffuse up into the water column. If the water column contains Fe or Al, the  $P_{Fe}$  fraction can scavenge P from the water column when evaporation concentrates mineral species and likewise act as a source of P when anoxic sediments are disturbed, or through the slower diffusion transport from anoxic sediments.

The  $P_{Ca}$  fraction represents Ca minerals that contain P. Utah Lake is unique in that it is near saturation levels for calcite because of high levels of evaporation and because of tributaries that flow through carbonate-dominated geology. Studies have shown that over 90% of P input to Utah Lake does not exit the lake, with various studies attributing this loss of P to coprecipitation with Ca minerals or sorption on solids [6, 9, 25]. The  $P_{Ca}$  fraction is not available to the water column under most circumstances due to the lake's high pH, though in periods when the water is not saturated with respect to calcite, such as from springtime inflows, these minerals can dissolve, releasing P.

The  $P_{res}$  fraction represents the P that remains following the extraction of all other fractions, including the P in residual mineral phases and organic materials, which is not generally available to the water column. While the  $P_{res}$  fraction can sometimes be assumed to represent organically-bound P, the quantification of specific organic-P subfractions would require the use of alternative analytical methods. And while it would be

interesting to evaluate different types of organically-bound P-fractions associated with suspended solids (such as from different types of algae or biochar), doing so is beyond the scope of our method development.

### 2.2.2 Study Materials

The primary materials for this study included suspended solids and lakebed sediment samples from Utah Lake which we used to test our method's effectiveness on small quantities of both suspended and settled material. We made the decision to use Utah Lake sediment for several reasons. First, Utah Lake is a eutrophic lake with sediments that are known to have a high P content, between 600-1,500 mg kg<sup>-1</sup> [6, 9, 28], making them ideal for P fractionation experiments. Second, Utah Lake is a turbid lake with high levels of suspended solids (Figure 2.1), which are presumed to be composed primarily of lakebed sediments. The lake's high turbidity also allowed us to collect a solid sample with less water than would be needed for most other water bodies. And third, a knowledge of the P-fractions associated with the lake's suspended solids would be helpful for lake management decisions as the lake has been held under public scrutiny due to its recurrent harmful algal blooms [25, 29, 30].

### 2.2.3 Method Development

As previously stated, our main objective was to create a fractionation method suitable for measuring P-fractions in very small quantities of suspended solids and sediments. Suspended solids can be collected from a water sample by either 1) centrifuging the sample and then decanting the excess water, or 2) allowing particulate matter to settle to the bottom of the sampling container and then siphoning off the excess water. Filtration is not recommended as suspended solids and extractants can be retained by the filter and thereby introduce complications introduced by their removal.

Centrifugation is generally considered the quickest method for separating suspended solids from water, but doing so requires a centrifuge that can process large quantities of water, and even then, centrifugation could still take hours to produce enough material for analysis if the concentration of suspended solids is low. If a cold room or a sufficiently large refrigerator is available, then allowing suspended sediments to settle out is a viable option and can be used as a pre-concentration step prior to centrifugation. Regardless of the method used, the quantity of wet solids required depends on the target amount of dry material for analysis as well as the desired number of replicate samples.

In small samples, the pore fluids can contain significant quantities of P, while these same amounts are insignificant with larger samples. We added wash steps to address the issue of P that is left behind in the pore fluids in smaller samples. For small sample sizes, the amount of pore fluid and

sample mass are similar, and thus the amount of P in the pore fluid remaining after an extraction step could be significant. This is not the case in the published methods, where extractant volumes are significantly larger than pore volumes [11]. The addition of this wash step helps ensure that extracted P was attributed to the correct fraction and reduced the likelihood of P sorbing back onto the sediments between fractionation steps.

We sought to experimentally determine a recommended minimum sample size threshold by subjecting an array of increasingly smaller quantities of P-rich sediments to our P-MF method. The wet sample sizes we evaluated included 1.4 g, 0.5 g, 0.4 g, 0.3 g, and 0.2 g samples, with the 1.4 g samples acting as a standard, given that many fractionation methods use between 1-2 g samples for their analysis.

Besides sample size, the primary modifications we made to the method by Casbeer et al. [11] included adjusting the ratio of the extractant to the sample size, the addition of washes after collecting the supernatant from each sequential extraction, and replacing the persulfate digestion step with microwave-assisted acid digestion.

In summary, we changed the sediment sample size, added washes between extractions, and adjusted extractant and wash volumes. We then followed these modified fractionation procedures to determine the minimum samples size that could be used to reliably ascertain P-fractions in small samples, such as those obtained from suspended sediments. In the following sections, we present details on the completed P-MF method and sample size selection results.

#### 2.2.4 Method Description

The Supplemental Information contains a detailed description of the final method. We summarize and describe the method in this section, but do not provide all the required details.

Our P-MF procedure quantified five P-fractions:  $P_{wat}$ ,  $P_{ion}$ ,  $P_{Fe}$ ,  $P_{Ca}$ , and  $P_{res}$ . The required extractants for our method are DI water for  $P_{wat}$ , 1.0 M KCl for  $P_{ion}$ , 0.1 M NaOH for  $P_{Fe}$ , and 0.5 M HCl for  $P_{Ca}$ . The remaining sample is then microwave digested to measure  $P_{res}$ . We used triplicate measurements, blanks, standard sample sizes, and  $P_{tot}$  as quality control checks.

We measured the first four fractions by sequentially applying extractants to a sediment sample and collecting and analyzing the resulting supernatants to determine the mass of P extracted. These are the same extractants used by Casbeer, et al. [11], though with different volume ratios. While Casbeer et al. used an extractant-to-sample ratio of 2 mL to 1 g of sediment, we opted to use a ratio of 10 mL of extractant per 1 g of sample material for our P-MF method. This constant ratio helped provide

comparability among the different sample sizes during the method development.

We also washed each sample between extraction steps in ratios of 10 mL of wash solution per 1 g of wet sample material. After a wash, we collected the resulting supernatants and combined the volume of wash solution with the supernatant of the P extractant for that step. We used washes of 1.0 M KCl for each fraction except the  $P_{wat}$ , for which we used DI water as the wash. We included the wash volumes in mass computations to determine the mass of P extracted from the solids at each step.

We analyzed P concentrations in the extracted supernatant using a Thermo Scientific iCAP 7400 ICP-OES. We added deionized water to the sample when the combined supernatant volume for a given fraction was insufficient for analysis. This additional liquid volume was accounted for in P mass computations.

$P_{res}$  constituted the final fraction and required digestion of any remaining solids, which are often organic in nature but can also be comprised of other mineral forms. We found that the persulfate digestion used by Casbeer, et al. [11] was insufficient to completely digest the remaining solids and we therefore chose to use microwave-assisted acid digestion (US EPA Method 3051A) to perform this step. However, there were several instances when there was not enough remaining sediment to perform a digestion for the final residual fraction. Microwave digestion requires a minimum of 0.1 g of material, and the analysis of lesser amounts may yield inaccurate results.

ICP-OES provides measurements of elemental P in units of ppm, which is essentially equivalent to mg L<sup>-1</sup> for the density of our aquatic or supernatant samples. These measurements include both the extractant volume and any water used for dilution when the concentration is too high or for augmentation if the sample volume is too small. Based on the Casbeer, et al. [11] method, we converted ICP-OES measurements to sample P solids concentrations in mg kg<sup>-1</sup> using the equation:

$$C_{P_{smp}} = \frac{C_{P_{aq}} \times \frac{L}{1000 \text{ mL}} \times V_{aq} \times D}{m_{smp} \times \frac{kg}{1000 \text{ g}}} \quad (2.1)$$

where:

$C_{P_{smp}}$  = the calculated sample P concentration (mg kg<sup>-1</sup>)

$C_{P_{aq}}$  = the measured aqueous P concentration (mg L<sup>-1</sup>)

$V_{aq}$  = the final volume of supernatant/solution (mL)

$D$  = the dilution factor (the undiluted volume divided by the diluted volume)

$m_{smp}$  = the estimated mass of dry sample subjected to P extraction (g)

The numerator on the right side of the equation is the mass of P in the analyzed liquid sample in mg, and the denominator is the original mass of the suspended solids or sediments, not the mass at the beginning of the extraction step. Care should be taken to distinguish between wet and dry sediment masses. Saturated samples such as suspended solids and lakebed sediments must be analyzed while wet in order to preserve their chemical integrity as drying the sample can change the chemical form of P and thus alter the P-fractions. However, the dry sediment mass of the original sample is required to calculate the sediment P concentrations of the measured fractions. To measure the dry mass, we collected sample duplicates to serve as proxies for measuring the water content and dry masses of the original samples. For this study, we will refer to samples used in the analysis by their dry masses and report the resulting P-fractions in mg kg<sup>-1</sup>.

The dilution factor in this equation is included for instances when the concentration of P in the supernatant or solution is above the analytical range of the instrument (i.e., is overrange) and therefore requires dilution in order for P to become measurable or when samples required augmentation to analysis. When dilution is not used, the dilution factor has a value of 1, thus becoming negligible for the purposes of this equation.

## 2.3 Results and Discussion

### 2.3.1 Baseline Results

#### 2.3.1.1 Detection Limits

Of the 156 samples we ran for P-MF analysis, 151 of them (97%) produced results that were within detection limits for the ICP-OES. The five exceptions were all underrange values representing water-soluble P or loosely-sorbed P, both of which tended to be less prevalent fractions for Utah Lake sediments. These measurements are marked in red numbering in Table 2.

#### 2.3.1.2 Dry Mass of Samples

For the P-MF analysis, we used wet sample sizes of 1.4 g, 0.5 g, 0.4 g, 0.3 g, 0.2 g for both our lakebed sediment and suspended solids samples. To estimate the dry mass for samples undergoing P-MF analysis, we dried duplicates and found that our lakebed sediments were 70% dry mass, while our suspended solids were 32% dry mass. This resulted in dry sample sizes of 0.99 g, 0.35 g, 0.28 g, 0.21 g, and 0.14 g for our lakebed sediment samples and 0.44 g, 0.16 g, 0.13 g, 0.09 g, and 0.06 g for our suspended solids samples. Each sample size for both sediment types was tested in triplicate as a quality control measure.

#### *2.3.1.3 Sample Controls*

Given that most P-fractionation methods for sediment require a minimum of 1 to 2 g of dried sample for analysis [2], we aimed to have the largest sample size for both our lakebed sediment and suspended solids samples be within that range so that these samples could act as a control or ground truth for their respective solid type, i.e., sediments or suspended solids. While we achieved this for our largest lakebed sediment samples, each having a dry mass of ~1 g per sample, the water content of our suspended solids samples was much higher than expected, causing the largest samples to each have a dry mass of only 0.44 g. This sample size consequently isn't large enough to act as a true control, but its inclusion still provides helpful insight for P-MF analysis.

#### *2.3.1.4 Results for Total Phosphorus*

After measuring the dry mass of our duplicate samples, we measured the  $P_{tot}$  (total P) of the duplicates and found them to be in the range of 310-320 mg kg<sup>-1</sup> for the lakebed sediments and 550-600 mg kg<sup>-1</sup> for the suspended solids. These raw values represent the actual levels of  $P_{tot}$  in the lakebed sediments and suspended solids samples. Estimated  $P_{tot}$ , which is determined by the sum of the P-fractions of each sample size, covered a much wider range than the raw measurements, being 180-390 mg kg<sup>-1</sup> for the lakebed sediments and 550-1450 mg kg<sup>-1</sup> for the suspended solids (Figure 2.2; Table 2.1).

The raw measurements are used primarily to check the accuracy of the estimated  $P_{tot}$  values, with similar results indicating a more accurate fractionation run. Some dissimilarity should be allowed, however, as sediment is often heterogenous by nature, and small sample sizes are more prone to be influenced by heterogeneity. Interestingly, the smallest sample sizes from both the lakebed sediments and suspended solids were the most similar to the raw  $P_{tot}$  measurements. The lakebed sediments overall were the most similar to the raw measurements, while the suspended solids varied quite markedly, particularly as sample size increased. Greater variation among suspended solids is to be expected, though, as their source materials are typically more diverse than those of lakebed sediments.

#### *2.3.1.5 Results for P-fractions*

Using the P-MF method described in section 2.2.4, we performed a total of 150 P-fraction measurements for our lakebed sediment and suspended solids samples (Figures 2.3, 2.4, 2.5, 2.6, and 2.7; Table 2.1). As a reminder, the individual fractions included in our analysis were water-soluble P ( $P_{wat}$ ), loosely-sorbed P ( $P_{ion}$ ), Fe- & Al-bound P ( $P_{Fe}$ ), Ca-bound P ( $P_{Ca}$ ), and residual P ( $P_{res}$ ).

Several trends emerged among the P-fraction results, most notably that while the water-soluble P concentrations were similar between the lakebed

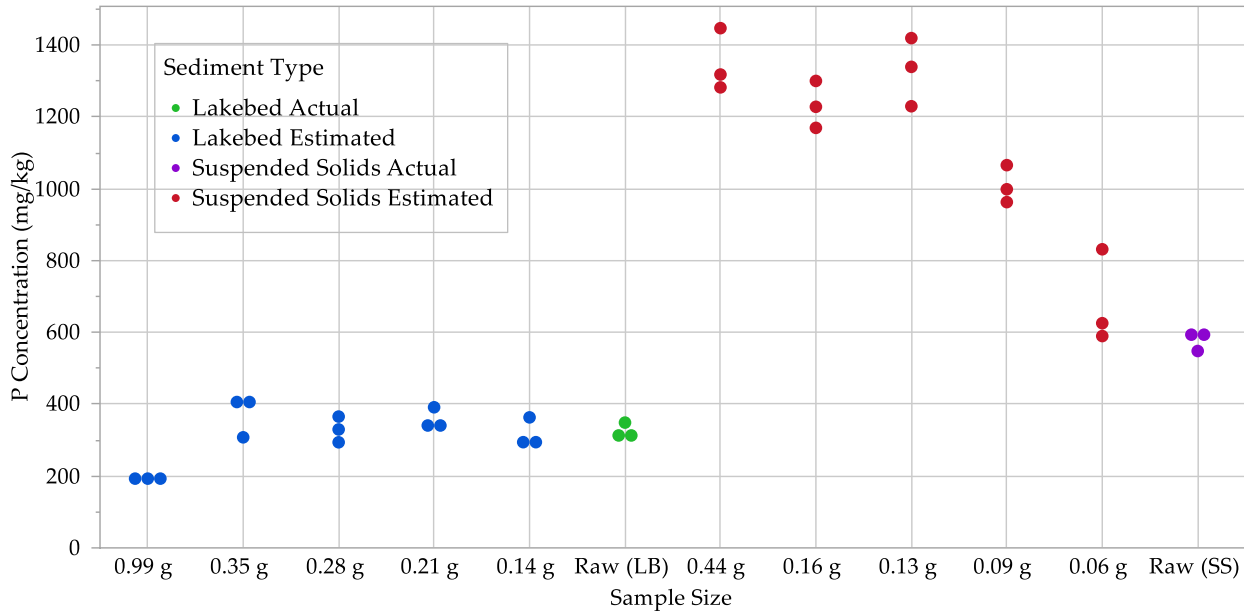


Figure 2.2. Results for both actual (raw) and estimated total P.

Table 2.1. P-MF results for total phosphorus (mg kg<sup>-1</sup>) with each sample size including three replicates. The controls, which had original wet masses of 1.4 g, are shaded in gray, and the raw (actual  $P_{tot}$ ) measurements are shown in blue numbering.

Lakebed Sediments						Suspended Solids						
	0.99 g	0.35 g	0.28 g	0.21 g	0.14 g	Raw	0.44 g	0.16 g	0.13 g	0.09 g	0.06 g	Raw
$P_{tot}$	194	391	358	392	363	316	1283	1228	1420	963	832	548
	181	421	294	350	294	310	1447	1300	1340	994	620	588
	204	308	325	332	295	320	1290	1170	1230	1066	590	600
avg	193	373	326	358	317	316	1340	1233	1330	1008	681	579

sediments and the suspended solids, all other P-fractions were significantly higher in the suspended solids. This is expected as previous work has shown that smaller particles sorb P at higher concentrations. This suggests that the suspended solids in Utah Lake may have a higher P bioavailability than lakebed sediments and may have more influence on dissolved P concentration from sediment-water equilibrium sorption interactions.

Another noticeable trend among the results is that the sample sizes used as controls—0.99 g for lakebed sediments and 0.44 g for suspended solids—differ visually from the other sample sizes for each fraction. The trends are different between sediment type, as the control for lakebed

sediments is consistently lower than other samples, while the standard for suspended solids is consistently higher.

With regard to the lakebed sediments, we found that the concentrations of water-soluble P and loosely-sorbed P tended to be small, ranging from 1-3 mg kg<sup>-1</sup>, with the loosely-sorbed fraction being the larger of the two. The next largest fractions were Fe- & Al-bound P, with concentrations ranging from 8-18 mg kg<sup>-1</sup>, followed by residual P, with concentrations ranging from 18-70 mg kg<sup>-1</sup>. Ca-bound P was by far the largest fraction for the lakebed samples, ranging from 150-360 mg kg<sup>-1</sup>.

As for the suspended solids, we found that, similar to the lakebed sediments, most water-soluble P ranged between 1-3 mg kg<sup>-1</sup>. The other P-fractions in the suspended solids were noticeably different from the lakebed sediments, with loosely-sorbed P ranging from 28-35 mg kg<sup>-1</sup>, and residual P ranging from 140-260 mg kg<sup>-1</sup>. The largest P-fractions for the suspended solids were the Fe & Al-bound P with a range of 130-390 mg kg<sup>-1</sup> and Ca-bound P with a range of 240-790 mg kg<sup>-1</sup> (Figures 2.3, 2.4, 2.5, 2.6, and 2.7; Table 2.2).

It should be noted that due to unavoidable sample loss during the fractionation process, all suspended solids samples except the 0.44 g control yielded less than the 0.1 g needed for the residual P measurement step. While mathematical corrections were made to account for the smaller sample masses used for this step, it is possible that these results for residual P may not be accurate. This oversight would have been avoided if we had not overestimated the dry mass content of our suspended sediment samples and used larger wet samples. We therefore suggest that the dry mass be measured in duplicate sediment samples before conducting P-MF analysis.

### 2.3.2 One-way ANOVAs

One of the primary objectives of this study was to determine the threshold for when sample size becomes the limiting factor for measuring P-fractions in small samples. Our approach for determining this threshold involved comparing the results of our standard samples to smaller sample sizes using one-way ANOVAs. This allowed us to determine if statistical differences were present in the data

We found that most of the P-fractions for both lakebed sediment and suspended solids had p-values that were well below our alpha value of 0.05, indicating a need for further analyses. On the other hand, the fractions with no statistically significant differences between sample sizes included water-soluble P and residual P for the lakebed sediments and loosely-sorbed P for the suspended solids, having p-values of 0.15, 0.26, and 0.20, respectively. Sample size consequently doesn't appear to affect the outcome of these fractions when analyzed using our P-MF method.

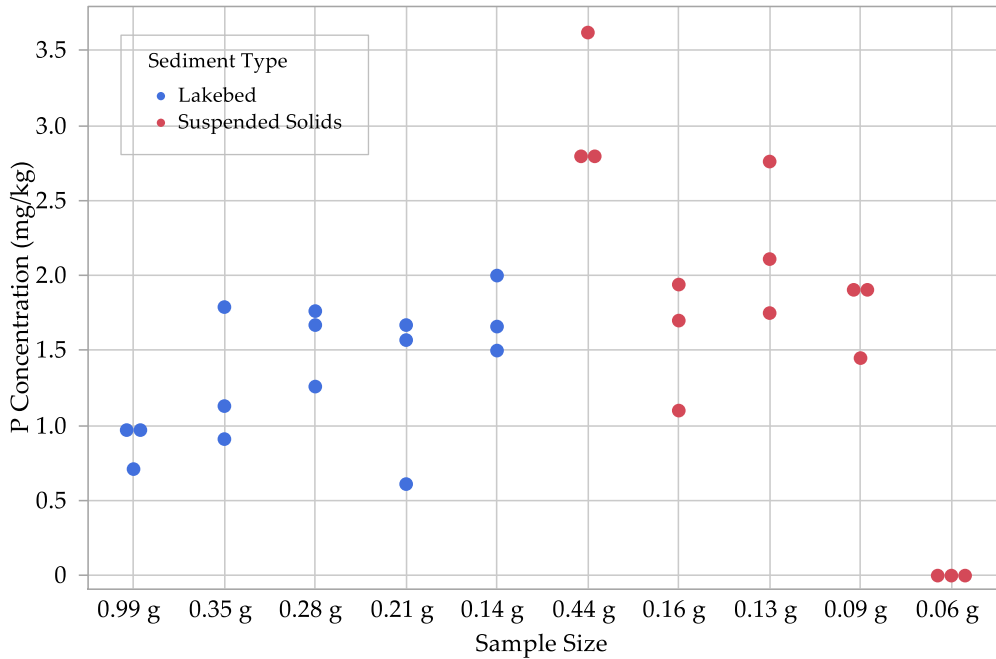


Figure 2.3. Results for water-soluble P. The 0.06 g results for suspended solids were below detection limits and are therefore set to zero.

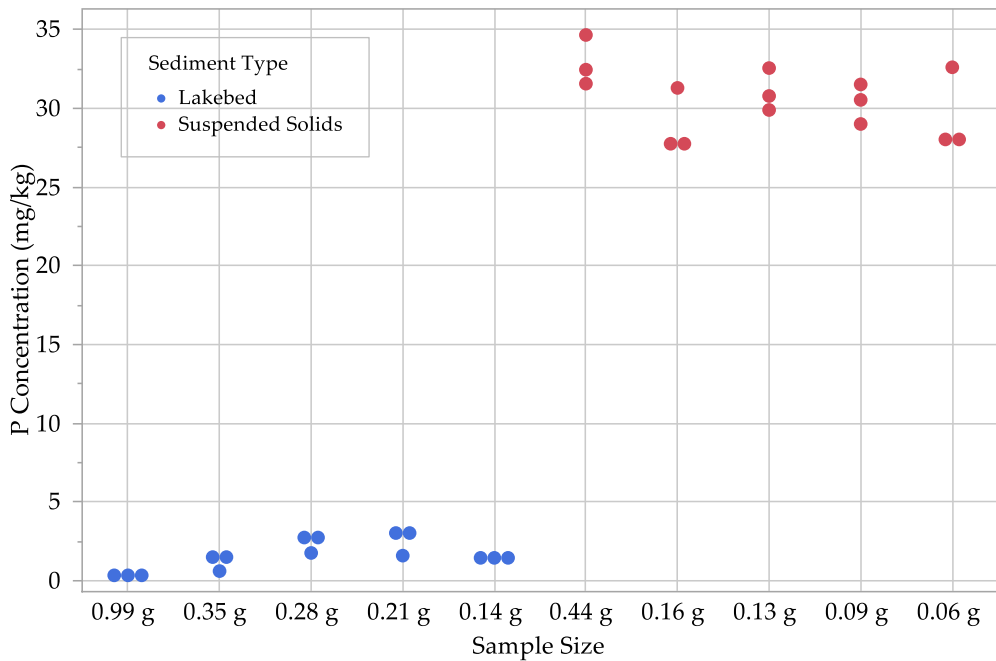


Figure 2.4. Results for loosely-sorbed P.

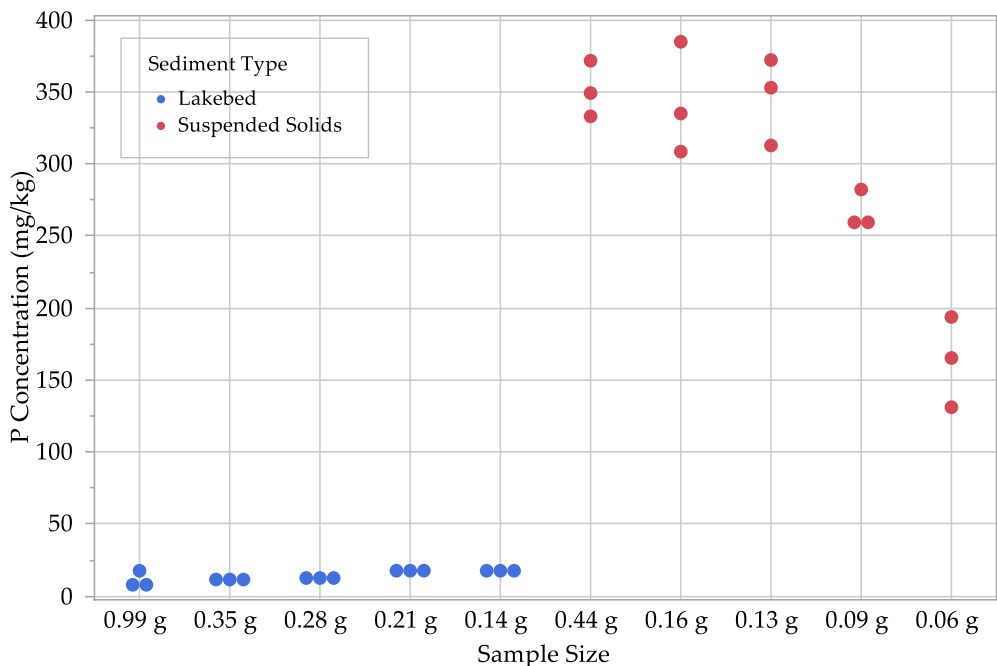


Figure 2.5. Results for Fe- & Al-bound P.

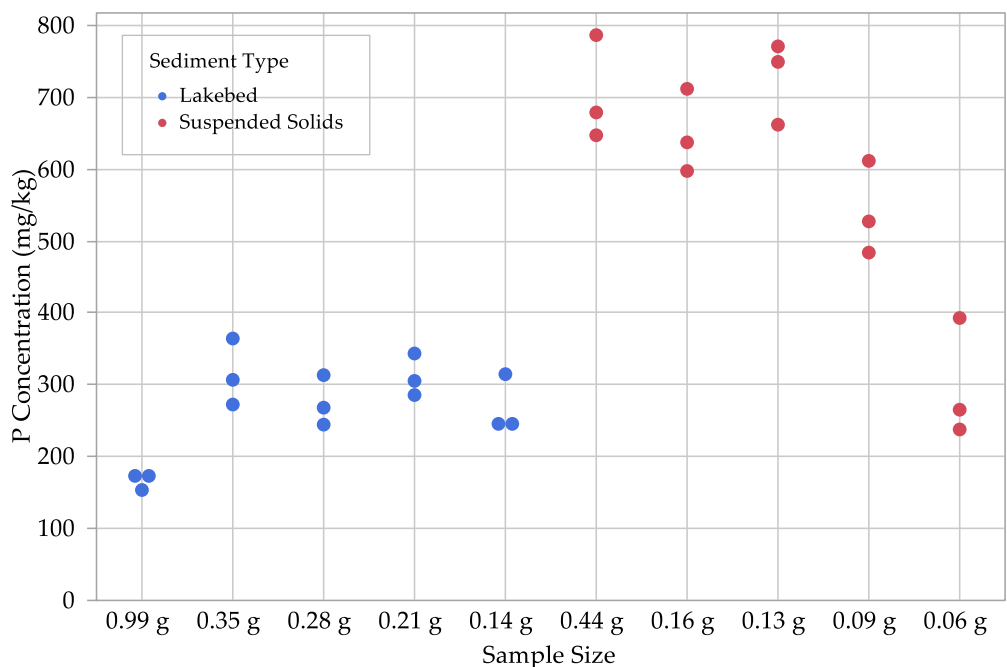


Figure 2.6. Results for Ca-bound P.

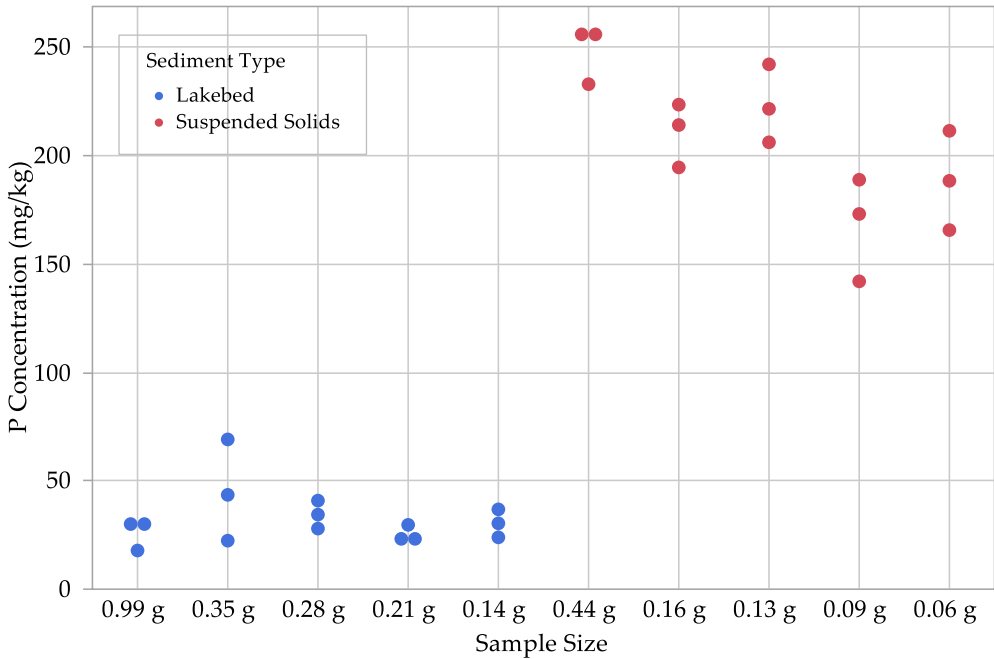


Figure 2.7. Results for residual P.

### 2.3.3 Post-hoc Tests

While one-way ANOVAs are useful for detecting whether the differences in sample size are significant, they are insufficient for determining which sample sizes are associated with significantly different P concentrations. To determine which sample sizes were significantly different from each other, we applied two post-hoc tests to the data, including the Student's T and Tukey-Kramer HSD tests (Table 3. Post-hoc Connected Letters Report for P-MF Samples. Rows marked in green signify fractions with large ANOVA p-values ( $> 0.05$ ), indicating no statistically significant differences among the sample sizes for the given sediment type.

For the lakebed sediment samples, the one-way ANOVA tests indicated that the fractions for loosely-sorbed P, Fe- & Al-bound P, and Ca-bound P had statistically significant differences based on their sample sizes. Both the Student's T and Tukey Kramer HSD tests grouped the two largest sample sizes together (0.99 g and 0.35 g) for loosely-sorbed P, suggesting that this fraction can yield consistent results down to dry sample mass of 0.35 g. This is not the case, however, for Fe- & Al-bound P and Ca-bound P, as the largest sample size (0.99 g) was grouped by itself while the remaining sample sizes were all grouped together. With the second largest sample size being 0.35 g, it is possible that the threshold for minimum sample size is an intermediate value between 0.35-0.99 g. Further experimentation is necessary to determine the value for that threshold.

For the suspended solids samples, the one-way ANOVA tests indicated that all P-fractions, with the exception of loosely-sorbed P, contained significant differences among their sample sizes. In most cases, the largest and third-largest sample sizes (0.44 g and 0.13 g) were grouped together for all P-fractions. The second largest was included with these groupings for both post-hoc tests on the for Fe- & Al-bound P and Ca-bound P fractions, as well as for the Tukey Kramer HSD test on the residual P fraction. This seems to suggest that consistent results could be obtained for

Table 2.2. P-MF results for individual fractions ( $\text{mg kg}^{-1}$ ) with each sample size including three replicates. The controls, which had original wet masses of 1.4 g, are shaded in gray, and underrange measurements are shown in red numbering.

		Lakebed Sediments					Suspended Solids				
		0.99 g	0.35 g	0.28 g	0.21 g	0.14 g	0.44 g	0.16 g	0.13 g	0.09 g	0.06 g
$P_{\text{wat}}$	1.01	1.79	1.73	0.61	1.66		2.80	1.10	2.11	1.45	0.00
	0.93	1.13	1.67	1.57	1.50		2.79	1.94	1.75	1.90	0.00
	0.71	0.91	1.26	1.67	2.00		3.62	1.70	2.76	1.91	0.00
	average	0.88	1.28	1.55	1.28	1.72	3.07	1.58	2.21	1.75	0.00
$P_{\text{ion}}$	0.99 g	0.35 g	0.28 g	0.21 g	0.14 g	0.44 g	0.16 g	0.13 g	0.09 g	0.06 g	
	0.41	1.30	2.71	1.60	1.69	34.7	31.3	32.6	30.5	32.6	
	0.20	0.84	2.79	3.28	1.64	31.6	27.5	29.9	31.5	28.1	
	0.44	0.62	1.77	2.79	1.05	32.0	28.0	30.2	29.0	27.9	
$P_{\text{Fe}}$	0.99 g	0.35 g	0.28 g	0.21 g	0.14 g	0.44 g	0.16 g	0.13 g	0.09 g	0.06 g	
	7.9	12.3	12.4	18.2	17.7	333	385	372	258	194	
	8.0	11.4	11.0	17.5	18.3	372	335	353	261	165	
	10.1	11.0	14.4	17.4	17.0	349	308	313	282	131	
$P_{\text{Ca}}$	0.99 g	0.35 g	0.28 g	0.21 g	0.14 g	0.44 g	0.16 g	0.13 g	0.09 g	0.06 g	
	156	307	313	343	315	679	597	771	484	393	
	154	364	245	305	240	786	712	749	527	238	
	161	273	268	286	251	647	637	662	611	265	
$P_{\text{res}}$	0.99 g	0.35 g	0.28 g	0.21 g	0.14 g	0.44 g	0.16 g	0.13 g	0.09 g	0.06 g	
	28.6	69.1	28.0	28.2	27.4	233	214	242	189	212	
	17.9	43.6	33.6	22.2	32.4	255	224	206	173	189	
	31.5	22.4	40.0	24.3	23.9	258	195	222	142	166	
average	26.0	45.0	33.9	24.9	27.9	249	211	223	168	189	

these fractions down to a dry sample mass of 0.13 g. Interestingly, the second-largest sample size (0.16 g) does not group with the largest and third-largest sample sizes (0.44 g and 0.13 g) for the water-soluble P fraction, which suggests that the minimum sample size threshold is > 0.16 g. Again, further experimentation is necessary to determine the value for that threshold.

Table 2.3. Post-hoc connected letters report for P-MF samples. Rows marked in green signify fractions with large ANOVA p-values (> 0.05), indicating no statistically significant differences among the sample sizes for the given sediment type.

		Lakebed Sediments					Suspended Solids				
		0.99 g	0.35 g	0.28 g	0.21 g	0.14 g	0.44 g	0.16 g	0.13 g	0.09 g	0.06 g
$P_{wat}$	Student's T	A	A	A	A	A	A	B	B	B	C
	Tukey Kramer HSD	A	A	A	A	A	A	B	B	B	C
$P_{ion}$	Student's T	A	A	B		A	A	A	A	B	
	Tukey Kramer HSD	A	A	A	B	A	A	A	A	A	
$P_{Fe}$	Student's T	A	B	B	C	C	A	A	A	B	C
	Tukey Kramer HSD	A	B	B	C	C	A	A	A	B	C
$P_{Ca}$	Student's T	A	B	B	B	B	A	A	A	B	C
	Tukey Kramer HSD	A	B	B	B	B	A	A	A	B	C
$P_{Re}$	Student's T	A	A	A	A	A	A	A	B	B	C
								C		D	D
	Tukey Kramer HSD	A	A	A	A	A	A	A	B	B	B
								C	C	C	

## 2.4 Conclusion

### 2.4.1 Study Limitations and Suggestions for Future Research

For this study, we created a P fractionation method designed to accommodate small samples of sediment and suspended solids, and we sought to determine the smallest sample size that still provides accurate results. While our method proves that microfractionation is possible, more work is needed in order to more clearly define the threshold for minimum sample size. With respect to Utah Lake, we expect the threshold to be between 0.35-0.99 g for lakebed sediments, and > 0.16 g for Utah Lake suspended solids.

We would like to highlight three limitations affecting this study, with the first limitation regarding the dry mass of our samples. A critical part of performing P-MF analysis is knowing the dry mass being tested. We conducted our experiments based on estimates for dry mass, and while this worked for our lakebed sediments, we overestimated the dry mass of our suspended solids samples. This caused the suspended solids samples to be smaller than expected, which consequently meant that we did not have a true control group for the suspended solids samples. Dry mass cannot be measured directly from samples undergoing analysis as doing so can jeopardize the integrity of the samples' P-fractions. Duplicate samples must be used as a proxy for determining dry mass. While we measured the dry mass of duplicate samples, we did so alongside the P-MF process, and so the true dry mass of our samples was only determined partway through. To avoid this issue, we recommend waiting to perform P-MF analysis until after the samples' dry mass has been determined.

A second limitation of this study was the number of sample sizes being tested. For each sediment type, we sought to have a sample size that acted as a control representing a standard P-fractionation sample along with four successively smaller sample sizes. While these sizes helped narrow the potential range for microfractionation samples from Utah Lake, the sample sizes tested weren't exhaustive, and future iterations of this study could more clearly define the lower sample size thresholds for sediments and suspended solids.

A third limitation of this study was that we only evaluated lakebed sediment and suspended solids from Utah Lake. Our results show that the lake's suspended solids have a significantly larger P content than the lakebed sediments, suggesting that the lake's suspended solids are a greater source of bioavailable P. While we would assume that sediment and suspended solids from other water bodies would behave similarly, additional experimentation is needed to confirm this, especially since the composition of sediments and suspended solids from other locations will vary and thereby impact the manner and degree to which they store and

release P. Future studies on P-MF processes should test sediments and suspended solids of diverse compositions from various locations.

Through development of these micro-fractionation methods, we demonstrated that suspended sediments in Utah Lake have significantly higher P concentrations, especially for the fractions that interact readily with the water column. These concentrations can be on the order of 10 to 100x for loosely sorbed P, to several hundred times for Fe- & Al-bound P. This highlights the need for an acceptable method to measure P-fractions in small samples, as measuring P-fractions in lake sediments are not a good analog for concentrations in suspended solids.

## 2.5 Supplemental Information – Phosphorus Microfractionation (P-MF) Method for Total Suspended Solids

### Scope and Application

- 1.01 This method is applicable for microscale samples of total suspended solids (TSS) from aerobic surface waters.

### Summary of Method

- 2.01 Sequential extraction is used to obtain five phosphorus (P) fractions from small samples of particulate matter, designed specifically for suspended solids. The P fractions included in this method are water-soluble P, loosely-sorbed P, iron- & aluminum-bound P, calcium-bound P, and residual P.

### Method Deviations

- 3.01 Suspended solids can be separated from surface waters either through centrifugation or sedimentation.
- 3.02 Extraction procedures for other P fractions could potentially be applied to this method, though further testing of those procedures on a microfractionation level is advised.
- 3.03 The required sample size can be reduced to a dry mass equivalent of 50 mg, but the residual phosphorus fraction will not be accurate.

### Interferences

- 4.01 Microfractionation analyses should begin on the day of sample collection as extended residence times appear to significantly affect the sample's calcium-bound fraction.

### Equipment and Supplies

- 5.01 Mass Balance and associated components
- 5.02 Centrifuge
- 5.03 Shaker Table

- 5.04      Microwave Digester and associated components
- 5.05      ICP-OES and associated components
- 5.06      Centrifuge tubes
- 5.07      ~20 mL luer lock syringes
- 5.08      0.45 µm syringe filters
- 5.09      Small, narrow spatula
- 5.10      Crucibles
- 5.11      Pestle and mortar

#### **Extractant Chemicals**

- 6.01      DI Water
- 6.02      1 M KCl
- 6.03      0.1 M NaOH
- 6.04      0.5 M HCl

#### **Sample Collection**

- 7.01      The amount of sample to be collected will depend on the water's concentration of TSS and the desired quantity of material. Duplicate samples are required, one for water content, one for fractionation. Samples should begin analysis on the day they are collected.

#### **Equipment and Extractant Preparation**

- 8.01      Five centrifuge tubes are needed per sampling location. The first centrifuge tube is designated as a "primary" tube and is used to combine extractants with the first duplicate sample from each sampling location. The remaining centrifuge tubes are used to store the resulting supernatants for each P fraction (i.e., the water-soluble, loosely-sorbed, Fe- & Al-bound, & Ca-bound fractions). 15-mL centrifuge tubes can be used for wet TSS samples ≤ 750 mg, and 50-mL centrifuge tubes can be used for wet TSS samples > 750 mg.
- 8.02      Four luer lock syringes and four syringe filters are needed per sampling location.

#### **Quality Control & Corrective Actions**

- 9.01      The second duplicate sample from each sampling location is used to approximate the solids-to-liquids ratio and the total phosphorus (TP) content of the first duplicate. The measurement of TP is used as a check to evaluate the effectiveness of the microfractionation procedure in extracting P from the first duplicate. This is done by comparing the TP content of the second duplicate against the sum of the P fractions from the first duplicate.

- 9.02 TSS samples should be weighed before and after each extraction step to determine if a significant amount of sample loss occurred. Since these include solids and supernatant, the measurements will not be exact. If sample loss has been detected, the new mass should be used for calculating P concentrations for each subsequent fraction. These changes will not apply to the residual P fraction which will instead use the value of ~100 mg, which is the amount required for microwave assisted acid digestion.

## Procedure

### Water-Soluble Phosphorus

- 10.01 Measure and record the empty mass of the primary tube (including the cap).
- 10.02 Add the desired amount of wet sample to the primary tube and record the mass.
- 10.03 Using an extractant-to-sample ratio of 10 mL g<sup>-1</sup>, add the appropriate amount of DI water to the primary tube.
- 10.04 Cap the primary tube and shake by hand until the sample and DI water are well-mixed. If the sample forms clumps or adheres to the walls of the primary tube, use a clean, narrow spatula to break up and stir the sample until it has become well-mixed with the extractant.
- 10.05 Centrifuge the primary tube at ~1,900 g for 20 minutes.
- 10.06 Attach a 0.45 µm syringe filter to the end of the luer lock syringe, remove the plunger from the barrel, and then decant the supernatant from the primary tube into the syringe. Reinsert the plunger into the syringe and then expel the supernatant into the centrifuge tube designated to store the water-soluble supernatant. Cap the centrifuge tube and set aside. (This technique for transferring and filtering will be used for all subsequent supernatants and washes).
- 10.07 Using an extractant-to-sample ratio of 10 mL g<sup>-1</sup>, wash the primary tube sample with DI water.
- 10.08 Cap the primary tube and shake by hand until the sample and DI water are well-mixed. If the sample forms clumps or adheres to the walls of the primary tube, use a clean, narrow spatula to break up and stir the sample until it has become well-mixed with the wash.
- 10.09 Centrifuge the primary tube again at ~1,900 g for 20 minutes.

- 10.10 Reuse the syringe and filter to transfer the wash to the centrifuge tube designated to store the water-soluble supernatant.
- 10.11 Discard both the syringe and filter.
- 10.12 Cap the centrifuge tube and then store at approximately 4°C until ready for ICP analysis.

**Loosely-Sorbed Phosphorus**

- 10.13 Measure and record the combined mass of the primary centrifuge tube and remaining sediment to determine if sediment loss occurred after the water-soluble P extraction step. This will not be exact, as some liquid remains.
- 10.14 Using an extractant-to-sample ratio of 10 mL g<sup>-1</sup>, add the appropriate amount of 1.0 M KCl to the primary tube.
- 10.15 Cap the primary tube and shake by hand until the sample and KCl solution are well-mixed. If the sample forms clumps or adheres to the walls of the primary tube, use a clean, narrow spatula to break up and stir the sample until it has become well-mixed with the extractant.
- 10.16 Centrifuge the primary tube at ~1,900 g for 20 minutes.
- 10.17 With a new syringe and filter, transfer the supernatant to the centrifuge tube designated to store the loosely-sorbed supernatant, cap the centrifuge tube, and then set it aside.
- 10.18 Using an extractant-to-sample ratio of 10 mL g<sup>-1</sup>, wash the primary tube sample with 1.0 M KCl.
- 10.19 Cap the primary tube and shake by hand until the sample and KCl are well-mixed. If the sample forms clumps or adheres to the walls of the primary tube, use a clean, narrow spatula to break up and stir the sample until it has become well-mixed with the wash.
- 10.20 Centrifuge the primary tube again at ~1,900 x g for 20 minutes.
- 10.21 Transfer the wash to the centrifuge tube designated to store the loosely-sorbed supernatant.
- 10.22 Discard both the syringe and filter.
- 10.23 Cap the centrifuge tube and then store at approximately 4°C until ready for ICP analysis.

**Iron- & Aluminum-bound Phosphorus**

- 10.24 Measure and record the combined mass of the primary centrifuge tube and remaining sediment to determine if

- sediment loss occurred after the loosely-sorbed P extraction step.
- 10.25 Using an extractant-to-sample ratio of 10 mL g<sup>-1</sup>, add the appropriate amount of 0.1 M NaOH to the primary tube.
- 10.26 Cap the primary tube and shake by hand until the sample and NaOH solution are well-mixed. If the sample forms clumps or adheres to the walls of the primary tube, use a clean, narrow spatula to break up and stir the sample until it has become well-mixed with the extractant.
- 10.27 Cap the primary tube and place horizontally on a reciprocating shaker table at 100 rpm for 17 hours.
- 10.28 Centrifuge the primary tube at ~1,900 g for 20 minutes.
- 10.29 Using a new syringe and filter, transfer the supernatant to the centrifuge tube designated to store the iron- & aluminum-bound supernatant, cap the centrifuge tube, and then set it aside.
- 10.30 Using an extractant-to-sample ratio of 10 mL g<sup>-1</sup>, wash the sample with 1.0 M KCl.
- 10.31 Cap the primary tube and shake by hand until the sample and KCl are well-mixed. If the sample forms clumps or adheres to the walls of the primary tube, use a clean, narrow spatula to break up and stir the sediment until it has become well-mixed with the wash.
- 10.32 Centrifuge the primary tube again at ~1,900 × g for 20 minutes.
- 10.33 Transfer the wash to the centrifuge tube designated to store the iron- & aluminum-bound supernatant.
- 10.34 Discard both the syringe and filter.
- 10.35 Cap the centrifuge tube and then store at approximately 4°C until ready for ICP analysis.

#### Calcium-Bound Phosphorus

- 10.36 Measure and record the combined mass of the primary centrifuge tube and remaining sediment to determine if sample loss occurred after the iron- & aluminum-bound P extraction step.
- 10.37 Using an extractant-to-sediment ratio of 10 mL g<sup>-1</sup>, add the appropriate amount of 0.5 M HCl to the primary tube. Exercise caution when adding HCl to samples containing CaCO<sub>3</sub> as the sample will effervesce due to the formation of CO<sub>2</sub> gas.
- 10.38a For samples containing CaCO<sub>3</sub>, carefully stir the mixture with a clean, narrow spatula until the sample stops

- effervescing, then allow the sample to off-gas for several minutes to help prevent leakage when capped due to the continued off-gassing of CO<sub>2</sub>. Cap the primary tube and then shake by hand until the sample and HCl solution are well-mixed. If the sample forms clumps or adheres to the walls of the primary tube, use a clean, narrow spatula to break up and stir the sample until it has become well-mixed with the extractant.
- 10.38b For samples not containing significant amounts of CaCO<sub>3</sub>, cap the primary tube and then shake by hand until the sample and HCl solution are well-mixed. If the sample forms clumps or adheres to the walls of the primary tube, use a clean, narrow spatula to break up and stir the sample until it has become well-mixed with the extractant.
- 10.39 Cap the primary tube and place horizontally on a reciprocating shaker table at 100 rpm for 24 hours.
- 10.40 Centrifuge the primary tube at ~1,900 g for 20 minutes.
- 10.41 Using a new syringe and filter, transfer the supernatant to the centrifuge tube designated to store the calcium-bound supernatant, cap the centrifuge tube, and then set it aside.
- 10.42 Using an extractant to sediment ratio of 10 mL g<sup>-1</sup>, wash the sediment with 1.0 M KCl.
- 10.43 Cap the primary tube and shake by hand until the sample and KCl are well-mixed. If the sample forms clumps or adheres to the walls of the primary tube, use a clean, narrow spatula to break up and stir the sample until it has become well-mixed with the wash.
- 10.44 Centrifuge the primary tube again at ~1,900 g for 20 minutes.
- 10.45 Transfer the wash to the centrifuge tube designated to store the calcium-bound supernatant.
- 10.46 Discard both the syringe and filter.
- 10.47 Cap the centrifuge tube and then store at approximately 4°C until ready for ICP analysis.

#### Residual Phosphorus

- 10.48 Using a clean, narrow spatula, scrape the sample from the primary tube into a crucible and dry the sample by either allowing it to air dry or by placing it in a drying oven overnight at 60°C or cooler.
- 10.49 Once dry, grind the sample into powder using a mortar and pestle.
- 10.50 Weigh out a minimum of 0.1 g of the powdered sample.

- 10.51      Microwave digest the sample using US EPA Method 3051A.  
 10.52      Store the resulting supernatant until ready for ICP analysis.

#### Data Analysis and Calculations

$$11.01 \quad C_{P_{smp}} = \frac{C_{P_{aq}} \times \frac{L}{1000 \text{ mL}} \times V_{aq} \times D}{m_{smp} \times \frac{kg}{1000 \text{ g}}} \quad (2.1)$$

where:

$C_{P_{smp}}$  = the calculated sample P concentration ( $\text{mg kg}^{-1}$ )

$C_{P_{aq}}$  = the measured aqueous P concentration ( $\text{mg L}^{-1}$ )

$V_{aq}$  = the final volume of supernatant/solution (mL)

$D$  = the dilution factor (the undiluted volume divided by the diluted volume)

$m_{smp}$  = the estimated mass of dry sample subjected to P extraction (g)

#### References for Standard Operating Procedure

- 12.01      Zhang, H.; Kovar, J. L. Fractionation of soil phosphorus. Methods of phosphorus analysis for soils, sediments, residuals, and waters 2009, 2, 50-60.
- 12.02      Kleinman, P. J. A.; Sharpley, A. N.; Gartley, K.; Jarrell, W. M.; Kuo, S.; Menon, R. G.; Myers, R.; Reddy, K. R.; Skogley, E. O. Interlaboratory comparison of soil phosphorus extracted by various soil test methods. Communications in soil science and plant analysis 2001, 32 (15-16), 2325-2345.
- 12.03      Kovar, J. L.; Pierzynski, G. M. Methods of Phosphorus Analysis for Soils, Sediments, Residuals, and Waters. In Southern Cooperative Series Bulletin, Second Edition ed.; Virginia Tech University, 2009.
- 12.04      Casbeer, W. C. Phosphorus Fractionation and Distribution across Delta of Deer Creek Reservoir. Master's Thesis, Brigham Young University, Provo, Utah, USA, 2009.
- 12.05      U.S. EPA. 2007. "Method 3051A (SW-846): Microwave Assisted Acid Digestion of Sediments, Sludges, and Oils," Revision 1. Washington, DC.

Flowchart

13.01

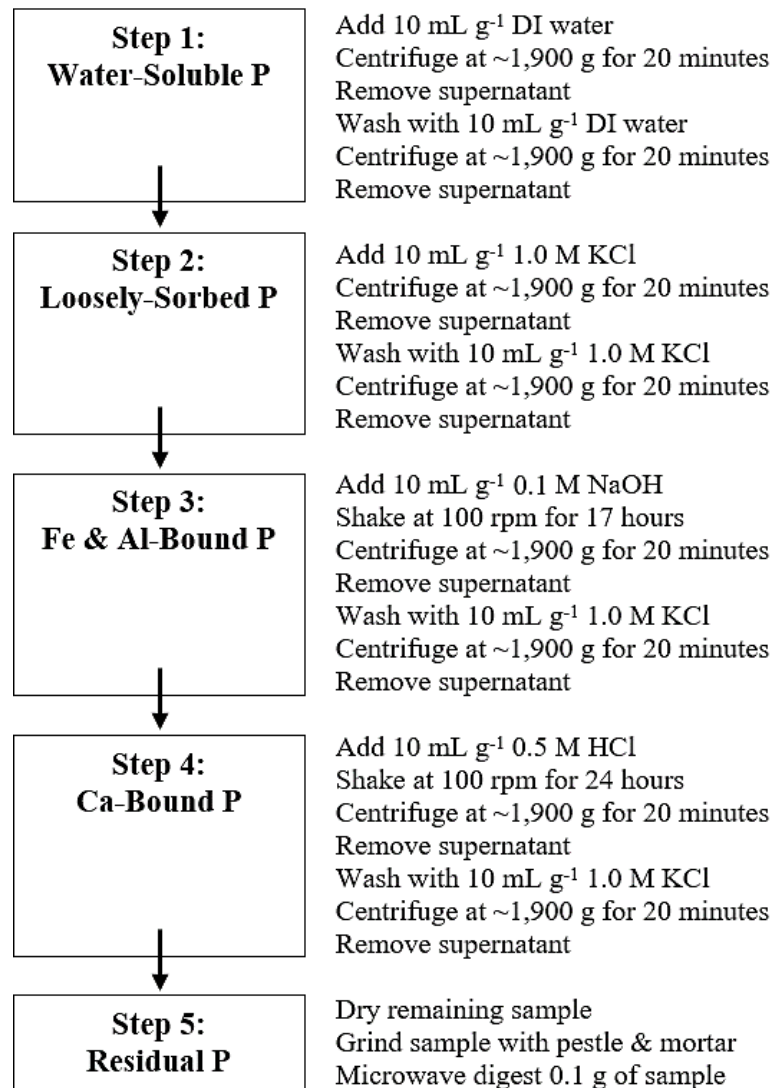


Figure 2.8. Stepwise P-MF procedure.

### **3 Historical Phosphorus Mass and Concentrations in Utah Lake: A Case Study with Implications for Nutrient Load Management in a Sorption-Dominated Shallow Lake**

*Jacob B. Taggart, Rebecca L. Ryan, A. Woodruff Miller, Rachel A. Valek, Kaylee B. Tanner, Anna C. Cardall, and Gustavious P. Williams*

**Abstract:** Utah Lake is unusual due to its large surface area, shallow depth, phosphorus-rich sediments, and well-mixed, unstratified waters. This creates conditions where water column phosphorous concentrations tend toward equilibrium, with lake sediments containing high concentrations of geologic phosphorus. To help understand the potential impact of phosphorous load reductions, we computed a time history of phosphorus mass in the lake using state and federal records of lake volume, dissolved phosphorus concentrations, and outflow. We show that historically, Utah Lake phosphorus concentrations have remained stable over time, in the range of 0.02 to 0.04 mg L<sup>-1</sup>, despite large changes in lake volume and internal phosphorus mass. We performed sorption calculations using data from the literature, demonstrating that it would take unrealistically large load changes to alter water column phosphorus concentrations under sorption processes. The sorption model produces results consistent with historical data that show relatively constant phosphorous concentrations despite large lake volume changes. We suggest, through several lines of evidence, that water column phosphorus concentrations are insensitive to external loads. Phosphorous load reduction is unlikely to have a significant effect on phosphorus concentrations in Utah Lake. These findings may apply to other sorption-dominated shallow lakes with phosphorus-rich sediment.

**Keywords:** historical data; mass balance; phosphorus; Utah Lake; sediments; sorption

### 3.1 Introduction

#### 3.1.1 Study Motivation

In November 2015, the Utah Division of Water Quality (DWQ) initiated the Utah Lake Water Quality Study (ULWQS) to develop nutrient criteria, particularly for phosphorus (P), to protect Utah Lake's designated beneficial uses. The ULWQS is a three-phase plan that involves (1) gathering and characterizing water quality data, (2) developing in-lake nutrient criteria, and (3) implementing plans to help Utah Lake reach the newly established nutrient criteria [31, 32]. In December 2018, DWQ released their Phase 1 Report [33].

During the summer of 2023, a mass balance model for P in Utah Lake was presented to members of the ULWQS Science Panel. The model estimates that wastewater effluent is the most significant P load to Utah Lake, contributing an estimated 133.4 metric tons (t) of total phosphorus (TP) per year. The model accounts for other P sources, including estimates of 49.6 t of TP year<sup>-1</sup> from tributaries, 45.0 t of TP year<sup>-1</sup> from internal loading, and 32.0 t of TP year<sup>-1</sup> from atmospheric deposition (AD) where P associated with particulates, dust, or precipitation is deposited in a water body. A decay factor is included in the model to account for internal P removal. Based on these criteria, this model predicts that Utah Lake will recover from its eutrophic state quickly—approximately 18 months—under a scenario where external P inputs, particularly wastewater effluent, are reduced [34].

There are conflicting estimates for Utah Lake P loads. For example, AD studies performed by Brown, et al. [35], Barrus, et al. [36], Olsen, et al. [37], and Telfer, et al. [38] measured AD rates from 75 to 350 t of TP year<sup>-1</sup> (approximately 2 to 10 times more AD mass than estimated by the ULWQS model). Other studies have shown that internal loading from lakebed sediments could contribute significantly to Utah Lake's P content. Hogsett, et al. [39] demonstrated that benthic sediments release P into Utah Lake's water column, suggesting that internal loading can contribute up to 1500 t of TP year<sup>-1</sup>.

Randall, et al. [40] found that Utah Lake sediments have P concentrations ranging from 300 to 1100 mg kg<sup>-1</sup>, with about 40% (120 to 440 mg kg<sup>-1</sup>) of sediment P being available to the water column through sorption/desorption reactions. Abu-Hmeidan, et al. [6] confirmed that the P content of Utah Lake sediments is high (with an average concentration of 666 mg kg<sup>-1</sup>) and that they are not statistically different from onshore lacustrine soils, signifying that internal loading and the overall P content of Utah Lake are likely geologically driven. The geologic source of these high sediment P concentrations is supported by Casbeer, et al. [11], who found similar P concentrations in sediments from Deer Creek Reservoir,

located on the Provo River approximately 40 km upstream from Utah Lake. These P-rich sediments act as P reservoirs and are able to support P equilibrium with the water column through sorption processes.

We wanted to evaluate the potential impacts of P load reduction on Utah Lake. We used publicly available data to characterize the mass changes of P in Utah Lake using historical lake volume data from the Bureau of Reclamation, historical P concentration data from the Utah Department of Environmental Quality, and historical outflow data from the Utah Division of Water Rights. We evaluated whether historical data trends could be explained using a sorption model based on data in the literature rather than through a mass balance approach. Using these data, we show that Utah Lake is likely dominated by sorption processes and that water column P concentrations move toward equilibrium with the P-rich sediment, resulting in water column P concentrations that are relatively constant over time despite large changes in lake volume and internal dissolved P (DP) mass.

### 3.1.2 Utah Lake Background

Utah Lake is a large, shallow, freshwater lake (surface area of 380 km<sup>2</sup> and an average depth of 3 m) located at 40°13' N latitude and 111°48' W longitude in the state of Utah, USA, in the easternmost portion of North America's Great Basin region. Utah Lake is classified as a semi-terminal lake, fed by multiple headwaters while having a single outlet, the Jordan River, which empties into the Great Salt Lake [41]. Utah Lake is managed as a reservoir, providing water for irrigation, agricultural, and municipal use in addition to supplying water for the Great Salt Lake [42]. Utah Lake is also an important wildlife habitat for fish, such as the threatened June Sucker, and migratory birds [43, 44].

The combination of Utah Lake's large surface area and semi-arid environment causes the lake to experience evaporative losses equivalent to nearly half of its annual inflow. These losses, in conjunction with groundwater seepage through local limestone formations, result in elevated levels of total dissolved solids that render the lake slightly saline, with concentrations near the solubility limits of calcite. Utah Lake has elevated levels of suspended solids due to bioturbation from the feeding behavior of Common Carp and wave-induced resuspension caused by the lake's overall shallowness and wind exposure [41]. Utah Lake is vertically well-mixed and does not stratify, though it is not well-mixed horizontally [45].

In 2016, the State of Utah Water Quality Board implemented a Technology-Based P Effluent Limit (TBPEL) of 1 mg L<sup>-1</sup> for wastewater treatment plants (WWTPs) to take effect in 2020 [46]. The implementation date has since been delayed, as the regulation allowed deferrals to 2025

based on construction requirements (Utah State regulation R317-1-3.3). Nonpoint P sources for Utah Lake are significant contributors and are difficult to assess and regulate. Lake-sediment interactions are even more difficult to control or even quantify but can dominate nutrient mass balance processes in lakes where sediments are rich in P and interact significantly with the water column.

### 3.1.3 Phosphorous-Rich Sediments

Utah Lake is located in a naturally P-rich geologic environment, which results in high P concentrations in lakebed sediment, surrounding lacustrine soils, and sediment transported from the watershed. Detrital P in Utah Lake likely originates from outcrops of the Delle Phosphatic and Meade Peak Members throughout the Utah Lake Watershed (Figure 3.1) [6, 47-51]. The Delle Phosphatic Member is a phosphate-rich sublayer of the Deseret Limestone (early Mississippian) found in Rock Canyon and the Lake Mountains adjacent to Utah Lake [48, 52]. The Meade Peak Member is a phosphatic shale within the Park City and Phosphoria Formation (late Permian) found in outcrops throughout the Utah Lake Watershed, with mineable grade phosphate in the Uinta Basin watershed, the neighboring watershed due east of the Utah Lake watershed [48, 51, 53, 54].

Due to erosion, the valley fill underlying Utah Lake is estimated to be as much as 4000 m thick [55] and includes P-rich source material from the Delle Phosphatic and Meade Peak Members [48]. Assessments of lakebed sediment and lacustrine soils surrounding Utah Lake found that they were not significantly different from each other with respect to their P content, with lakebed sediment TP concentrations ranging from 280 to 1710 mg kg<sup>-1</sup> with an average TP concentration of 666 mg kg<sup>-1</sup> (n = 85). The surrounding lacustrine soils range from 603 to 1114 mg kg<sup>-1</sup> and have an average TP concentration of 786 mg kg<sup>-1</sup> (n = 10) [6]. Sediments from Deer Creek Reservoir, about 40 km upstream of Utah Lake, have higher TP concentrations, with average measured values of 1107 mg kg<sup>-1</sup> (n = 12) and 2573 mg kg<sup>-1</sup> (n = 19) [11]. We infer that the high P content of Utah Lake sediment is primarily derived from geologic sources rather than having been precipitated from the water column or settled out from anthropogenic sources. This hypothesis is supported by data that show that the surrounding lacustrine soils and upstream reservoir sediments have similar or higher P concentrations.

### 3.1.4 Nutrient Mass Balance Models

The construction of nutrient mass balance models is a well-established process that offers insight into a lake ecosystem [56, 57]. Mueller [57] lists five general input-output mass balance approaches initially proposed by Vollenweider [56]. In general, mass balance models consist of model inputs

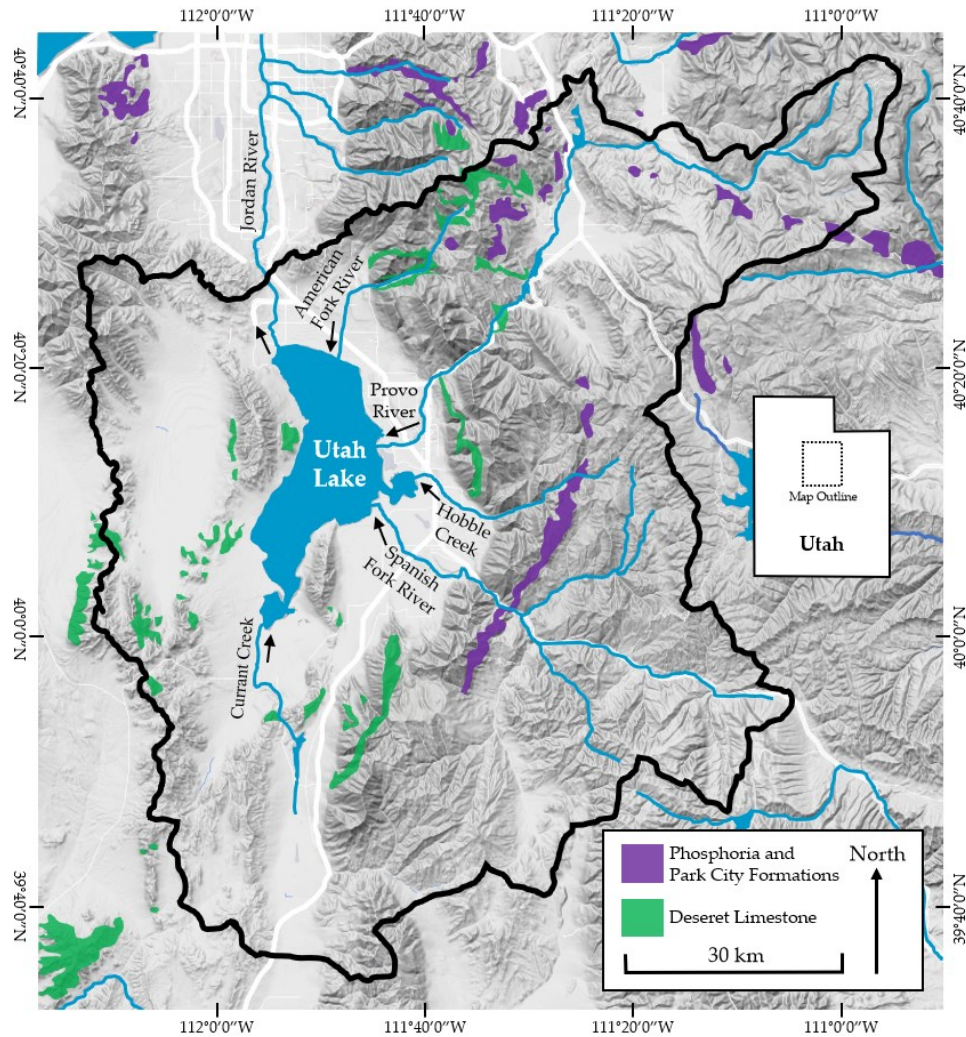


Figure 3.1. Geologic phosphate sources in the Utah Lake Watershed. The phosphate from these outcrops originates primarily from the Meade Peak Member of the Phosphoria and Park City Formations (marked in purple) and the Delle Phosphatic Member of the Deseret Limestone (marked in green) [47-50].

such as point and nonpoint sources, internal sources or sinks, and outflows [56-58]. Model results are used to help manage or understand nutrient sources and predict impacts from changes to nutrient loads or lake processes [56, 59-63].

TP mass balance models have proven useful for characterizing eutrophication and for predicting lake behavior in response to changes in the lake environment [62, 64]. Estimated changes in nutrient concentrations are important considerations for lake restoration as management strategies are often focused on nutrient load reduction [64-68]. Studies on large, shallow, eutrophic lakes worldwide have demonstrated that Utah Lake

and similar lake ecosystems can benefit from nutrient mass balance studies [67, 69-72].

Mueller [57] highlights that one large source of uncertainty in P mass balance models is internal nutrient cycling, i.e., how nutrients are added to or removed from the water column due to sediment-water interactions. As such, studies that account for sediment-water interactions greatly increase the accuracy and value of these models [69, 70, 73]. These models, which included analyses of sediment-water interactions, provided important insight into each lake's potential for P uptake or release by sediments and have been used to guide lake restoration measures.

We did not develop a mass balance model for this study. We instead used historical datasets for lake volume from the Bureau of Reclamation, lake outflow from the Utah Division of Water Rights, and water column P concentrations from the Utah Division of Water Quality to estimate the mass of P in Utah Lake and the Jordan River outflow. We also found that a sorption model can account for the patterns and changes we see in the data. This approach implies that Utah Lake water column concentrations of P are largely insensitive to external loads.

### 3.1.5 Sorption

Sorption is defined as the reversible partitioning of dissolved substances (i.e., solutes) with solid materials (i.e., sorbents) through the processes of adsorption, absorption, or ion exchange. When a solute becomes sorbed, it is called a sorbate. Most sorption can be modeled as an equilibrium process where the dissolved and sorbed concentrations are mathematically related [74]. Because of this equilibrium partitioning, sorption can act as either a sink or a source depending on solute concentrations as the system moves toward equilibrium [75].

In lake systems, P can sorb to clays, amorphous oxyhydroxides, carbonates, and similar materials and be readily desorbed depending on various physical, chemical, and biological conditions within the lake [76]. While sorption processes are not often included in mass balance models, they have been incorporated when sorption has been found to have a significant impact on water column concentrations. To demonstrate the importance of accounting for sorption, van der Salm, et al. [74] evaluated five phosphate models with increasing complexity and found that the model that included sorption was the most accurate. Subsequent work has developed more involved models that include sorption, such as Wang, et al. [75] and Chapra [61].

Sorption can be a dominant process in freshwater systems, making water column concentrations insensitive to other loads. Studies of the Kis-Balaton reservoir system in Hungary found that even though input mass was significantly reduced, the reservoir system exhibited little response

because of nutrient interchange with sediments through sorption processes. Pollman and James [71] developed a mass balance model that included sorption for shallow Lake Okeechobee, Florida, USA. They showed that the sorption model performed better than models that treated sediments as either a sink or a source. This model estimated that P contribution from internal sources exceeded external loads by a factor of 2.6. Research on the Three Gorges Dam, a deep reservoir in China, showed that sorption played a significant role in P-retention, though less interaction with the water column was observed because of the limited soil–water interaction [77].

### 3.1.6 Research Overview

We used datasets collected by state and federal agencies from 1989 to 2023 to estimate internal P mass and associated changes in Utah Lake. Section 3.2.1 describes these datasets in depth, including their source, sampling frequency, statistical descriptions, and general observations. Section 3.2.2 presents the statistical methods and calculations we used to determine the mass of P in the lake and its outflow.

Using the methods outlined in Section 3.2, we present an analysis in Section 3.3 that demonstrates the high variability of lake volume and the estimated P mass in the lake over the study period. We show that this variability in lake mass and volume is in stark contrast to the consistency of DP concentrations over the same time, where we would expect lake volume to be correlated with concentrations. This includes characterizing monthly mass changes in the system. We show that estimated monthly external P loadings to Utah Lake are not large enough to account for the monthly mass changes seen in Utah Lake. We then used a hypothetical sorption model based on data in the literature to show that these trends and changes are consistent with a sorption-dominated system.

Section 3.4 discusses variability in lake volumes and concentrations and the associated implications. We discuss example sorption calculations and show how they explain both the historical data and support the conclusion that water column concentrations are insensitive to external loads. We conclude in Section 3.4 with numerous lines of evidence that all independently imply that Utah Lake water column concentrations are dominated by a sorption system, not external loads.

Section 3.5 summarizes our conclusion that internal P cycling, through sorption processes, is responsible for maintaining elevated P concentrations in Utah Lake despite the presence of other P loads and sinks. This leads to the conclusion that reducing external P sources to the lake, such as WWTP loads, would have a minimal impact on DP concentrations in the water column. We also discuss implications for

similar reservoirs where restoration efforts may be more effective if focused on areas other than nutrient load reduction.

### 3.1.7 Hypothesis

Our hypothesis is that the water column and sediments in Utah Lake behave as a sorption system that is in equilibrium with respect to P. We assumed this hypothesis because Utah Lake is shallow, the water column is well mixed with the sediment, and the sediment has high concentrations of geologic P. If this hypothesis is true, then water column concentrations should be relatively insensitive to changes in nutrient loads or lake volumes. We evaluated this hypothesis using several lines of inquiry. This hypothesis has implications for the management of lakes with similar conditions (i.e., shallow waters that are well mixed with high P sediments) and ultimately means that P load reductions will have minimal impact on water column P concentrations in these types of lakes.

## 3.2 Data and Methods

### 3.2.1 Data Sources and Descriptions

#### 3.2.1.1 Utah Lake Volume

We obtained Utah Lake daily volume data from the Bureau of Reclamation (BOR), which provides data since 1 January 1932 [78]. The BOR uses a rating curve to convert lake elevation to volume.

We used data from 13 July 1989 to 4 August 2023, as this period coincides with the available nutrient data (Figure 3.2). Utah Lake volumes exhibit an annual pattern, with peak volumes in the spring and lows near the end of the summer, though the timing of the peaks and troughs are variable. For example, the peak volume in 2019 occurred on 8 July, while peak volumes for 2018 and 2020 occurred on 15 April and 18 April, respectively (Figure 3.2). The lake also exhibits long-term volume trends. For example, the high volume in 2011 of  $1.3 \times 10^9 \text{ m}^3$  dropped to the low in 2016 of  $1.3 \times 10^8 \text{ m}^3$ , an order of magnitude difference. The peak in 2016 was only  $6.2 \times 10^8 \text{ m}^3$ , a peak-to-peak change of  $6.8 \times 10^8 \text{ m}^3$  in just over 5 years. Similar long-term drops in lake volume appear to be part of a semi-regular wet and dry cycle experienced by the lake.

#### 3.2.1.2 Jordan River Outflow

We obtained Jordan River outflow data from the Utah Division of Water Rights, which has archived data from 1937 to the present [79]. For this study, we used data from 1 January 1989 to 1 July 2023 to coincide with the lake volume and nutrient datasets (Figure 3.3).

Jordan River outflow volumes from Utah Lake are right-skewed, with a mean monthly flow volume of  $2.4 \times 10^7 \text{ m}^3$  and a median flow volume of  $1.9 \times 10^7 \text{ m}^3$ . In most winters, there is little to no flow from November

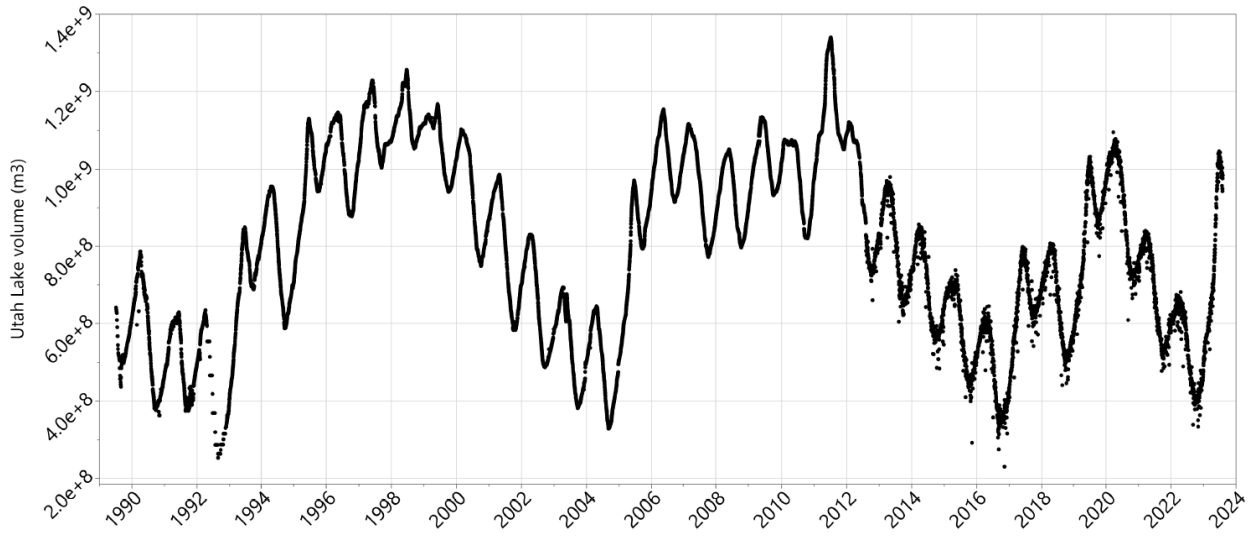


Figure 3.2. Daily Utah Lake volumes in cubic meters ( $\text{m}^3$ ) from 13 July 1989 to 4 August 2023. We assume the data become more variable after 8 August 2012 because of automated measuring systems.

until March (Figures 3.3 and 3.4). For our study period, 20% of the flows are below  $2.5 \times 10^5 \text{ m}^3$ , with no outflow about 10% of the time. During most years, there are no winter releases; however, winter flows occurred from 1997 to 2000 and from 2011 to 2012 during high water years to maintain reservoir levels below the legally required maximum lake elevation [42].

Monthly outflows from Utah Lake are highest in the late spring and early summer months (Figure 3.4). Average flows from June to August are similar. Only a small decrease in flows is observed during May and September (Figure 3.4). Median flows (the notches in Figure 3.4) show more variation, with July having the highest outflows, while June and August are similar, and May and September have noticeably lower median outflows. Spring flows, which occur from March to May, are variable, with low-water years having small releases and wet years having large releases.

### 3.2.1.3 Phosphorus Concentrations

We obtained P concentration data from the Ambient Water Quality Management System (AWQMS) database provided by the Utah Department of Environmental Quality [32]. We accessed the AWQMS website in the fall of 2023. We searched for all measurements that included “Utah Lake” in the location field, then excluded samples from the marinas because they are not representative of the lake body and generally exhibit higher concentrations. We also excluded samples labeled as “field blanks” or “duplicates”. We included samples labeled as “surface” or “water column” as our goal was to estimate the average concentration of P in the lake. This yielded 3269 samples collected from 31 August 1978 to

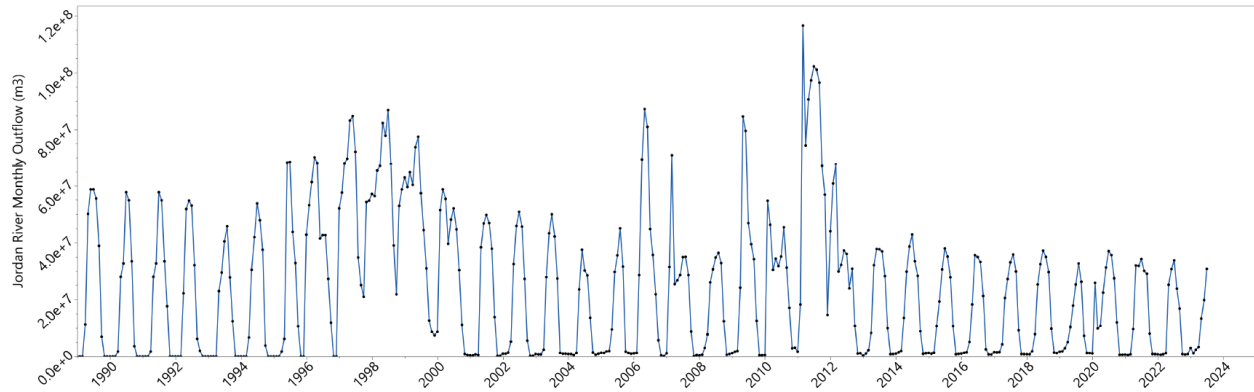


Figure 3.3. Jordan River outflow volumes in cubic meters ( $\text{m}^3$ ) reported as cumulative monthly volumes from 1 January 1989 to 1 July 2023.

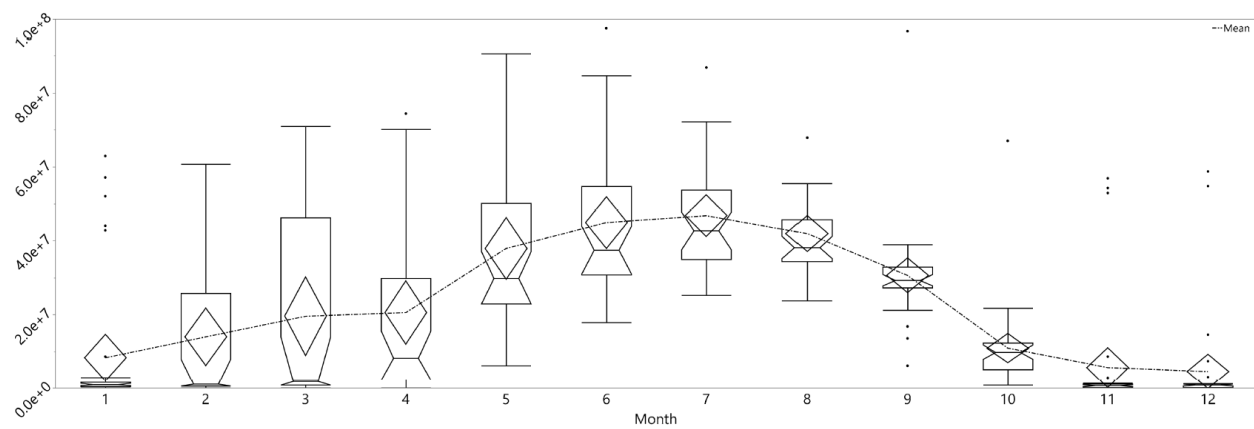


Figure 3.4. Distribution of Jordan River outflow volumes by month in cubic meters ( $\text{m}^3$ ) from 1 January 1989 to 1 July 2023. Mean values are shown by the diamonds, with the diamond's extent equal to the 95% certainty range. The median is shown by the notch, and the box ends are the 25th and 75th percentiles. The whiskers extend to 1.5 times the interquartile range. The mean monthly values are connected by the dashed line.

20 September 2022. The sampling frequency has continually increased with time. There are only two samples in 1978, and the next samples are from 11 July 1989, so our effective data timeline runs from 1989 to 2023.

The AWQMS measurements represent two fractions, TP and DP, which were measured using three different methods described as “Orthophosphate”, “Phosphate\_mixed”, and “Phosphate\_retired”. The “Phosphate\_retired” method was used from the beginning of the dataset until 15 September 2021; after that time, the reference switched to the “Phosphate\_mixed” method until the end of the dataset. There is no overlap in time between the two methods. Measurements with the method labeled “Orthophosphate” are only available after 23 September 2020.

For this study, we used DP values and included the data from all three methods, resulting in a usable sample size of 1658 samples, as approximately half of the original P samples were for TP concentrations. We did not use TP data because TP includes non-sorbed P associated with suspended solids, and we are interested in P available for sorption. DP is the portion of P that is related to the P sorbed onto solids, both suspended and in the sediment. This means that TP values include P sorbed onto the suspended sediments, while DP values characterize the P dissolved in the water column.

Figure 3.5 shows both the sample locations and the number of P sample measurements available in the AWQMS database. Panel A (left) summarizes the location and number of all the P samples, both TP and DP. Panel B (right) presents the DP samples we used in our analysis. The map

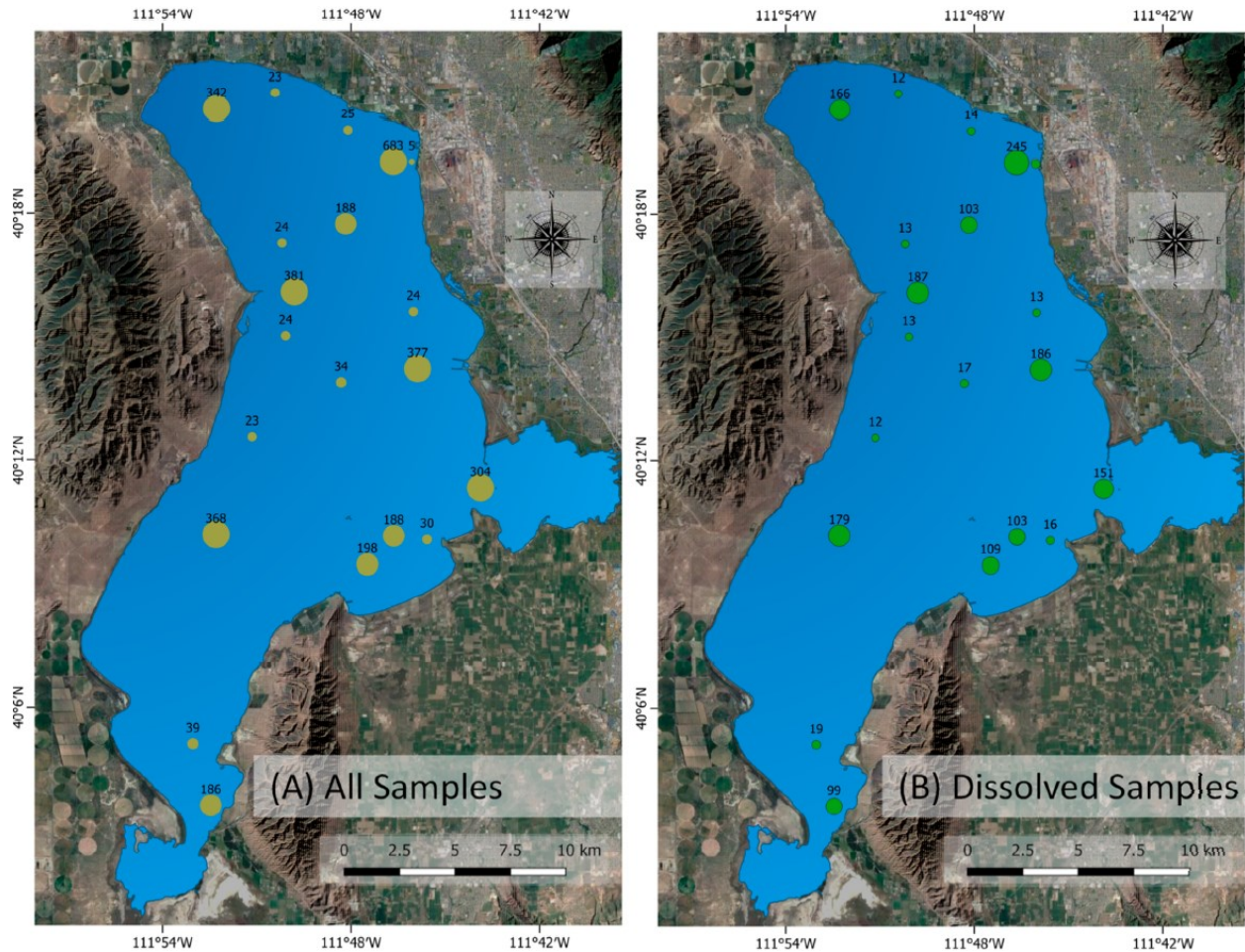


Figure 3.5. Locations and number of phosphate samples available from the AWQMS database. The figure shows all 3466 P (both total and dissolved) samples shown as brown dots (panel A) on the left, and 1658 dissolved P (DP) measurements shown as green dots (panel B) on the right.

shows that the samples are spatially distributed, and these data should provide a representative overview of lake conditions. Many of the larger clusters of samples are near WWTP discharges, so the data are skewed towards these areas and may be slightly higher than average lake conditions. This represents a conservative assumption. There are a large number of samples in the northwest corner of the lake near the Jordan River outfall, presumably to represent outflow concentrations. The cluster of 245 samples and a nearby single sample in the northeast corner close to shore is approximately 1500 m directly south of the outfall for Timpanogos Special Service District, the largest WWTP that discharges to Utah Lake. The single sample is about the same distance south but approximately 750 m to the east, closer to the shoreline. There is a large cluster of 186 samples directly west of Provo Harbor near the discharge point of the Provo River and the outfall from the Orem WWTP. There is also a cluster of 151 measurements at the mouth of Provo Bay, on the east side of the lake. The Provo City WWTP discharges into Provo Bay.

Table 3.1. A list of sampling locations and IDs for Utah Lake P data from the AWQMS database.

Location ID	Location Name
4917770	Utah Lake Outside Entrance to Provo Bay
4917380	Utah Lake 0.5 mi S of American Fork Boat Harbor #14
4917310	Utah Lake 0.5 mi W of Geneva Discharge #15-A
4917320	Utah Lake 0.5 mi W of Geneva Discharge #15-A Replicate Of 4917310
4917530	Utah Lake 0.7 mi East of Pelican Point
4917370	Utah Lake 1 mi East of Pelican Point
4917710	Utah Lake 1 mi NE of Lincoln Point #03
4917410	Utah Lake 1 mi NE of Pelican Point #10
4917420	Utah Lake 1 mi SE of Pelican Point #09
4917390	Utah Lake 1 mi West of Provo Boat Harbor
4917715	Utah Lake 1 mile Southeast of Bird Island
4917400	Utah Lake 1.5 mi NW of Provo Boat Harbor #16
4917520	Utah Lake 2 mi E of Saratoga Springs #12
4917365	Utah Lake 2 miles West of Vineyard
4917700	Utah Lake 2.5 mi NE of Lincoln Point #02
4917500	Utah Lake 3 mi W/NW of Lincoln Beach
4917300	Utah Lake 300 ft Offshore from Geneva Steel
4917510	Utah Lake 4 mi E of Saratoga Springs #11
4917330	Utah Lake 5mi N/NW Of Lincoln Beach/1 mi Offshore
4917620	Utah Lake Goshen Bay Midway Off Main Point On East Shore
4917600	Utah Lake Goshen Bay Southwest End
4917340	Utah Lake W of Provo Boat Harbor/6 mi N Of Lincoln Beach #08

Figure 3.6 shows the 1658 DP measurements used in this study. There are four points with anomalously high values, one point in 1989 and three points in 1991, with values of 1.42, 0.85, 0.60, and 0.59 mg L<sup>-1</sup>, respectively, which are not included in the plot as they compress the scale. While these excluded measurements appear to be outliers, we included them in the analysis presented in this study. Figure 3.6 shows that no data, except the four excluded measurements, have values above 0.21 mg L<sup>-1</sup>.

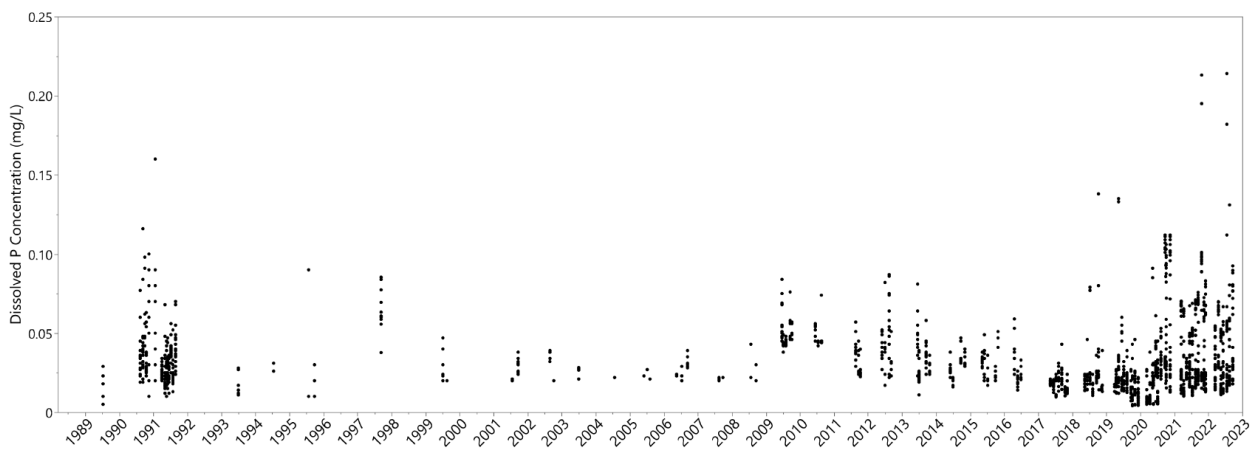


Figure 3.6. Dissolved P (DP) concentrations in Utah Lake from 1989 to 2022.

### 3.2.2 Analysis Methods

#### 3.2.2.1 Statistical Analyses

We evaluated the variability of both lake volumes and P concentrations using standard analytical techniques and plots. To compare different data groups or times, we used analysis of means (ANOM) and the Tukey–Kramer test as implemented in JMP Pro 17® [80, 81]. We grouped data by both month and year and compared the distributions of the population for a given year or month to the distribution of the entire data population over the study period using ANOM. We also performed pair-wise comparisons using the Tukey–Kramer test. We present the ANOM results using plots in which the annual mean is plotted along with the upper and lower decision boundaries for that time period. These plots graphically show the relative similarities between the annual mean and the population mean. We present the Tukey–Kramer results of connected letter reports in tables.

#### 3.2.2.2 Phosphorus Mass Calculations

We computed DP mass in Utah Lake at any specific time as follows:

$$M_{Lake} = C_P V_L C_f \quad (3.1)$$

where  $M_{Lake}$  is the mass of DP in the lake in kg,  $C_P$  is the concentration of DP in the lake in mg L<sup>-1</sup>, and  $V_L$  is the lake volume in m<sup>3</sup> all at a point in time.  $C_f$  is a conversion factor defined as follows:

$$C_f = C_P \left( \frac{mg}{L} \right) V_L (m^3) \left( \frac{1000}{m^3} \right) \times \left( \frac{kg}{10^6 mg} \right) C_f = 10^{-3} \frac{L \, kg}{m^3 \, mg}$$

We computed  $M_{out}$ , which is the mass of DP leaving Utah Lake via the Jordan River outflow, using the same equations, assuming that the DP concentration in the outflow was the same concentration as the overall lake (which we show to be valid in Section 3.3.2.3) and that the volume of the outflow ( $V_{out}$ ) was the total volume (m<sup>3</sup>) released during the examined time period—typically on a monthly basis.

We computed the mass of DP removed from the lake via the Jordan River as follows:

$$M_{out} = C_P C_f V_{out} \quad (3.2)$$

where  $V_{out}$  is the volume of water that flows out of Utah Lake (m<sup>3</sup>), and  $M_{out}$  is the mass of P removed (kg) from the lake via the Jordan River over the time period.

We evaluated monthly mass changes in the lake using a simple mass balance approach:

$$M_{Lake} = M_{in} - M_{out} \quad (3.3)$$

where  $M_{Lake}$  is the mass of DP in Utah Lake,  $M_{in}$  represents the cumulative DP load from all sources or sinks except the Jordan River over a given time period, and  $M_{out}$  is the amount of DP removed by the Jordan River over the same period. This means that  $M_{in}$  includes or accounts for all other P sinks or sources. External sources for Min include WWTP effluent, tributary inflows, nonpoint sources, atmospheric deposition, and groundwater. Internal fluxes for  $M_{in}$  include precipitation and sedimentation from the water column (which removes DP mass from the lake), and release from the sediment (which increases DP mass in the lake), as well as any other sources or sinks, including sorption (which can act as either a sink or a source depending on the relative concentration of P in the water column and the sediment).

We computed the change in mass for each month by subtracting the mass at the beginning of the previous month from the mass at the beginning of each given month for both the lake,  $M_{Lake}$  and the mass removed by the Jordan River over the month,  $M_{out}$ , as follows:

$$\Delta M_{in} = \Delta M_{Lake} + \Delta M_{out} \quad (3.4)$$

where  $\Delta$  represents the monthly change in the mass in any compartment over the study period.

We estimated the DP concentration at the beginning of each month,  $C_P$ , by interpolating the measured values using the pandas python library with the PCHIP spline interpolation method, which eliminates over and undershoots [82]. On days with multiple measurements, we used either the daily mean or the median values, resulting in two different interpolated values of  $C_P$ . We term these resulting monthly values  $C_{P\text{avg}}$  and  $C_{P\text{med}}$  for interpolated values using the mean or the median, which is shown in Figure 3.7 as blue or black lines, respectively. The y-axis is limited to 0.5 mg L<sup>-1</sup>; therefore, the four large measurements in 1989 and 1991 that are shown in Figure 3.6 are off-scale. These measurements affect the mean values, with their influence being shown by large spikes in the blue line for these two years; however, they have less impact on the median values. A similar case occurs in 2021 and 2022, as shown in Figure 3.7B, where large, isolated values affect the mean but have less impact on the median. The interpolation based on daily median values, the black line, does not show these large excursions.

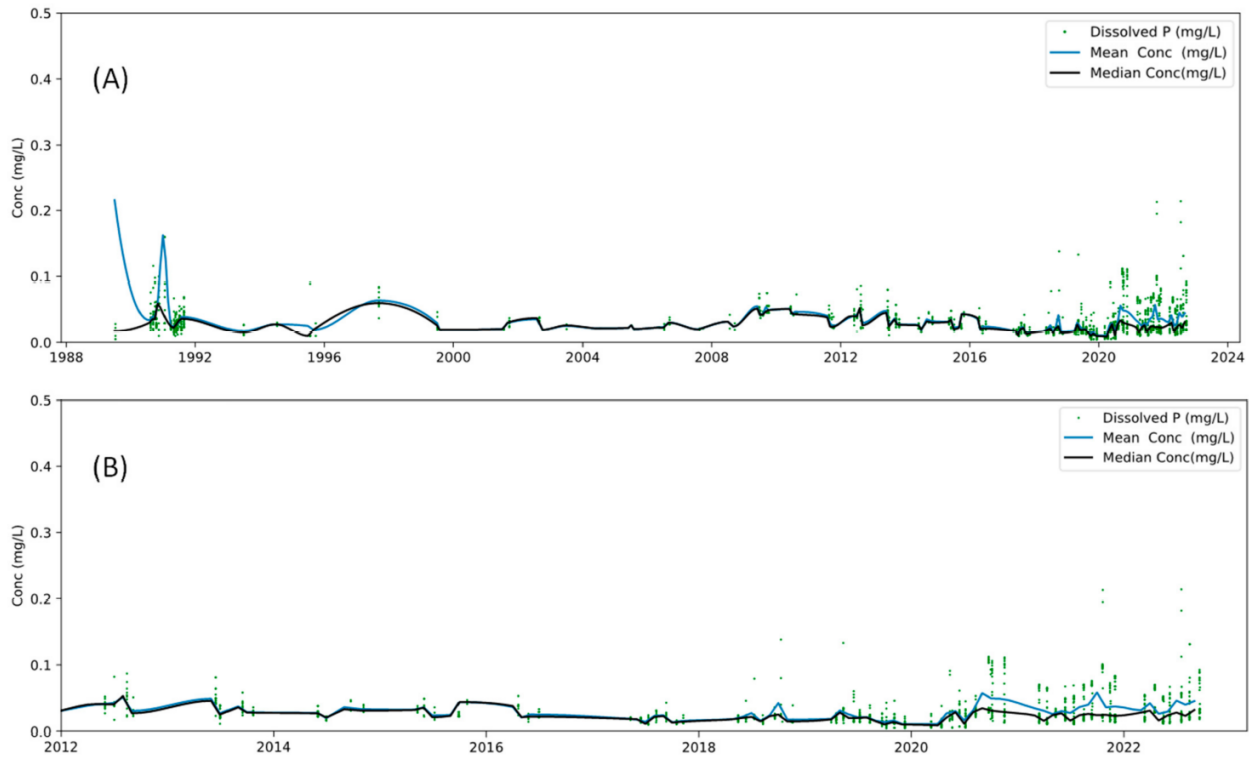


Figure 3.7. Interpolated dissolved P (DP) concentrations in Utah Lake based on either the mean or median values measured on the same day. The top (panel A) shows the entire study period, and the bottom (panel B) shows details from 2012 to 2023.

P samples were usually only taken in the summer months for most of the study period, but since about 2019, the sampling frequency has increased to include the majority of the year (Figures 3.6 and 3.7). For most of our analyses, we used interpolated values based on the median concentrations, though we occasionally reference interpolated values based on the mean concentrations.

We used measured daily values for lake volume at the beginning of each month and the interpolated monthly lake concentrations to compute the mass of DP at the start of each month. We used the month-to-month difference in DP mass to compute the change in in-lake DP mass,  $\Delta M_{Lake}$ . The Jordan River outflow data provide monthly volume release measurements. We multiplied these measured volumes by the interpolated concentrations at the beginning of each month to estimate the change in outflow mass,  $\Delta M_{out}$ . We computed the cumulative mass of DP into the lake during the month,  $\Delta M_{in}$ , according to Equation 3.4.

Figure 3.8 presents the annual mean DP value for each year, with dots representing each measurement and bars showing the interquartile range. This graph shows that the mean DP concentration has not varied significantly over the study period. The one larger mean value in 1997 of about  $0.06 \text{ mg L}^{-1}$  is based on 12 measurements that were mostly taken in July. The remaining annual mean values are all below  $0.05 \text{ mg L}^{-1}$ , with most below  $0.04 \text{ mg L}^{-1}$ .

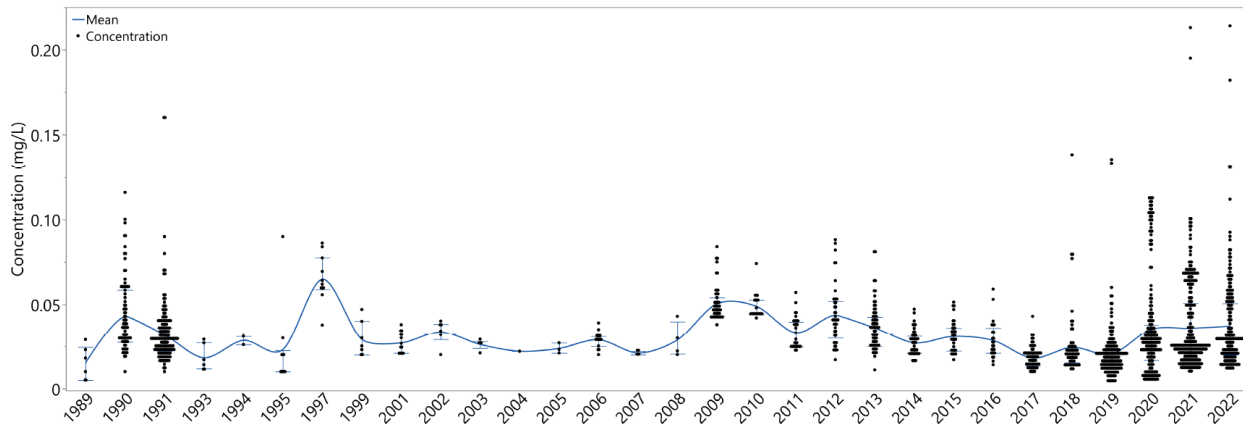


Figure 3.8. Dissolved P (DP) concentrations in Utah Lake from 1989 to 2022 grouped by year, with a line connecting the mean annual value and the bars showing the interquartile range. One point in 1989 and three points in 1991, with values of 1.42, 0.85, 0.60, and  $0.59 \text{ mg L}^{-1}$ , respectively, are not shown on the graph.

#### 3.2.2.3. Sorption Calculations

In addition to our phosphorus mass calculations, we also performed sorption calculations using data from the literature to demonstrate how sorption could impact water column P concentrations in Utah Lake.

Equilibrium-based sorption models, such as Freundlich or Langmuir models, can be used to mathematically define the concentration ratio of solutes and sorbates [77]. These models are called isotherm models, as sorption processes are temperature-dependent. While isotherm models are helpful for describing and predicting sorption activity, they do not define the specific reaction mechanisms that occur during a sorption event. Rather, they provide a simplified model that characterizes the relationship between concentrations in the solid and liquid phases [83].

We used the Freundlich model for example calculations as it is the simplest model and is generally accurate over concentration ranges found in reservoirs. The Freundlich model is defined as follows:

$$C_{solid} = K_d C_{liq}^{1/n} \quad (3.5)$$

where  $C_{solids}$  is the concentration in the solids or sediment ( $\text{mg kg}^{-1}$ ),  $C_{liq}$  is the concentration in the liquid ( $\text{mg L}^{-1}$ ),  $K_d$  is a fitted constant called the distribution coefficient, and  $n$  is the correction factor for non-linear relationships. When  $n$  is 1,  $K_d$  is the slope of the isotherm [77, 84].

### 3.3 Results

#### 3.3.1 Lake Volume Variability

##### 3.3.1.1 Volume Annual Variability

Utah Lake volumes are quite variable when compared to the variation in DP concentration, both on an annual and longer-term scale. The change in average Utah Lake volumes ranged from approximately  $4 \times 10^8 \text{ m}^3$  in 1997 to  $1 \times 10^9 \text{ m}^3$  in 1998 and 2011 (Figures 3.2 and 3.9). The one-year change from the lowest volume in 2004 to the highest in 2005 ( $6.4 \times 10^8 \text{ m}^3$ ) is even larger, as the reservoir started filling in early autumn of 2004, with the low of  $3.3 \times 10^8 \text{ m}^3$  occurring on 15 September 2004 and the high of  $9.7 \times 10^8 \text{ m}^3$  occurring on 28 June 2005. Utah Lake volumes show changes over longer terms (Figures 3.2 and 3.9) as well. The lowest-volume period in our data occurred in 1992, and the highest occurred in 2011. Additionally, annual mean volumes exhibited approximately 10-year trends of increasing and decreasing volumes (Figures 3.9 and 3.10). Monthly volume variation (Figure 3.11) shows that lake average volumes peak in May, but in any given month, the lake volume is quite variable, with historical peak volumes in any month, including those with the lowest average volume, being higher than the May average. The effect of climatic conditions can be seen in the longer-term trends; wet and dry cycles are reflected in lake storage patterns (Figure 3.9).

An ANOM analysis of average lake volumes grouped by year (Figure 3.10) shows that, with few exceptions, annual lake mean volumes are significantly different from the average lake volume over the study period

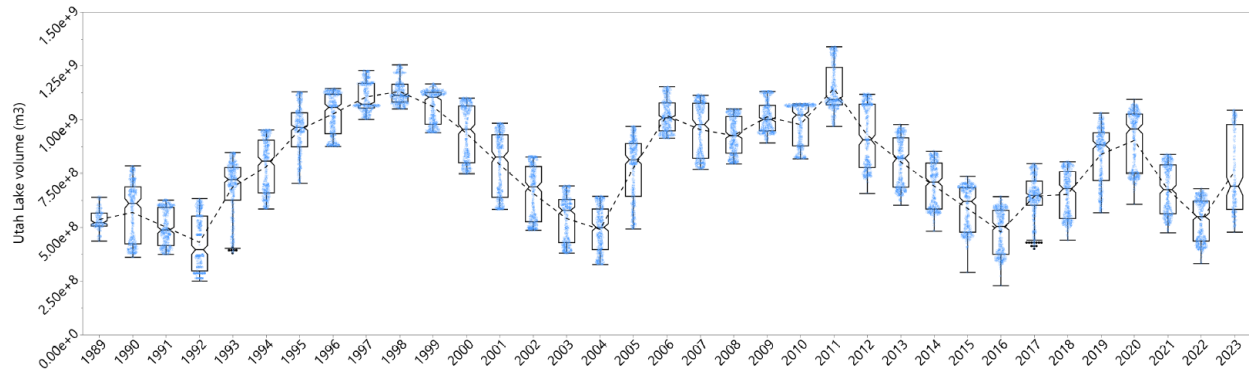


Figure 3.9. Annual distributions of Utah Lake volume (m<sup>3</sup>) from 13 July 1989 to 4 August 2023 with box plots showing the distribution and blue dots representing all individual values. The dashed line connects the mean values for each year, and the notches in the boxes represent the median values.

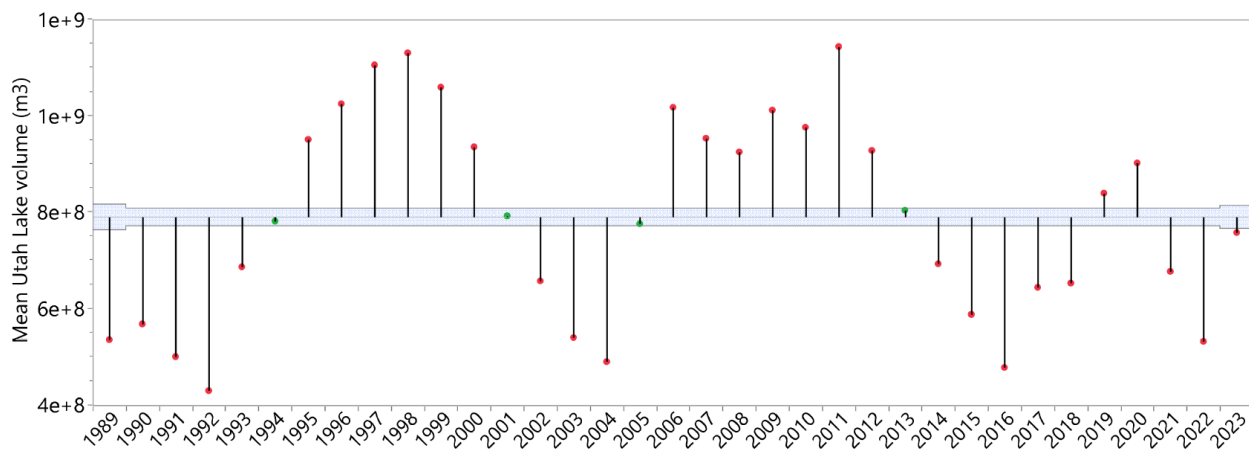


Figure 3.10. Analysis of means (ANOM) results of Utah Lake volume data grouped by year. The plot includes the mean for each year (green or red dots) and the blue decision region, bounded by the lower and upper decision boundaries, LDL and UDL, respectively, which represents the area where differences are not statistically significant at the p = 0.05 level. This shows that the majority of mean values for the majority of years are statistically significantly different from the mean for the entire population.

at the p = 0.05 level. This is in sharp contrast to mean DP concentrations, which, at a significance level of p = 0.05, are only statistically different from the population mean for a very small number of years, and those that are different are relatively close to the decision boundary (Figure 3.12). Thirty-one of the thirty-five average annual lake volumes are well outside the decision boundary. The four years in which the annual average lake

volume is not significantly different from the population mean, 1994, 2001, 2005, and 2013, appear to be the result of a regular cycle in lake volumes, which go from below the average to above the average in those four years.

### 3.3.1.2 Volume Monthly Variability

Figure 3.11 shows the distribution of monthly volumes over the ~34-year study period. Monthly volumes generally peak in May but can peak as late as July (Figure 3.11). These volumes exhibit large variations. Lake volumes in May range from about  $4 \times 10^8 \text{ m}^3$  to  $1.3 \times 10^9 \text{ m}^3$ , a difference of  $9 \times 10^8 \text{ m}^3$ . The lake is generally at its lowest point in September or October, after which the lake gradually fills again. While these are the general trends, Figures 3.9 and 3.11 show that any given year can vary considerably, with peak monthly values in any given month exceeding the peak average value in May.

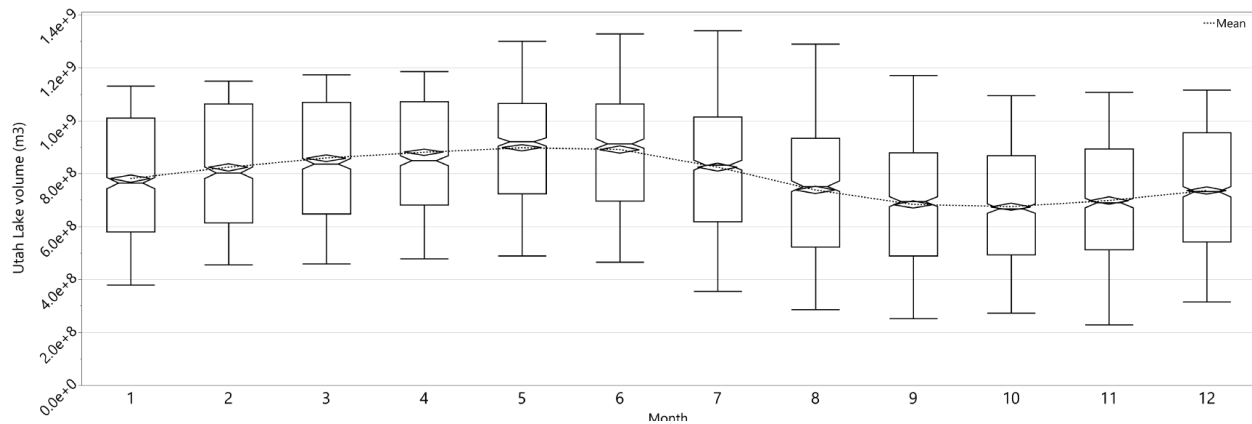


Figure 3.11. Monthly distributions of Utah Lake volumes in cubic meters (m<sup>3</sup>). However, for the average peaks in May, the volumes are quite variable, with peak volumes in any month higher than the June average.

### 3.3.2 Phosphorus Concentration Variability

#### 3.3.2.1 Phosphorus Concentration Annual Variability

Figure 3.8 shows the 1658 measurements of DP grouped by year, with the solid line connecting the annual mean value and the whiskers showing the interquartile range. The data show little variation in DP concentration over the period, with the annual means ranging from approximately 0.02 to 0.06 mg L<sup>-1</sup>. In the initial years of 1990 to 1991 and the later years of 2018 to 2022, more of the data fall outside the interquartile range, but the interquartile ranges in these years are not significantly larger than in other years. The data show little trend, with a high in 1997. There is a slight decreasing trend from 2009 to 2019, then a slight increase from 2019 to 2020, after which mean annual concentrations have remained steady.

If we group DP concentrations by year, the annual mean values show a relatively narrow range from  $0.015 \text{ mg L}^{-1}$  to  $0.064 \text{ mg L}^{-1}$ , which occurred in 1989 and 1997, respectively (Figures 3.8 and 3.12). We used both the analysis of means (ANOM) and the Tukey–Kramer test to determine how similar each year is to each other.

Except for 1997, the annual mean values are not statistically different from the mean of the entire dataset at the  $p = 0.05$  level, though in several years (1990, 2009, 2010, 2012, and 2017–2019), the mean value for the year is slightly outside the ANOM decision boundary (Figure 3.8). While variation can be observed across the different years of our study period, that variation is either statistically insignificant (with the exception of 1997) or only slightly outside the decision boundaries.

The results from the pair-wise Tukey–Kramer test are presented in Table 3.2. This table orders the years based on the mean value from largest to smallest. If two years share a letter, then they are not statistically different. For example, 2002 has all seven letters assigned (A, B, C, D, E, F, G), indicating that it is not significantly different from any other year. The years 2017 and 2019, which only have the letter G assigned, are significantly different from years without a ‘G’, such as 1997.

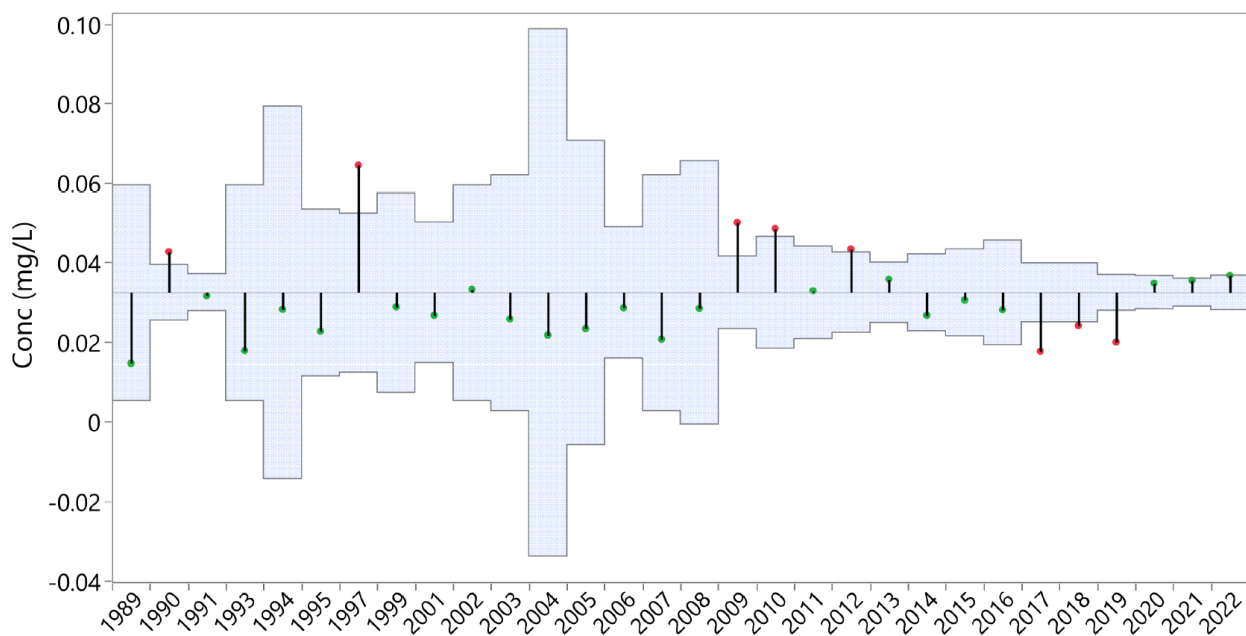


Figure 3.12. Analysis of means (ANOM) results on Utah Lake dissolved P (DP) concentration data grouped by year. The plot includes the mean for each year (green or red dots) and the blue region, bounded by the lower and upper decision boundaries, LDL and UDL, respectively, which represents the area where differences are not statistically significant at the  $p = 0.05$  level. The boundary locations are based on the number of samples in each year.

Table 3.2. Tukey–Kramer pair-wise connecting letter report for annual means.

Year	Connecting Letter							Mean	Year	Connecting Letter							Mean
1997	A							0.065	2008	A	B	C	D	E	F	G	0.029
2009	A	B						0.050	1994	A	B	C	D	E	F	G	0.029
2010	A	B	C	D				0.049	2016		C	D	E	F	G	0.028	
2012	A	B	C	D	E			0.044	2001		B	C	D	E	F	G	0.027
1990	A	B	C					0.043	2014			E	F	G		0.027	
2022		C	D	E				0.037	2003	A	B	C	D	E	F	G	0.026
2013		B	C	D	E	F		0.036	2018					F	G	0.024	
2021		C	D	E				0.036	2005	A	B	C	D	E	F	G	0.024
2020		C	D	E				0.035	1995		B	C	D	E	F	G	0.023
2002	A	B	C	D	E	F	G	0.034	2004	A	B	C	D	E	F	G	0.022
2011		B	C	D	E	F	G	0.033	2007		B	C	D	E	F	G	0.021
1991			D	E	F			0.032	2019						G	0.020	
2015			C	D	E	F	G	0.031	1993		B	C	D	E	F	G	0.018
1999	A	B	C	D	E	F	G	0.029	2017						G	0.018	
2006		B	C	D	E	F	G	0.029	1989		C	D	E	F	G	0.015	

Note: levels not connected by the same letter are significantly different.

The significance of a difference in mean value depends on several parameters, including the mean value itself, the variability of the data in that year, and the number of samples.

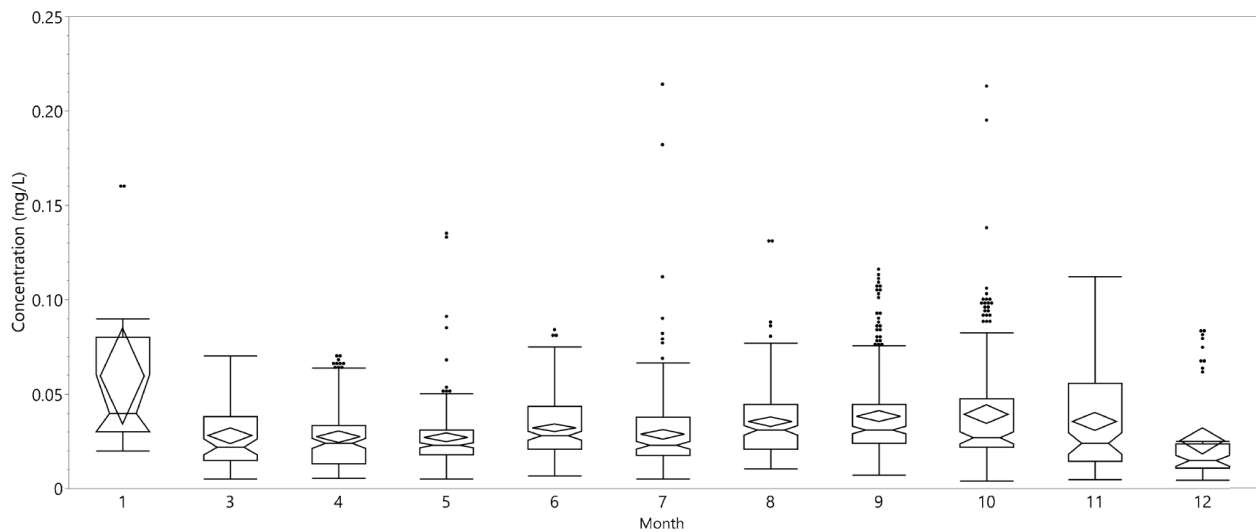


Figure 3.13. Distribution of Utah Lake dissolved P (DP) concentration by month. Mean values are shown by the diamonds, with the diamond's extent equal to the 95% certainty range. The median is shown by the notch, with the box ends at the 25th and 75th percentiles. The whiskers extend to 1.5 times the interquartile range. Dots represent every measurement with values outside 1.5 times the interquartile range.

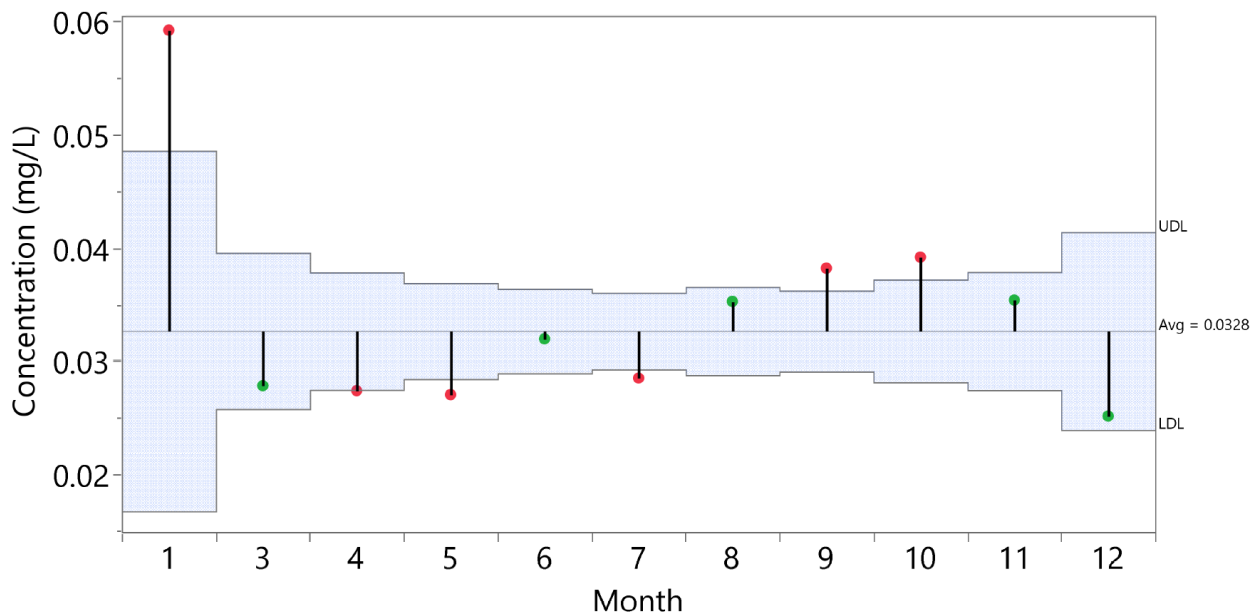


Figure 3.14. ANOM analysis of Utah Lake monthly dissolved P (DP) mean values. The plot includes the mean for each month (green or red dots) and the blue region, bounded by the lower and upper decision boundaries, LDL and UDL, respectively, which represents the area where differences are not statistically significant at the  $p = 0.05$  level. The boundary locations are based on the number of samples in each month.

### *3.3.2.2 Phosphorus Concentration Monthly Variability*

Monthly P concentrations show a pattern of slightly higher average values in the fall and slightly lower average values in the spring, though the observed changes are not large (Figure 3.13). In Figure 3.14, the highest mean DP value is reported in January, but we only have a limited number of January samples, all of which were collected in 1991, so this value is not as representative of typical lake conditions as the DP values reported in other months (Figure 3.8).

If we group DP concentrations by month, the monthly mean values range from  $0.025 \text{ mg L}^{-1}$  to  $0.059 \text{ mg L}^{-1}$  for December and January, respectively (Figure 3.14), falling in a relatively narrow range. ANOM analysis reveals a sinusoidal pattern, with higher values in the fall and lower values in the spring. We believe that the January value is an outlier since we only have a few measurements that were collected in January. Figure 3.14 supports this assertion with the large decision boundary (blue area), which is based on the number of samples. While there is variation in the monthly means, the variation is not large. Most monthly means that are significantly different from the population mean are only slightly outside the decision boundary (Figure 3.14).

The results from the pair-wise Tukey-Kramer test are presented in Table 3.3. The months are ordered by mean value from largest to smallest. January is significantly different from all the other months, while most other months are similar. The letters generally align with the calendar, with the 'B' group being the fall months, the 'C' group being the late summer through early fall, and the 'F' group being the late spring through early summer. Groups 'D' and 'E' represent transition periods and include months throughout the calendar year. While there is an annual sinusoidal pattern, the monthly data have relatively similar concentration values.

Table 3.3. Tukey-Kramer pair-wise connecting letter report for monthly means.

Month	Connected Letters					Mean	
1	A					0.059	
10		B				0.039	
9		B	C			0.038	
11		B	C	D	E	0.036	
8		B	C		E	0.035	
6			C	D	E	F	0.032
7				D		F	0.029
3				D	E	F	0.028
4				D		F	0.028
5						F	0.027
12				D	E	F	0.025

Note: levels not connected by the same letter are significantly different from each other.

### 3.3.2.3 Phosphorus Concentration Variability by Location

In Figure 3.15, the DP measurements are grouped by location; the measurement locations are designated by the number codes assigned to them in the AWQMS records. This figure shows that the distribution of DP concentrations is similar for all the measurement locations. The 4917300 and 4917530 locations only have a single measurement. To examine the spatial distribution data, both the analysis of means (ANOM) and the pair-wise Tukey-Kramer test showed that there is no statistically significant difference in the means at the different locations at the  $p = 0.05$  level either from the entire population (ANOM) or individual pairs (Tukey-Kramer).

Figure 3.16 presents the results of the ANOM test, which shows that the mean value for site 4917770 of  $0.0385 \text{ mg L}^{-1}$  slightly exceeds the upper decision limit. The ANOM plot presents the mean value for the data at each location (green or red dot), the mean of the entire dataset (horizontal line), and the upper and lower decision boundaries at the  $p = 0.05$  level (LDL and UDL, respectively). The plot shows that, except for site 4917770, the means for each site are well within the decision boundaries. Site 4917770 is located at the mouth of Provo Bay and experiences more algal blooms than the rest of the lake [30, 85]. The high values for site 4917770 (Figure 3.15) occurred

in 2021 and 2022 and are visual outliers (Figure 3.8). While site 4917770 is slightly different based on the ANOM analysis, there is no statistically significant difference at the  $p = 0.05$  level, with the Tukey–Kramer test using pair-wise comparisons with all the other locations. This implies that we can treat the lake samples as a single distribution that characterizes the lake spatially.

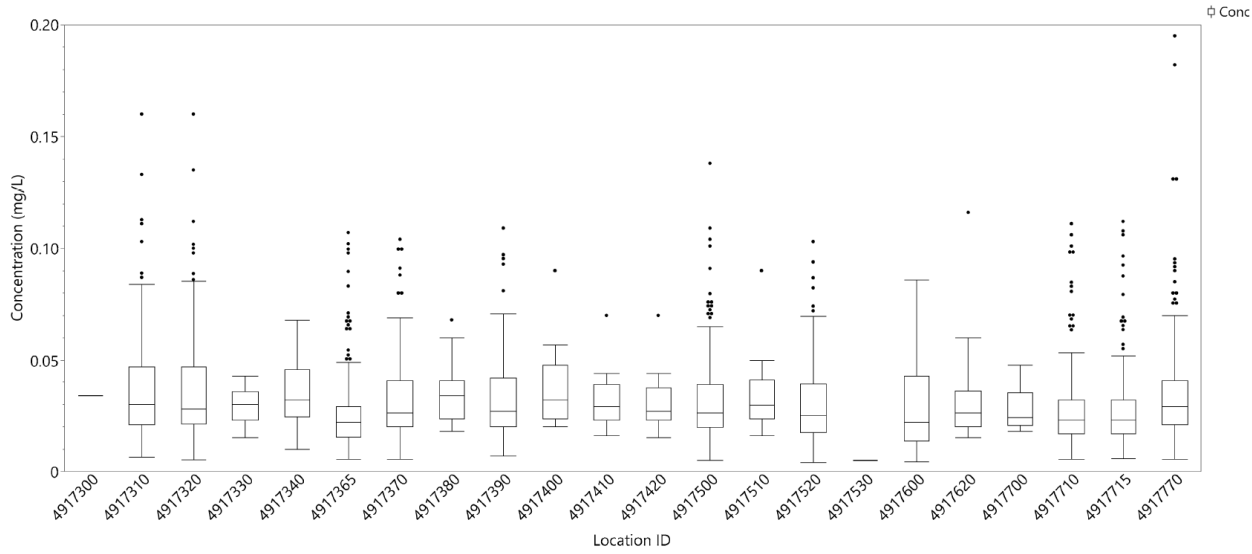


Figure 3.15. Utah Lake dissolved P (DP) concentrations sorted by measurement location ID. The median is shown by the line dividing each box, with the box ends at the 25th and 75th percentiles. The whiskers extend to 1.5 times the interquartile range. Dots represent every measurement with values outside 1.5 times the interquartile range. See Table 3.1 for a list of which ID numbers are assigned to each sampling location.

### 3.3.3 Phosphorous Outflow—Jordan River

We estimated the monthly outflow of DP in the Jordan River using Equation 3.2. Figure 3.3 shows that the Jordan River often has no outflows in winter months. This is reflected in Figure 3.17, where mass outflows are zero in most winter months. Figure 3.18 presents both the monthly mass of DP ( $t$ ) removed by the Jordan River as blue and the total mass of DP ( $t$ ) in Utah Lake as gray.

DP mass outflows in the Jordan River (Figure 3.17) for the 113 months in which we have measurements are slightly right skewed with mean and median values of 0.90 and 0.77 t, respectively. These statistics include only a few winter months, where outflows are generally zero, and the measured DP values are infrequent, so actual mean and median values are likely lower with a larger skew. We did not include months where we had no concentration measurements, and if we had concentration data but the

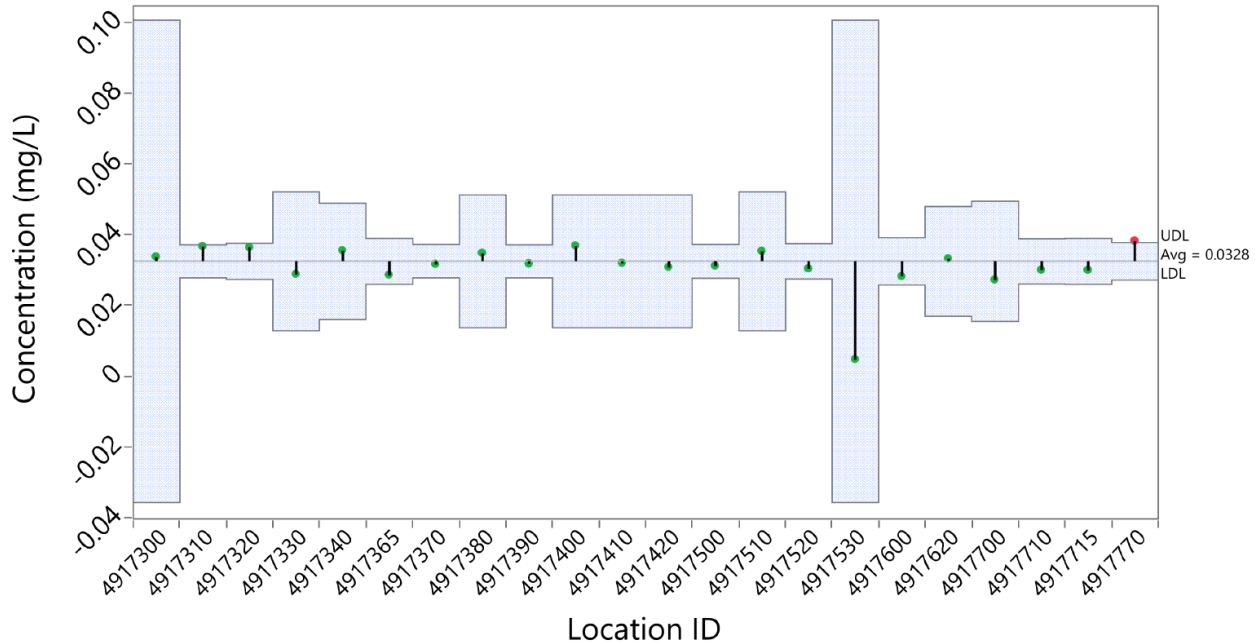


Figure 3.16. Analysis of means (ANOM) report for the 22 different Utah Lake sampling sites. The plot includes the mean for each site (green or red dots), the blue region, bounded by the lower and upper decision boundaries, LDL and UDL, respectively, represents the area where differences are not statistically significant at the  $p = 0.05$  level. The boundary locations are based on the number of samples at each location.

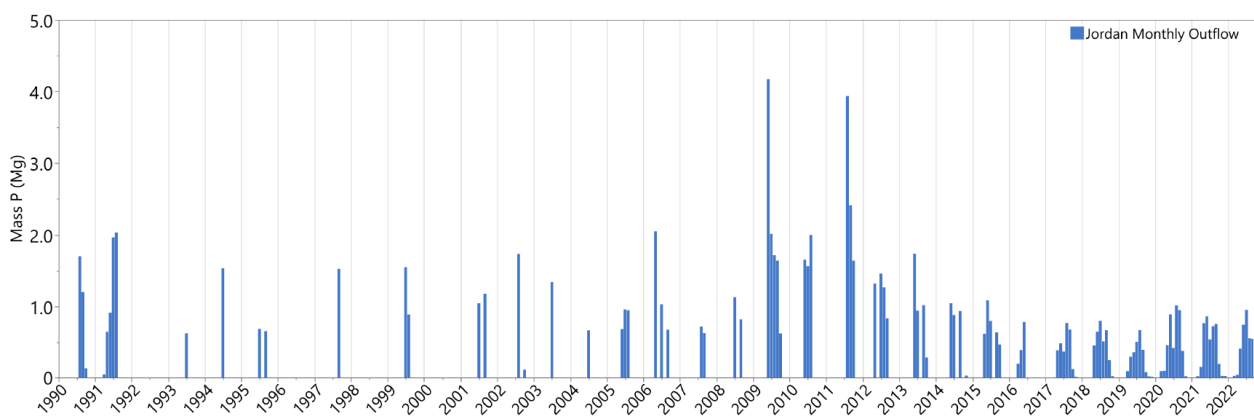


Figure 3.17. Monthly mass outflow (Mg or t) of Utah Lake dissolved P (DP) in the Jordan River for months in which we have measured data. We have flow data every month but limited concentration data. Large mass outflows correspond to large outflow volumes as the concentrations are relatively constant.

flow was zero, we still included the data. DP mass outflows correspond to volumetric outflows (Figure 3.3), as the concentrations are relatively constant.

DP mass outflow is correlated with the mass of P in Utah Lake (Figure 3.19), as volumetric outflows are larger in years when the lake is full. The monthly DP mass outflow is 2.5% of the mean lake DP mass and 3% of the

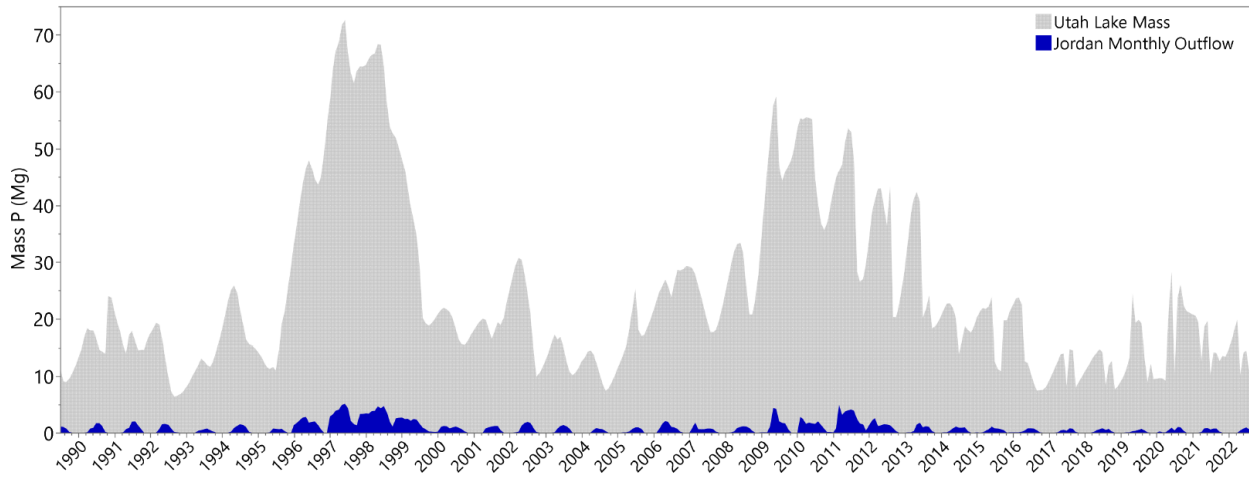


Figure 3.18. Monthly mass outflow (Mg or t) of Utah Lake dissolved P (DP) in the Jordan River as blue, with the total mass of P in Utah Lake as gray. These data use interpolated P concentrations to compute mass estimates in months with no data.

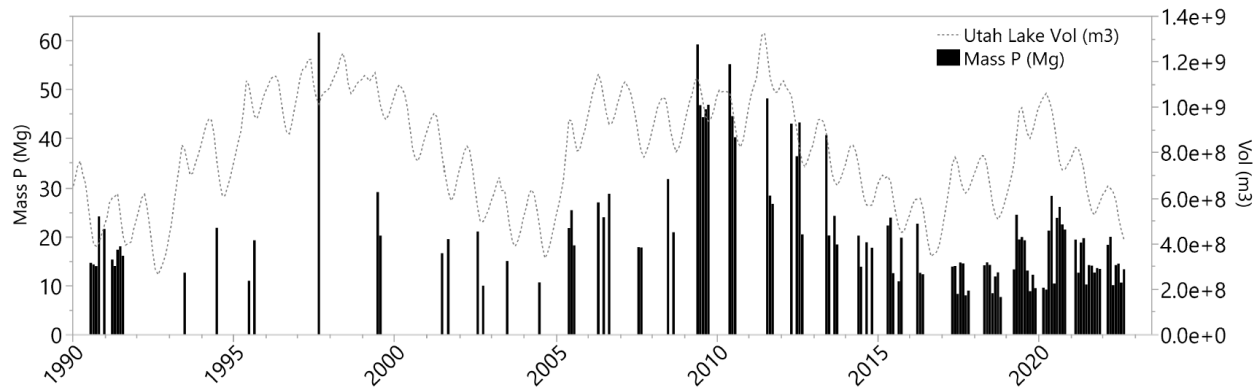


Figure 3.19. Monthly values of the mass (Mg or t) of Utah Lake dissolved P (DP) as bars and the volume of Utah Lake ( $m^3$ ) as the dashed line on the left and right axis, respectively. While the values generally follow each other, the mass of DP typically follows rather than leads the lake volume as the lake moves toward equilibrium concentrations after the lake volume changes.

median lake DP mass for any given month in which we have measurements. The Jordan River outflow is zero for slightly over 2% of the

months for which we have measurements. Previous studies have shown that in the long term, Utah Lake acts as a P sink, retaining about 10% of the P inflow [41]. These data, shown in Figure 3.18, demonstrate that P mass outflows, while not large, do impact mass balances.

### 3.3.4 Phosphorus Mass Variability

Figure 3.19 presents the mass of DP ( $t$ ) and the volume of water ( $m^3$ ) in Utah Lake at the beginning of each month. We only show mass values in months for which DP concentration measurements exist. Contrary to the behavior expected in a strict mass balance model, the mass of DP increases and decreases with lake volumes, though the change in mass lags behind the change in volume to some degree. This is consistent with lake concentrations moving toward equilibrium values under a sorption system. The lake is reacting to either dilution events (e.g., desorption during spring runoff) or concentration (e.g., sorption during late summer evaporation). Without dominant sorption processes, we would expect the in-lake mass to be relatively insensitive to volume changes unless accompanied by external loads. As WWTPs and AD account for a large portion of the load, we do not expect large load changes over time. For Utah Lake, water influent loads are a small portion of the total estimated DP loads, and we would not expect large mass changes due to DP contributed by spring inflows. These data show that Utah Lake volume and DP mass have a correlation coefficient of 0.56, where the correlation is significant at the  $p < 0.001$  level. This implies that changes in volume and mass are related, an observation consistent with a sorption system.

We computed the change in the mass of P in Utah Lake using Equations 3.1 through 3.4. To compute the DP mass in Utah Lake at the beginning of each month,  $M_{Lake}$ , we used Equation 3.1 and the outflow of mass in the Jordan River with the estimated concentration at the beginning of each month. The total monthly mass inflow of DP from all sources (Figure 3.20B) is equal to the monthly change in mass for the entire lake (Figure 3.20A) plus the monthly outflow in the Jordan River. This includes DP from point sources such as tributaries and WWTPs, from nonpoint sources such as AD and overland flow, and from internal sources such as lakebed sediments. We used concentration estimates based on the median of values on days with multiple measurements for the interpolation (Figure 3.7).

If DP inputs from external sources remain relatively constant, the mass of DP in the lake should remain relatively constant, and the concentration should decrease due to dilution from spring runoff and increase in the summer because of evaporation. In Utah Lake, however, the concentration of DP stays relatively constant. As shown in Figure 3.19, mass increases with increasing volume and decreases with decreasing volume, consistent with a sorption-dominant system.

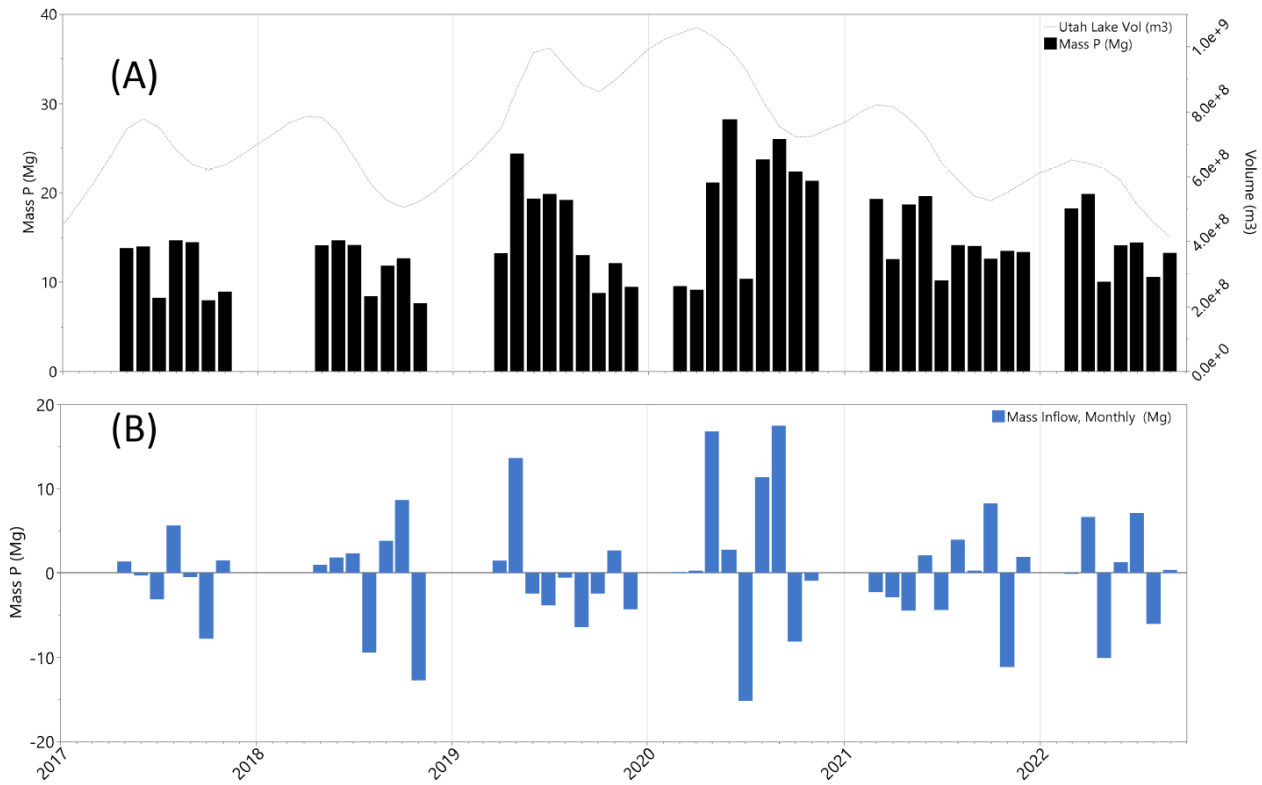


Figure 3.20. Panel (A) is a detail of Figure 3.19, which shows the total mass (Mg or t) of dissolved P (DP) in Utah Lake, while panel (B) shows monthly DP total mass inflows (Mg or t) from all sources including sorption into Utah Lake. These are computed as the change in the lake mass plus the mass outflow in the Jordan River. Data are shown only for months in which we have DP concentration measurements. Total mass DP inflows range from positive 17 t per month to negative 15 t per month. The graph is restricted to the period since 2017 for visualization purposes and because prior years have only a few data points per year.

### 3.3.5 Sorption Calculations

We do not have sorption isotherm data for Utah Lake, but to show how sorption in Utah Lake could affect water column concentrations, we use data from Sposito [86], who measured P sorption on sandy clay loam soil. Utah Lake sediments are similar in texture, with an abundance of clays and sands [40]. We fit a Freundlich isotherm to these data (Figure 3.21), which resulted in a  $K_d$  of 1039 and n of 2.08:

$$C_{solid} = 1039 \times C_{liq}^{1/2.08} \quad (3.6)$$

where  $C_{solid}$  is the sediment concentration of P ( $\text{mg kg}^{-1}$ ) and  $C_{liq}$  is the water column concentration of DP ( $\text{mg L}^{-1}$ ). In Utah Lake, water column DP concentrations are generally below 0.1  $\text{mg L}^{-1}$ ; the literature data used for the isotherm have a larger range (Figure 3.21).

The average Utah Lake water column DP concentration of 0.03  $\text{mg L}^{-1}$  (Figure 3.12) using a  $K_d$  of 1039 results in a sediment concentration of 192.5  $\text{mg kg}^{-1}$ , as shown in Equation 3.6. This concentration, 192.5  $\text{mg kg}^{-1}$ , is consistent with the published values for Utah Lake sediment. Studies show that about 40% of the P in the sediment is loosely sorbed or associated with redox-sensitive P, both fractions that would be involved with sorption processes in Utah Lake [40]. This means that about 266  $\text{mg kg}^{-1}$ , with a range of 120 and 440  $\text{mg kg}^{-1}$ , would be the sediment concentration in equilibrium with the water column [6, 40]. If the water column were in equilibrium with sediment concentrations in a range of 120 and 440  $\text{mg kg}^{-1}$ , the range of water column equilibrium concentrations would be about 0.010 to 0.16  $\text{mg L}^{-1}$  using this isotherm.

To show how the sorption process acts as a buffer to water column concentrations from large mass inflows or removals from the system, we

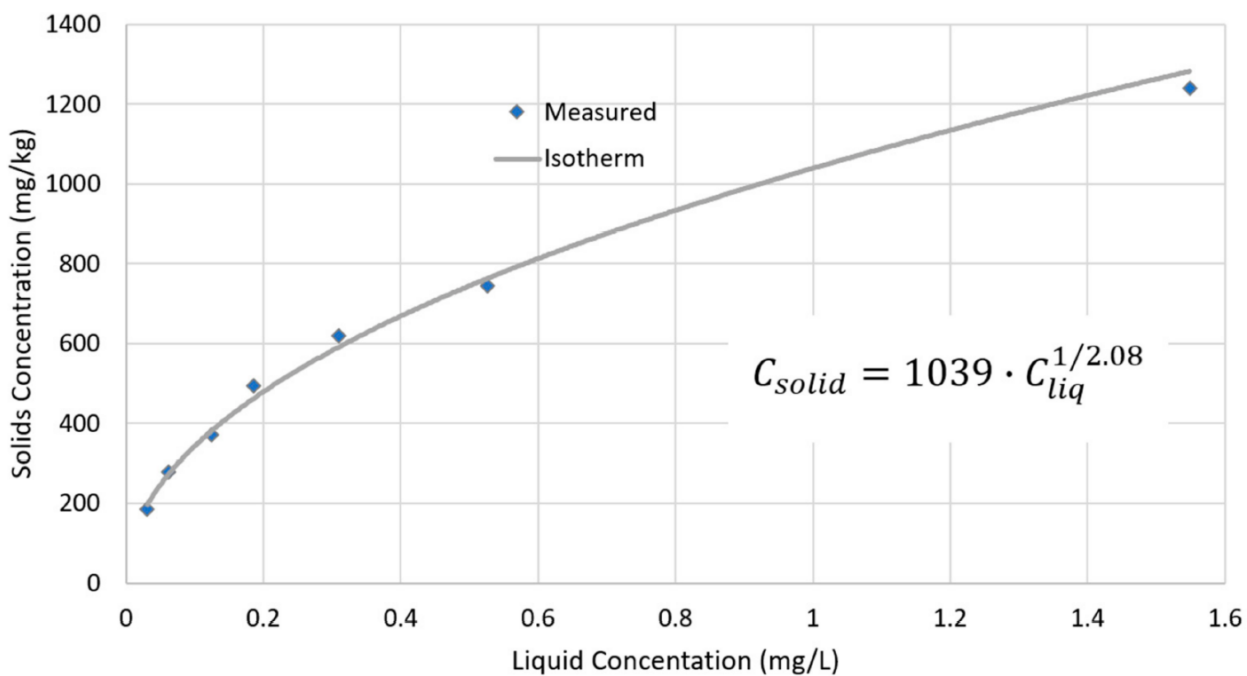


Figure 3.21. Example data that represent P adsorption to a sandy clay loam soil (from Sposito [86]) fit with a Freundlich isotherm. As is conventional for isotherm plots, the y-axis represents the concentration of P sorbed to the soil, while the x-axis represents the concentration of P in solution.

present example calculations. If we assume Utah Lake is 3 m deep and interacts with 10 cm of sediment, with a density of 1.8 in a water column that has an area of 10 cm<sup>2</sup> (0.001 m<sup>2</sup>), this gives a water volume of 3 L and a sediment mass of 0.18 kg. If we assume the concentrations presented above, 0.03 mg L<sup>-1</sup> and 192.5 mg kg<sup>-1</sup>, this results in 0.09 mg and 34.65 mg of P in the water column and sediment, respectively, with a total of 34.74 mg of P in the system.

Using concentrations of 0.03 mg L<sup>-1</sup> and 192.5 mg kg<sup>-1</sup> as a baseline, we can compute the total mass of P that would need to be added or removed from the system to adjust the water column concentration from 0.02 mg L<sup>-1</sup> to 0.07 mg L<sup>-1</sup>, which is about the range of observed values in Utah Lake over the last 30 years (Table 3.4).

Table 3.4. Equilibrium concentrations, mass, and dissolved P (DP) mass added to a column of water that is 3 m deep, has a cross-sectional area of 10 cm<sup>2</sup>, and interacts with sediment that is 10 cm deep. This equates to 3 L of water and 0.18 kg of sediment, respectively. This table assumes a water concentration of 0.03 mg L<sup>-1</sup> as the baseline (with the corresponding row shaded in gray) to compute the amount added or removed from the system to achieve different concentrations. Example data that represent P adsorption to a sandy clay loam soil (from Sposito [86]) fit with a Freundlich isotherm. The y-axis is the concentration of P sorbed to the soil, while the x-axis is the concentration of P in solution.

$C_{liq}$ (mg/L)	$C_{solid}$ (mg/kg)	$P_{solid}$ (mg)	$P_{liq}$ (mg)	$P_{tot}$ (mg)	$P_{added}$ (mg)
0.020	158.41	28.51	0.060	28.57	-6.17
0.025	176.35	31.74	0.075	31.82	-2.92
0.030	192.51	34.65	0.090	34.74	0.00
0.035	207.32	37.32	0.105	37.42	2.68
0.040	221.07	39.79	0.120	39.91	5.17
0.045	233.95	42.11	0.135	42.25	7.50
0.050	246.11	44.30	0.150	44.45	9.71
0.055	257.65	46.38	0.165	46.54	11.80
0.060	268.65	48.36	0.180	48.54	13.80
0.065	279.19	50.25	0.195	50.45	15.71
0.070	289.32	52.08	0.210	52.29	17.55

Where  $C_{liq}$  and  $C_{solid}$  are defined by Equation 3.6,  $P_{solid} = M_{solid}C_{solid}$ ,  $P_{liq} = V_{liq}C_{liq}$ ,  $P_{tot} = P_{solid} + P_{liq}$ , and  $P_{added}$  is the mass difference in  $P_{tot}$  at the baseline concentration ( $C_{liq} = 0.03$  mg L<sup>-1</sup>) and the current concentration. In Table 3.4, we assume that  $V_{liq} = 3$  L and  $M_{solid} = 0.18$  kg.

The data in Table 3.4 show that in order to change the water column concentration from 0.03 mg L<sup>-1</sup> to 0.035, the system would require 2.68 mg of P in just 3 L of water. If this amount were added to the water column and not allowed to partition into the sediment, it would result in a concentration of 0.92 mg L<sup>-1</sup>, a concentration over 25 times higher than the

equilibrium concentration with the sediment. Similarly, one would need to remove 2.92 mg of P from the system to change the water column concentration from 0.030 mg L<sup>-1</sup> to 0.025 mg L<sup>-1</sup>. The amount that would need to be removed from the system (from both the sediment and water column) is over 32 times the total amount of P in the water column at the beginning. Doubling the water column P concentration to 0.06 mg L<sup>-1</sup> would require the addition of 13.8 mg of P, an amount which, if added to 3 L of lake water with an initial concentration of 0.03 mg L<sup>-1</sup>, would result in water with a concentration of 4.63 mg L<sup>-1</sup>—more than 77 times the equilibrium concentration of 0.06 mg L<sup>-1</sup>.

We can evaluate Utah Lake using the same approach, assuming a water depth of 3 m and a sediment depth of 10 cm. If we use the average Utah Lake volume of about  $8 \times 10^8$  m<sup>3</sup> ( $8 \times 10^{11}$  L), this gives  $4.8 \times 10^{10}$  kg of sediment. Changing the water column concentration from 0.030 to 0.035 mg L<sup>-1</sup> changes the sediment concentration from 192.5 to 207.3 mg kg<sup>-1</sup>. The initial P mass in the water and sediment is 24 and 9240 t, respectively, with a total mass of 9264. The final P mass in the water and sediment would be 28 and 9951 t, respectively, with a total mass of 9979 t, a total change of about 715 t of P. This amount of added P is larger than the total estimated annual load from all sources. The addition of 715 t, with no outflow, would only change the water column concentration by 0.005 mg L<sup>-1</sup>.

If we assume a much lower  $K_d$  value of 500, then changing water column concentrations from 0.030 to 0.035 mg L<sup>-1</sup> would result in sediment concentration changes from 92.6 to 99.8 mg kg<sup>-1</sup>. The initial DP mass in the water column is about 24 t, with about 4446 t of P in the sediment. The final mass is 28 t in the water, 4789 t in the sediment, and 4817 t in total, an increase of 347 t. While about half the amount using a  $K_d$  of 1039, this increase in P mass is about the same as the estimated annual load and only changes the water column concentration by 0.005 mg L<sup>-1</sup>.

Conversely, reducing water concentrations from 0.030 mg L<sup>-1</sup> to 0.025 mg L<sup>-1</sup> would reduce sediment concentrations from 207.3 mg kg<sup>-1</sup> to 192.5 mg kg<sup>-1</sup> ( $K_d = 1039$ ) or from 99.76 mg kg<sup>-1</sup> to 92.63 mg kg<sup>-1</sup> ( $K_d = 500$ ) and require a total P mass reduction in the system of 780 t or 377 t, respectively. This corresponds to water column mass reductions from 28 t to 24 t, a reduction of 4 t for either case, as the water column concentration reductions are the same. To achieve the total mass reductions of 780 t or 377 t would require flushing the entire reservoir about 27 times or 13 times for  $K_d = 1039$  or  $K_d = 500$ , respectively. This assumes that we flush 28 t of P each time, which is the mass of P in the water column at a concentration of 0.030 mg L<sup>-1</sup>. This highlights how well-buffered water column concentrations are in Utah Lake. Even with a  $K_d$  as low as 100, it would require three complete flushing events to reduce water column concentrations from 0.030 mg L<sup>-1</sup> to 0.025 mg L<sup>-1</sup>, with sediment

concentrations changing from  $20.0 \text{ mg kg}^{-1}$  to  $18.5 \text{ mg kg}^{-1}$  and reducing the total mass in the system to 72 t of P.

### 3.4 Discussion

#### 3.4.1 Variability

The volume of Utah Lake varies significantly over time. From 1989 to 2023, the average lake volume was  $7.9 \times 10^8 \text{ m}^3$ , with a standard deviation of  $1.1 \times 10^8 \text{ m}^3$ . Yearly, the lake volume fluctuated by  $3.7 \times 10^8 \text{ m}^3$ , about half the lake's volume. Monthly variation showed that the volume increased by as much as  $4.5 \times 10^7 \text{ m}^3$  or decreased by as much as  $8.0 \times 10^7 \text{ m}^3$  depending on the time of year. Lake volumes typically peak in May and reach a trough in October. Between 1989 and 2023, lake volume reached an all-time high in 2011, peaking at  $1.3 \times 10^9 \text{ m}^3$ , which is 1.7 times larger than the lake's average volume. In contrast, the all-time low during the same period was in 1992, with a trough of  $2.5 \times 10^8 \text{ m}^3$ , about a third of the lake's average volume. Statistical analyses show that Utah Lake volumes for most years are different from the mean. Meanwhile, Jordan River outflows are on the order of  $4.5 \times 10^7 \text{ m}^3$  per month (Figures 3.3 and 3.4), with P outflows that are about 10% of the total mass of P in the lake.

Despite large fluctuations in lake volume, DP concentrations remained relatively constant in Utah Lake from 1989 to 2023. Average values frequently ranged between  $0.02$  and  $0.06 \text{ mg L}^{-1}$ , with no statistically significant variation in annual mean values in any given year or month besides a few minor exceptions (see Section 3.2). DP did follow a pattern of being slightly higher in the fall and slightly lower in the spring, but these variations were not statistically significant over our study period. The data for DP did contain outliers, including one sample from July 1989, two samples from January 1991, and eleven samples from September 1997. The presence of these outliers, however, was insignificant given the 1658 total measurements used in this study. These data points were included in the analysis and did not change the results.

Lake volume variability and relatively constant P concentrations are best illustrated by Figures 3.10 and 3.12, respectively. ANOM graphically presents individual group comparisons with the overall mean for the population. It uses decision boundaries based on the number of samples and the variability of the population to determine if any group is different from the entire population. Figures 3.10 and 3.12 present the ANOM analysis with lake volume and lake concentration grouped by year and compared to the complete data set. Figure 3.10 shows that except for 1994, 2001, 2005, and 2013, the lake volume in all years is very different from the 34-year mean. The years that are not different are where the lake volume is transitioning from a wet to a dry period. In stark contrast, Figure 3.12 shows that with eight exceptions, in none of the years is the lake DP

concentration statistically different from the long-term average. For the eight years where the concentrations are different from the average, the values are only slightly outside the decision boundaries. This constant concentration behavior is distinctly different from the variable volume data, where nearly all the years were considerably outside the decision boundaries.

We estimate the mass of DP in Utah Lake to be between 10 and 50 t at any given time (Figure 3.19), with monthly mass changes that can be either positive or negative, increasing or decreasing by as much as 15 t (Figure 3.20). Current estimates for external TP loading, however, are between 18 and 35 t month<sup>-1</sup> and are always positive [34–38]. We show that the monthly change in DP mass in Utah Lake is comparable in magnitude or exceeds the estimated total P load to the lake and that the differences in loading must be attributable to internal cycling caused by sediment-water interactions.

For a simple mass balance model, like the one presented in Equation 3.5, a lake would be expected to have its P concentration reduced by 50% if the lake's volume was doubled based on dilution. Conversely, if the lake's volume were decreased by 50% (half the volume), we would expect a concentration increase of 100%. The volume of Utah Lake often doubles in response to spring runoff, but the DP concentration only decreases slightly. Conversely, in late summer, the lake loses half its volume from evaporation with little increase in P concentration. The average monthly P concentration in the spring is not statistically different from the annual DP concentrations, nor is the concentration in the summer statistically different from the average DP concentration (Figures 3.13 and 3.14). This implies that sorption is so dominant that lake concentrations are insensitive to external P loads.

### 3.4.2 Isotherm Calculations Implications

While we do not have isotherm data specific to Utah Lake, we showed in Section 3.5 that using  $K_d$  values of 1039 (from the literature) and 500 (an assumed reduction) still require additions of 714 t and 346 t of P, respectively, to change the water column concentration of Utah Lake from 0.030 mg L<sup>-1</sup> to 0.035 mg L<sup>-1</sup>, a change of only 0.005 mg L<sup>-1</sup>. Conversely, changing the water column concentration from 0.030 mg L<sup>-1</sup> to 0.025 mg L<sup>-1</sup> would require flushing Utah Lake approximately 27, 13, or 3 times, assuming  $K_d$  values of 1039, 500, or 100, respectively.

These calculations assume the water column only interacts with sediments down to a depth of 10 cm. P-rich sediments are 1000s of meters deep, and because diffusion processes transport P upward from the deeper sediments, the amount of sediment that could interact with the water column is practically infinite. If P is depleted from the near surface

sediments, additional P will diffuse from the anoxic regions with high P values in the pore water. If additional P is added, the P in the sediment will form calcite complexes, essentially removing the P from shorter-term equilibrium sorption processes. The sediment acts as a buffer to keep Utah Lake water column concentrations constant and insensitive to external loads.

We hypothesize that the variations seen in Utah Lake water column P concentrations are due to short-term kinetics, where the system is temporarily moved away from equilibrium by events such as high spring inflows, which dilute the P concentration in the water column, or late summer evaporation, which increases water column P concentrations. As concentrations move from the equilibrium concentration, sorption processes either add or remove P from the water column to re-establish equilibrium. This sorption-dominated model is supported by the limited variability of P concentrations in the water column over our 34-year study period, and the data that show that measured sediment P concentrations in the fractions associated with sorption processes match those predicted by the model.

This simple example, using isotherm data from the literature and an assumed reduction, demonstrates that water column concentrations of P in Utah Lake are essentially independent of external P loads and will remain constant even if external P sources, such as WWTP effluent, are significantly reduced.

### 3.4.3 Sorption Lines of Evidence

Using publicly available data, we presented analyses and data that strongly support the hypothesis that water column concentrations of P in Utah Lake are governed by sorption processes. This is unusual, as water column P concentrations in most lakes are better modeled by a mass balance approach, where reducing or increasing nutrient loads will reduce or increase water column concentrations, respectively. Utah Lake is unique in a number of aspects that allow sorption processes to dominate mass balance flows to the point where other loads or removals have a limited impact. While we have no concrete data to prove our hypothesis, there are several lines of evidence that all strongly support our theory.

The main arguments and data that support the hypothesis that Utah Lake water column concentrations are governed by sorption processes are as follows:

1. Utah Lake sediments are high in P that is available for partitioning. This P is geologic in origin rather than anthropogenic. Lakebed sediments [40], surrounding lacustrine soils [6], and sediment 40 km upstream [11] all have P concentrations on the order of 1000 mg kg<sup>-1</sup>, with about 40% of the P in the fractions being

available to the sorption process [40]. In addition, the sediments underlying the lake are deep [55], and because of the potential for anaerobic releases, the sediments represent an essentially infinite reservoir of P.

2. Utah Lake is very shallow, with a long fetch (~40 km), and strong winds. The lake does not stratify, and because of the depth, fetch, and winds, the lake's sediments are continually mixed with the water column. We regularly measure total suspended solid concentrations on the order of  $1000 \text{ mg L}^{-1}$  and Secchi depths of a few 10s of cm. Because of this mixing with sediments, the water column can equilibrate with sediments in a sorption process.
3. Utah Lake has a large population of invasive carp. These fish contribute to sediment water column mixing through bioturbation, continually stirring up the sediment through bottom feeding and by preventing the establishment of vegetation that could armor the lakebed and help isolate the sediment from the water column [41].
4. Utah Lake volumes are variable, easily changing volume by a factor of 2 in any given year, and often more (Section 3.1.1). Conversely, DP concentrations in Utah Lake are relatively constant, with values ranging from about 0.02 to  $0.06 \text{ mg L}^{-1}$  but remain mostly in the 0.03 to 0.04 range (Section 3.2). With large changes in lake volume, we would expect P concentrations to be diluted in the spring after spring runoff fills the lake and then be concentrated in the late summer, as about half the lake volume is lost to evaporation. While we do see changes in water column DP, they are small and are better explained by the kinetics of sorption processes.
5. An ANOM analysis of Utah Lake volume (Figure 3.10) and water column DP concentrations by year (Figure 3.12) shows that, for most years, the volume is outside of the decision boundaries and is significantly different from the mean, while the opposite is true for the concentration data—only a few years are outside the boundaries and only by a small amount. Statistically, the different annual average concentrations are not different from the population mean when nearly all the annual average yearly volumes are different from the population mean.
6. Monthly changes in the mass of DP in the water column show that large changes can occur in just a month's time (Section 3.4). When we estimate P inflows using lake mass and Jordan River mass outflows, we see that monthly mass inflows are large and switch from loads to removals in short time periods (Section 3.4). These estimated monthly mass inflows are larger in magnitude than estimated loads. More importantly, these loads are both positive and negative, switching from month to month. This can easily be

explained using a sorption approach, where the sorption term is significantly larger than other P loads or sinks. This same phenomenon is difficult to explain using external loads alone.

7. Using an isotherm fitted to data taken from the literature (as we do not have an isotherm for Utah Lake sediments) and an assumed value of half the literature's  $K_d$  value, we can show the following:
  - a) The sediment concentration at equilibrium with a water column concentration of  $0.03 \text{ mg L}^{-1}$  (the average) is consistent with measured sediment P concentrations in the fractions available for sorption.
  - b) Because of the large sediment reservoir, it would require large P loads to cause even small changes in water column P concentrations when the system is at equilibrium. In a system without this large sediment reservoir in equilibrium with the water column, loads this large would increase water column concentrations by almost two orders of magnitude.
  - c) In most lakes, the water column is not vertically-mixed well enough to be in equilibrium with reservoir sediments and the reservoir sediments are not enriched in P from geological sources. These two unique features, shallow waters that are well mixed with sediments enriched in geologic P, allow sorption processes to dominate water column P concentrations.
  - d) It would require the addition of either 714 t or 346 t of P to change water column concentrations by only  $0.005 \text{ mg L}^{-1}$  for  $K_d$  values of 1039 and 500, respectively; this buffering process is supported by the constant water column concentrations observed over our 34-year study period.

These separate lines of evidence all support the hypothesis that water column P concentrations in Utah Lake are dominated by sorption processes and that water column concentrations are insensitive to external loads. This evidence supports the assertion that changing anthropogenic P loads to Utah Lake would have little to no impact on water column concentrations. For example, if WWTP loads were able to be reduced to zero, this analysis shows that water column P concentrations would not be decreased but would instead remain similar to historical levels.

### 3.5 Conclusions

We used publicly available data to analyze the variability of lake volumes, water column DP concentrations, and water outflow of Utah Lake. Using

these data, we estimated the mass of DP in Utah Lake over time, along with changes in the mass of DP in the lake.

Through statistical analysis, we showed that volumes are variable but that DP concentrations are relatively constant. Further, water column DP concentrations do not change as expected; we would expect the dilution of P as the lake fills as well as the concentration of P as the lake evaporates.

We show that monthly changes in mass are large compared to estimated loads to the lake and that these changes switch from representing net sinks to net sources from one month to the next, a finding that is not consistent with simple mass balance models. Using an assumed isotherm, we show how these large mass changes, switching from a sink to source, are consistent with a mass balance model dominated by sorption processes.

We estimate, using assumed isotherm data, that reducing or even eliminating external loads to Utah Lake will have little impact on water column P concentrations. This has important implications regarding the efficacy of additional nutrient reductions currently being considered by the regulatory community. Our analysis suggests that even very large reductions in nutrient inputs will have a minimal effect on DP in Utah Lake.

Data from published studies highlight the fact that P sediments and soils in and around Utah Lake are geologic in origin, not anthropogenic, and represent a very large, essentially infinite reservoir of P. Importantly, we computed that measured average lake water column P concentrations of  $0.03 \text{ mg L}^{-1}$  are consistent with measured sediment P concentrations in the fractions available for sorption.

This study also has implications for other shallow lakes with significant sediment–water interactions. If these lakes have sediments with high concentrations of P from geologic sources, water column concentrations could behave independently from external loads. For sorption to dominate in this manner requires several unique circumstances, including shallow water with no stratification, significant water–sediment interaction, and high background P concentrations in the sediment. While these conditions are unusual, they are not unique. We present this case study as a framework that can be used to evaluate and study other lakes or reservoirs.

For lakes and reservoirs that have water column P concentrations primarily driven by sorption processes, costs and efforts aimed at nutrient load reductions may prove ineffective. Other remedial or restoration efforts, such as measures that stabilize sediments and limit sediment–water interactions, may prove more feasible.

### 3.6 Afterword

This chapter is based on an updated version of the research article: "Historical Phosphorus Mass and Concentrations in Utah Lake: A Case Study with Implications for Nutrient Load Management in a Sorption-Dominated Shallow Lake" published in the journal *Water* [25]. I hereby confirm that the use of this article is compliant with all publishing agreements.

## 4 A Geochemical Study of Near-Shore Sediment Cores from Utah Lake, Utah, USA

*Jacob B. Taggart, Lauren M. Woodland, Kaylee B. Tanner, and Gustavious P. Williams*

**Abstract:** A variety of sediment core studies have been performed on Utah Lake over the past century with recent studies reporting detailed information regarding the lake's depositional history based on a small number of shallow core samples. Given the lake's large surface area (~380 km<sup>2</sup>), we sought to provide more comprehensive coverage by collecting 10 sediment cores throughout the lake and analyzing them for ICP-OES detectable elements, fractional calcium carbonate, and fractional organic matter. Our core samples were at least 140 cm deep, which ensured the collection of depositional material from before the arrival of European settlers. The quantity and geographical spread of our core samples enabled us to gather data that still effectively represented Utah Lake even though exceptionally high-water levels and equipment limitations restricted us to collecting core samples in near-shore areas with non-rocky sediment. Our core samples showed noticeable chemostratigraphic variability across the lake, demonstrating that lakebed sediment is not as homogenous as previously thought. Elements from Utah Lake sediments with higher normalized mean concentrations tend to have more strong correlations with other elements. Depth trends reveal that certain elements correlate positively or negatively with depth, and geochemical shifts at 30–40 cm align with research claims that this depth marks the onset of European settlement. Phosphorus in the sediments is linked to calcium, iron, and several trace metal pollutants, indicating that both natural processes and human activities influence elemental distribution in lakebed sediments.

**Keywords:** calcium carbonate; ICP-detectable elements; organic matter; phosphorus; sediment cores; Utah Lake

---

## 4.1 Introduction

### 4.1.1 Study Motivation

Of the various techniques used for paleolimnological research, sediment core collection has proven to be an invaluable means of revealing a lake's environmental and depositional history. In comparison to seismic imaging and ground penetrating radar, which are used to broadly characterize a lake's stratigraphy and bathymetry, sediment cores are the principal method for determining the biogeochemical properties of lakebed sediment and how lake conditions have changed throughout time [87].

Despite the large quantity of data that can be extracted from a single sediment core, the spatially heterogeneous nature of lakebed sediment necessitates the collection of numerous sediment cores from different areas to adequately represent an entire lake. This is especially true for large lakes, as their size makes them prone to localized impacts from anthropogenic and physiographic phenomena. As such, Last and Smol [88] recommend collecting a minimum of five to ten core samples in order to generate representative sediment profiles for a given lake.

Over the past century, a variety of paleolimnology studies have been performed on Utah Lake sediments, including several which indicate that the lake experienced an ecological regime shift beginning in the mid-to-late 19th century, coincidental to the onset of European settlement in the area [89-101]. The lake has since transitioned from a less turbid (but not necessarily clear) state, dominated by benthic productivity, to a more turbid state, dominated by water column productivity [96, 98, 100-102].

While phosphorus (P) is known to play a prominent role in the productivity of aquatic environments, a relatively small number of paleolimnological studies have measured the concentration of P in Utah Lake sediment cores [91, 97-100]. These studies did so as part of high-resolution analyses of multiple variables on a small number of relatively shallow core samples ( $n \leq 4$ ), with analytical costs likely prohibiting the collection and assessment of additional samples or deeper cores. Most of these studies included core samples from semi-isolated portions of the lake, such as Provo Bay and Goshen Bay. This consequently left one or two core samples from each study to represent the main body of Utah Lake. With the exception of Bolland [91], the depths of these core samples were all less than one meter.

Given Utah Lake's large surface area (~380 km<sup>2</sup>), we sought to provide supplementary representation of sediments throughout the lake by collecting 10 deeper sediment cores. These cores, ranging from 140 to 240 cm deep, were intentionally deep enough to include pre-settlement deposits found below 30–40 cm deep [99-101]. We analyzed these cores for 25 ICP-OES detectable elements, fractional calcium carbonate (CaCO<sub>3</sub>), and fractional organic matter (OM). We hypothesize that although European

settlement may have influenced Utah Lake sediments to some extent, certain lakebed features, such as sediment P profiles, are more likely shaped by natural processes [6, 40, 103].

#### 4.1.2 Background on Utah Lake

Utah Lake is a semi-terminal, basin-bottom lake in north-central Utah, USA. Despite its large surface area (~380 km<sup>2</sup>), Utah Lake is relatively shallow (~3 m). Fluctuations in storage consequently result in a highly dynamic shoreline, as a depth change of 30 cm can alter the lake's surface area by over 10 km<sup>2</sup> [104].

Since the formation of Utah Lake as a remnant of Lake Bonneville approximately 13,000 years ago, several Native American tribes have lived adjacent to the lake and relied on it for sustenance. Europeans began establishing settlements around Utah Lake in the mid-1800s, eventually driving out the native inhabitants and altering the lake in many significant ways [102]. These changes include the following: the overharvesting of native fish species and introduction of nonnative fish species such as the Common Carp (*Cyprinus carpio*) [101], the construction of a dam and pump house at the lake's outlet for managing lake levels and the flow of water downstream [42], and the introduction of pollutants from industrial, municipal, and agricultural sources [99, 102].

Utah Lake functions as a wildlife habitat for a variety of flora and fauna, notably the threatened June Sucker fish species and the waterfowl that migrate along the Pacific Flyway. For humans, the lake is primarily used for recreational activities and as a reservoir for downstream irrigation. However, these uses are threatened by harmful algal blooms which occur in the lake on a near-annual basis. Algal blooms are typically a product of nutrient-laden waters, with P often presumed to be the limiting nutrient. While there is no increasing trend in algal blooms outside of Provo Bay [30], it is still important to take action towards reducing the number of harmful algal blooms in order to protect the lake's beneficial uses for both humans and wildlife.

Many efforts are being made to better understand the chemical behavior of P in Utah Lake in order to improve lake management practices. As such, the study of sediment cores from Utah Lake can help demonstrate how P and other ICP-detectable elements have varied in lakebed sediments both spatially and temporally relative to the arrival of European settlers and subsequent increases in population around the lake. This, in turn, will improve our understanding of the lake's geochemical response to anthropogenic activity and thereby inform management strategies for Utah Lake.

#### 4.1.3 Core Collection Sites

Our criteria for selecting core collection sites in Utah Lake were based on three conditions: 1) the number of cores we planned to collect, 2) our sampling equipment's ability to access the lakebed, 3) and the suitability of the sediment for core sampling. As previously mentioned, Last and Smol [87] recommend collecting 5-10 sediment cores to adequately represent an entire lake. Due to Utah Lake's large size, we chose to collect 10 sediment core samples from within the lake.

The target depth for each of our core samples was 2.4 m (8 feet) beneath the sediment surface. While our equipment had a total reach of 6.7 m (22 feet), much of this length was needed to extend the equipment down through the water column and into the lake sediment. The Utah Lake watershed experienced an exceptionally good water year at the time of this study, causing the lake to be particularly full during the summer of 2024. We were consequently limited to sampling in near-shore areas along the lake's perimeter, as the offshore portions of the lake had become too deep to be accessible for our equipment. A few of the previous Utah Lake paleolimnological studies [91, 97-100], were conducted during typical water years when the lake level was lower and collected core samples toward the center of the lake. By limiting our collection sites to near-shore areas, we acquired a unique dataset that complements the data collected by previous studies.

We discovered that the portions of the near-shore lakebed next to the Lake Mountains and West Mountain were too rocky for us to collect core samples. This limited us to collecting 10 sediment cores across Utah Lake in near-shore areas that were nonadjacent to mountainous terrain. The sites for these core samples as well as the approximate location of Utah Lake's original shoreline are shown in Figure 4.1. Further details regarding all sediment cores are found in Table 4.1.

We use the following abbreviations to refer to each sample location: A – Airport; B – Benjamin; GN – Goshen North; GS – Goshen South; LM – Lindon Marina; M – Mosida; NS – North Shore; PB – Provo Bay; PS – Powell Slough; SS – Saratoga Springs (Figure 4.1). We generally named our core samples after nearby geographic features, though they were not always collected directly from those locations (Figure 4.1). For example, the Lindon Marina sample were taken about  $\frac{1}{2}$  km ( $\frac{1}{3}$  mi) north of the marina itself to avoid collecting sediments disrupted by the construction and use of the marina.

## 4.2 Materials and Methods

### 4.2.1 Sample Collection and Preparation

We used an AMS® Soggy Bottom Sampling System to obtain our sediment core samples. This system includes an open barrel, manually driven

Table 4.1. Sediment core sample information. The Appendix contains a more detailed table with collection date, sampling coordinates, site elevation, and lake surface elevation.

Site Name	Water Depth	Penetration Depth	Core Length	% Shortened
Airport	2.33 m / 7.66 ft	1.62 m / 5.33 ft	0.90 m / 2.95 ft	45%
Benjamin	1.80 m / 5.91 ft	2.44 m / 8.00 ft	1.15 m / 3.77 ft	53%
Goshen North	1.73 m / 5.67 ft	1.52 m / 5.00 ft	0.95 m / 3.12 ft	38%
Goshen South	1.75 m / 5.75 ft	2.44 m / 8.00 ft	0.94 m / 3.08 ft	61%
Lindon Marina	1.72 m / 5.63 ft	2.44 m / 8.00 ft	1.00 m / 3.28 ft	59%
Mosida	1.73 m / 5.67 ft	1.60 m / 5.25 ft	0.69 m / 2.26 ft	57%
North Shore	1.17 m / 3.83 ft	2.44 m / 8.00 ft	0.85 m / 2.79 ft	65%
Powell Slough	1.65 m / 5.42 ft	1.83 m / 6.00 ft	1.00 m / 3.28 ft	45%
Provo Bay	2.18 m / 7.16 ft	2.44 m / 8.00 ft	0.90 m / 2.95 ft	63%
Saratoga Springs	1.74 m / 5.72 ft	1.60 m / 5.25 ft	1.10 m / 3.61 ft	31%

sampler and removable plastic liners that are 4 cm wide and either 61 cm or 122 cm long (1.5 in wide and either 2 ft or 4 ft long) to contain core samples during and after extraction. Instead of using a hydrostatic seal to prevent sample loss, the Soggy Bottom Sampler uses core catchers that are inserted into the bottom of each liner prior to sampling. Core catchers have small plastic fingers that are curled inward to allow material to enter the liner as the sampler is driven into the lakebed. These plastic fingers then close when the core sampler is extricated from the lakebed, preventing the sample from sliding out of the liner (Figure 4.2).

Once the core sampler was assembled, we attached 91-cm (3-foot) metal extenders to the sampler so it could be lowered through the water column to the lakebed. We then attached a slide hammer to the top-most metal extender, allowing us to drive the sampler down to the desired depth. This depth was typically deeper than the length of the core sampler due to core shortening, a phenomenon that causes sediment cores to be shorter than the penetrated depth of the core sampler. Core shortening will be discussed in greater detail in Section 2.6.

After the sampler was driven down to the desired depth, we extracted it by either reverse hammering with the slide hammer or by ratcheting the sampler upward with a fixed crane. We then removed the plastic liner containing the sediment core from the sampler and sealed the ends with parafilm followed by duct tape. The core sample was then placed on ice with the top elevated while in transit to our laboratory. Within 24 hours of acquiring a core sample, we cut the core open to collect subsamples. We then dried and ground the subsamples for laboratory analysis. As recommended by Wrath [105], we aimed to collect subsamples from the center of each core to avoid contamination from sediments smeared along

the inner walls of the plastic liners during sampling. We collected ~2 g subsamples every 5 cm along each core for elemental analysis as well as ~15 g subsamples from 6 sites along each core for the analysis of fractional CaCO<sub>3</sub> and OM.

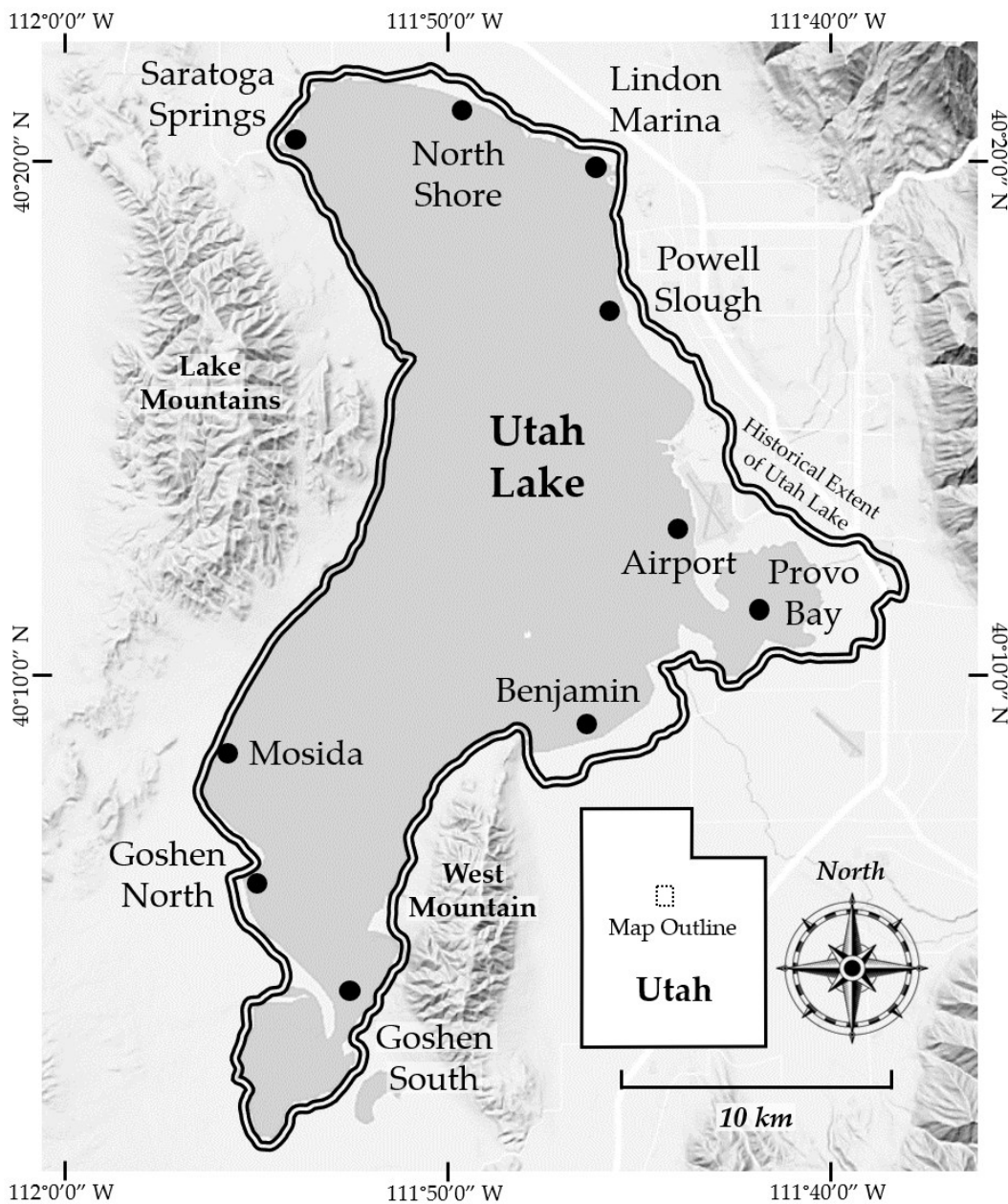


Figure 4.1. Core sampling locations throughout Utah Lake. The historical extent of Utah Lake is included to show the lake's approximate shoreline prior to European settlement, with a surface elevation of 1372 m (4500 ft).

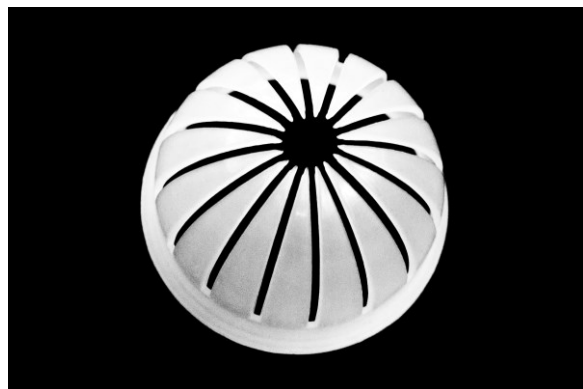


Figure 4.2. Photograph of a core catcher.

#### 4.2.2 Microwave Digestion and ICP-OES

We used U.S. EPA Method 3051A [106] to conduct microwave assisted acid digestion on our sediment core subsamples. While this method digests most components in sediments and soils, it is not a complete digestion and may leave behind some refractory substances, such as oxides. While we occasionally observed trace amounts of solid residue after the digestion of our samples, this material appeared to consist primarily of quartz and other silicate minerals. It is possible that the undigested residue included other unaccounted materials, but if this is the case, all of our core samples are subject to the same bias.

After digesting our samples, we performed elemental analysis using a Thermo Scientific iCAP 7400 ICP-OES. Assuming that the liquid from our digested samples had a mass density of  $1 \text{ g ml}^{-1}$  (the same density as water), we converted our results from units of ppm to  $\text{mg L}^{-1}$ . We then converted the results from the ICP analysis to units of mass concentration ( $\text{mg kg}^{-1}$ ) by multiplying them by the sample volume (L) produced from digestion and dividing them by the mass of the sediment (kg) used for digestion.

#### 4.2.3 Fractional Calcium Carbonate

We used the Plant, Soil and Water Reference Methods for the Western Region (WREP) Carbonate Qualitative Test [107] to measure the fractional  $\text{CaCO}_3$  content of our sediment core samples. This is a gravimetric method that involves weighing samples before and after their immersion in hydrochloric acid. The acid reacts with the  $\text{CaCO}_3$  to form carbon dioxide, calcium chloride, and water. The mass lost due to the formation of carbon dioxide is used to calculate the mass of  $\text{CaCO}_3$  present in the original sample.

#### 4.2.4 Fractional Organic Matter

We used the WREP Loss On Ignition Method [107] to measure the fractional soil OM in our sediment core samples. We heated the samples at 105°C for 24 hours to remove all traces of moisture, including the water incorporated into the molecular structure of clay minerals. We then weighed the samples before and after incinerating them at 360°C for 4 hours. The sample mass lost due to the combustion of OM is used to calculate the mass of OM present in the original sample.

#### 4.2.5 Color and Texture

We used Munsell Soil Color Charts [108] to identify the Munsell color categories of each subsample. Due to insufficient mass for particle size analysis, we classified the texture of the subsamples based on their feel and appearance as either sand, silt, gravel, or a transitional phase between two textures. We did not differentiate between clay and silt, instead categorizing all fine-grained subsamples as having a silty texture.

#### 4.2.6 Core Shortening

The use of open-barrel core samplers often produces sediment cores that are shorter than the penetrated depth. This phenomenon, known as core shortening, can be caused by multiple processes, including sediment thinning, physical compaction, and sediment bypassing [87, 109, 110]. Sediment thinning (Figure 4.3A) is the most common form of core shortening. It occurs when a penetrating object stretches and compresses

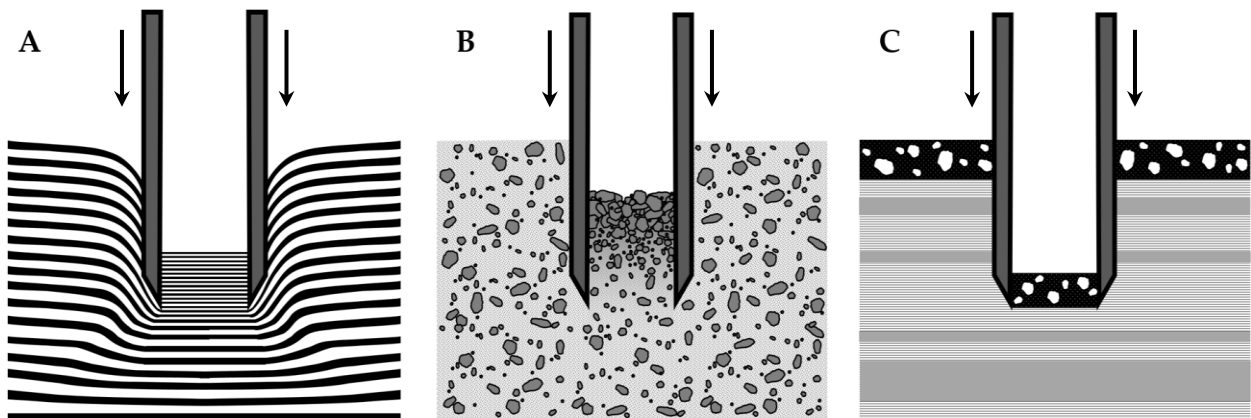


Figure 4.3. Side view of core shortening mechanisms within an open-barrel core sampler, including sediment thinning (A), physical compaction (B), and sediment bypassing (C). Panel A is adapted from Hongve and Erlandsen [109]. In reality, multiple core shortening mechanisms can occur simultaneously during sample extraction.

the sediment as the object is bored downward. All sediment layers are still present, but both the mass and volume of the sediment have been reduced, as manifested by thinner sediment layers within the core sample [87, 109, 110]. A second form of core shortening is physical compaction (Figure 4.3B) which occurs when water or air is forcibly expelled from a sediment layer, causing the sediment to become more densely packed, reducing the sediment's volume while maintaining its mass [110]. A third form of core shortening is sediment bypassing (Figure 4.3C). It occurs when a core sampler becomes clogged and excludes sediment layers during the sampling process. Sediment bypassing typically occurs when sampling firm sediment layers overlying softer sediment [110].

We used an open-barrel sampler and observed significant core shortening in all the cores we collected, with an average reduction of 50%. Following the recommendation by Zheng, et al. [111], we have included the amount of shortening for each core in Table 4.1 to facilitate comparison with both these and future sediment cores from Utah Lake.

The sediment-water interface throughout Utah Lake is poorly defined due to sediment resuspension caused by wind-driven wave action and the bottom-feeding behavior of the Common Carp (*Cyprinus carpio*). Together, these phenomena result in a loosely consolidated layer of sediment at the top of the lakebed that gradually transitions downward into firmer sediment. We therefore expect that the uppermost sections of our lakebed samples experienced core shortening in the form of physical compaction, while the primary cause of core shortening in the underlying layers was through sediment thinning. Although sediment bypassing may have affected the Mosida core due to the presence of a gravel layer overlying layers of silt, the occurrence of sediment bypassing is difficult to confirm without stratigraphic and sedimentological assessments of the lakebed in that location. With this one exception, we did not see any indication of potential barrel plugging.

To account for core shortening, we linearly corrected the sample length and subsample intervals of the cores to match their approximate depth in the undisturbed sediments (Figure 4.4). We performed these corrections under the assumption that all sediment layers within a given sample were equally impacted by core shortening. In reality, core shortening can affect sediment layers unequally depending on sediment type and their degree of consolidation. For the sake of this study, we assumed that these effects were insignificant.

Because our sediment core samples experienced varying amounts of core shortening, the intervals between subsample depth were not the same for each core. To compare the data among the different cores, we interpolated the elemental concentration data from the corrected subsample depths using a Piecewise Cubic Hermite Interpolating

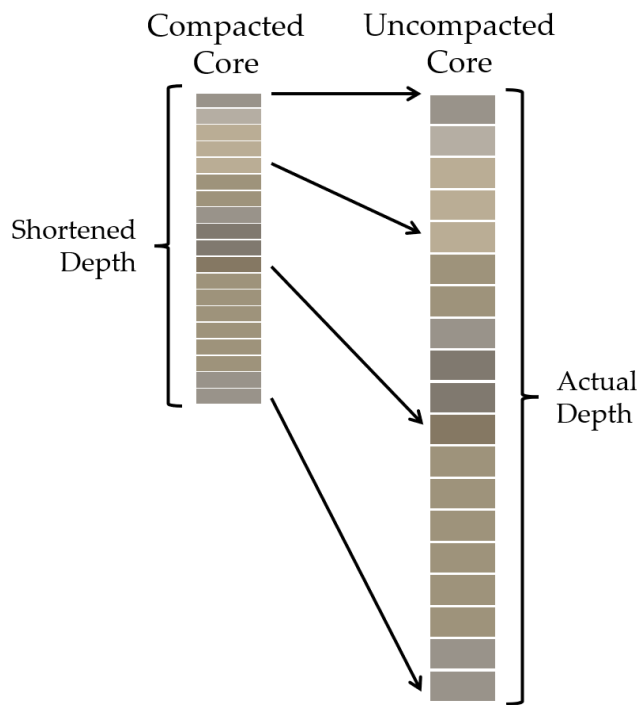


Figure 4.4. Depth comparison between a compacted and uncompacted sediment core sample. Cores collected from open-barrel samplers are prone to core shortening and require depth correction to represent the correct layer placement of undisturbed sediment.

Polynomial (PCHIP) at 5-cm intervals. This enabled comparative analysis of our sediment cores in 5-cm intervals down to 140 cm. PCHIP interpolation is a non-linear polynomial that has a continuous first derivative and a discontinuous second derivative. This results in a smooth interpolation that honors the data extent – i.e., without any over- or under-shooting that often occurs with spline interpolation methods.

#### 4.2.7 Methods of Analysis

We analyzed three categories of data—chemical composition, core depth, and sample location—and evaluated their interrelationships. The category of chemical composition can be further divided into the elemental concentration for 25 ICP-detectible elements and the fractional mass content for  $\text{CaCO}_3$  and OM.

Before analysis, we used Microsoft Excel 365 to normalize the data using min-max normalization which transforms the variables to a range of 0-1 using its minimum and maximum values. We used the Pearson Correlation to quantify the strength of a relationship between two

variables which is computed by dividing the covariance of the two samples by the product of their standard deviations.

We explored clustering and relationships among our data using multidimensional scaling (MDS) which is a statistical technique used to visually represent the distances between multiple datasets, with similar variables plotted close together and dissimilar variables plotted far apart from each other. MDS maintains the multidimensional distances between each sample pair while presenting all the samples in two-dimensional plots. The patterns in the MDS plots are not relevant, only the relative distance among the points.

Any distance metric can be used to construct MDS plots. For our analysis, we evaluated six different distance measures: Euclidean, Manhattan, Minkowski, Canberra, Spectral Angle, and Pearson Correlation (which is considered measure of distance). While they can all provide insight into the relationships among our data, we give the greatest weight to the distance measures that produced the highest Spearman Rank Correlation Coefficients ( $\rho$ ), as those measures are considered the best relational representations of the data. We generated these distance measures and MDS plots using R version 4.4.1 and the base R stats package.

### 4.3 Results and Discussion

#### 4.3.1 Core Depth, Color, and Texture

Our initial experimental design was to collect 2.4-meter-deep cores from each sampling site, and while we managed to do this for several core samples, we could not drive the core sampler down to 2.4 m at most locations. To ensure fair comparisons across core samples, we excluded sediment core data beyond the depth of the shortest core when making comparisons between cores. We established this limit at 1.4 m, the depth of the Goshen North core sample, which was the shallowest core we collected. Figure 4.5. Comparison of core depths and colors, with subsamples shown as individual rectangles within each core. The core depths have been corrected for core shortening, resulting in unequal intervals between subsamples (see Section 2.6). The subsample colors are the actual colors observed using Munsell color matching charts [108]. The red dashed line indicates the depth of the shallowest core sample (rounded to 140 cm), which was used as the comparison limit for sediment core data across all samples above this depth. presents all the core samples after adjusting for core shortening along with a red dashed line indicating the depth at 1.4 m.

We visually examined all 5-cm subsamples and assigned colors from the Munsell color index (Figure 4.5). The core depths have been corrected for core shortening, resulting in unequal intervals between subsamples (see Section 2.6). The subsample colors are the actual colors observed using

Munsell color matching charts [108]. The red dashed line indicates the depth of the shallowest core sample (rounded to 140 cm), which was used as the comparison limit for sediment core data across all samples above this depth.). The resulting colors were generally gray or brown, with hues in the 2.5Y and 10YR categories, lightness values between 4 and 8, and chroma values between 1 and 3. We included the color names (i.e. Gray, Light Gray, etc.) in Figure 4.5. Comparison of core depths and colors, with subsamples shown as individual rectangles within each core. The core depths have been corrected for core shortening, resulting in unequal intervals between subsamples (see Section 2.6). The subsample colors are the actual colors observed using Munsell color matching charts [108]. The

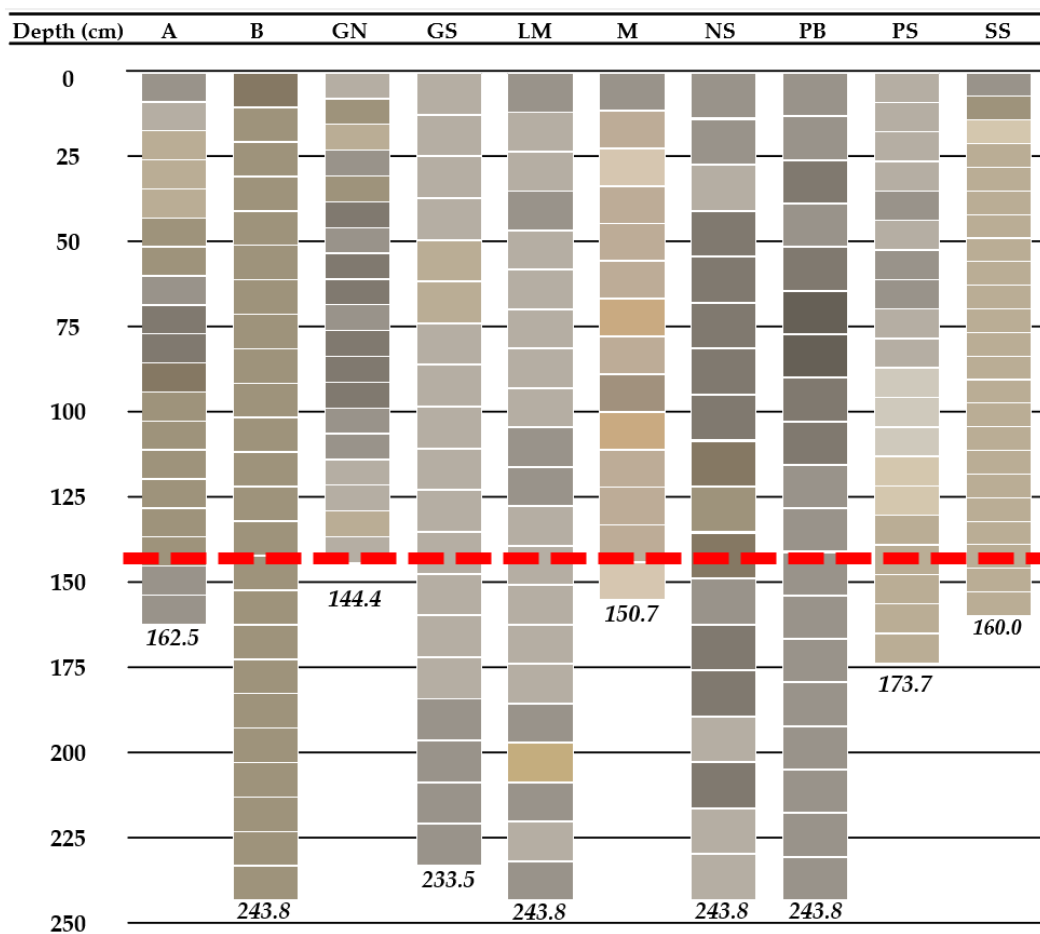


Figure 4.5. Comparison of core depths and colors, with subsamples shown as individual rectangles within each core. The core depths have been corrected for core shortening, resulting in unequal intervals between subsamples (see Section 2.6). The subsample colors are the actual colors observed using Munsell color matching charts [108]. The red dashed line indicates the depth of the shallowest core sample (rounded to 140 cm), which was used as the comparison limit for sediment core data across all samples above this depth.

red dashed line indicates the depth of the shallowest core sample (rounded to 140 cm), which was used as the comparison limit for sediment core data across all samples above this depth, but noted that the names can apply to multiple Munsell notation categories [108] and can therefore be applied to multiple, albeit similar colors.

Core samples lake-wide were primarily silty with occasional gravel and sandy layers (we did not attempt to distinguish between clay and silty textures). The Airport core appeared to be an anomaly among the core samples, being composed almost exclusively of sand. Other studies have observed sandy sediments along the shoreline of Utah Lake and near the mouths of its major tributaries [90, 94]. Because the site of the Airport core located 3.15 km (2 mi) south of the mouth of the Provo River, the sand within this core was likely transported to the lake by the Provo River and then moved southward by longshore drift [112]. A summary of the textures and colors exhibited by the Airport core is shown in Table 4.2; similar information for the 9 other sediment cores is provided in the Appendix.

Table 4.2. Texture and color of the Airport core sample.

Depth (cm)	Texture	Munsell Notation	Color Name	Color
0.00	Sandy	2.5Y 6/1	Gray	
9.03	Silty Sand	2.5Y 7/1	Light Gray	
18.05	Silty	2.5Y 7/2	Light Gray	
27.08	Silty	2.5Y 7/2	Light Gray	
36.10	Silty	2.5Y 7/2	Light Gray	
45.13	Silty Sand	2.5Y 6/2	Light Brownish Gray	
54.15	Silty Sand	2.5Y 6/2	Light Brownish Gray	
63.18	Silty Sand	2.5Y 6/1	Gray	
72.20	Sandy	2.5Y 5/1	Gray	
81.23	Sandy	2.5Y 5/1	Gray	
90.25	Sandy	2.5Y 5/2	Grayish Brown	
99.28	Sandy	2.5Y 6/2	Light Brownish Gray	
108.31	Sandy	2.5Y 6/2	Light Brownish Gray	
117.33	Sandy	2.5Y 6/2	Light Brownish Gray	
126.36	Sandy	2.5Y 6/2	Light Brownish Gray	
135.38	Sandy	2.5Y 6/2	Light Brownish Gray	
144.41	Sandy	2.5Y 6/2	Light Brownish Gray	
153.43	Sandy	2.5Y 6/1	Gray	
162.46	Sandy	2.5Y 6/1	Gray	

## 4.3.2 Elemental Concentrations

### 4.3.2.1 Analysis and Detection

Elemental analysis with a Thermo Scientific iCAP 7400 ICP-OES allowed us to measure the concentration of the following 25 elements from our sediment core subsamples: Al, As, B, Ba, Ca, Cd, Co, Cr, Cu, Fe, K, Mg, Mn, Mo, Na, Ni, P, Pb, S, Se, Si, Sr, Ti, V, and Zn (Table 4.3). Calcium (Ca) was the predominant element across all cores, followed by major elements Al, Fe, K, and Mg. Minor elements included Ba, Mn, Na, P, S, Si, Sr, and Ti, and the remaining ICP-detectable elements are considered trace elements.

Across the lake, we found that elemental concentrations were right-skewed, suggesting that while high levels are uncommon, they do occur occasionally (Table 4.3; Figure 4.6). Measurements for all elements were generally within detection limits, with the minimum detection limits ranging between 2-50 ppb, depending on the element. On the occasion when measurements did fall below these limits—most often for Se and Mo—we replaced the values with zeroes.

Table 4.3. Summary statistics for elemental concentrations across all sediment cores.

Element	Mean	Median	Standard Deviation	Skewness	Element	Mean	Median	Standard Deviation	Skewness
Al	3577	3024	1921	1.3	Mo	1.9	0.77	3.5	3.1
As	7.0	4.6	9.2	3.2	Na	537	463	303	1.8
B	13	12	6.1	0.8	Ni	8.3	7.4	3.6	0.6
Ba	112.5	85	86	2.5	P	530	498	143	0.7
Ca	89543	84941	43819	0.5	Pb	6.9	5.9	4.6	1.8
Cd	0.71	0.66	0.3	0.5	S	1462	578	1879	2.1
Co	3.2	2.9	1.4	1.2	Se	0.98	0.31	1.3	1.5
Cr	26.3	25	11	1.1	Si	372	378	202	0.3
Cu	7.7	6.2	4.6	0.8	Sr	280	217	212	1.4
Fe	6906	6309	2992	0.7	Ti	121	102	84	4.1
K	1491	1096	1115	1.7	V	31	28	14	1.2
Mg	9484	8600	4979	1.8	Zn	33	28	18	2.1
Mn	387	333	193	1.2					

### 4.3.2.2 Relationship Between Elements

Pearson Correlation analysis of all sediment cores revealed that 43% of all element comparisons were strongly correlated ( $r > 0.5$ ; Figure 4.6). The most frequent elements among these comparisons were B, Cd, Cu, Fe, K, and Mn. On the other hand, As, Se, and Ti were not strongly correlated with any other elements. All remaining elements were strongly correlated with at least one other element.

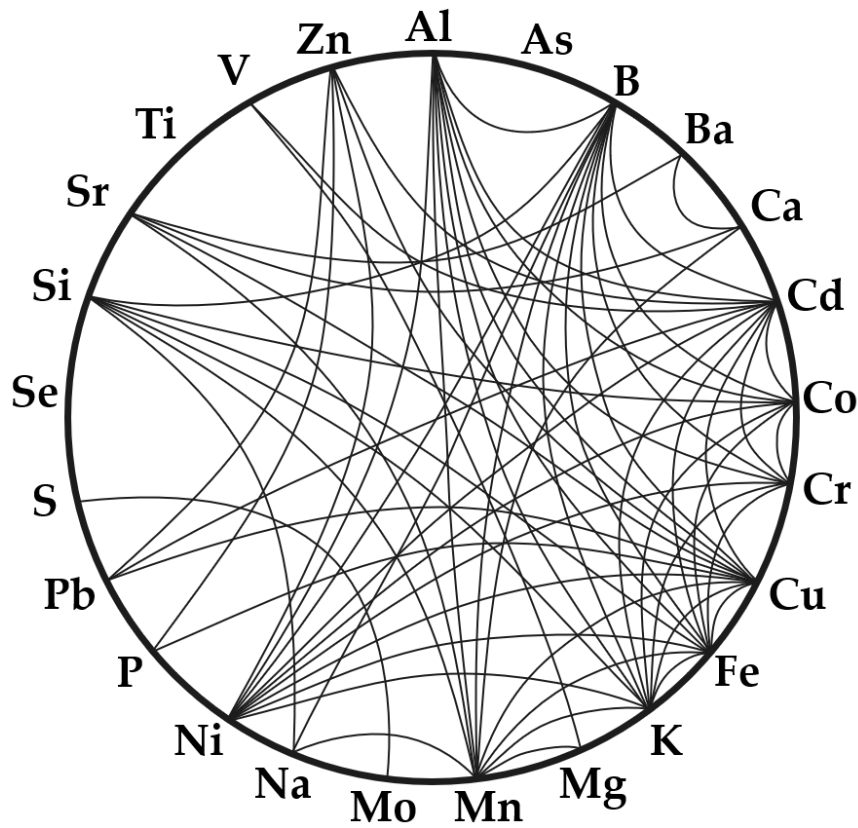


Figure 4.6. Strongly correlated ICP-detectable elements ( $r > 0.5$ ) from all 10 sediment cores.

When the normalized distribution of these elements is plotted (Figure 4.7), the elements that frequently show strong correlations with others tend to have the highest normalized mean concentrations. The opposite is also true, with the elements having the fewest strong correlations with others tending to also have the lowest normalized mean concentrations. This seems to indicate a connection between an element's concentration and the frequency with which it strongly correlates with other elements. There are several notable exceptions to this, such as P, Ca, and V which have high normalized mean concentrations while only having a few strong correlations with other elements. Another notable exception is K, which only has a moderate normalized mean concentration while having a high number of strong correlations.

For our MDS analyses of elemental concentration (Figure 4.8), the Manhattan and Euclidean distance metrics had the highest Spearman rank correlations, with  $\rho = 0.922$  and  $0.875$ , respectively. When plotted, the Manhattan and Euclidean distances form a similar distribution pattern, isolating P, Se, and Si, while creating a loose cluster with As, Mo, S, and Ti,

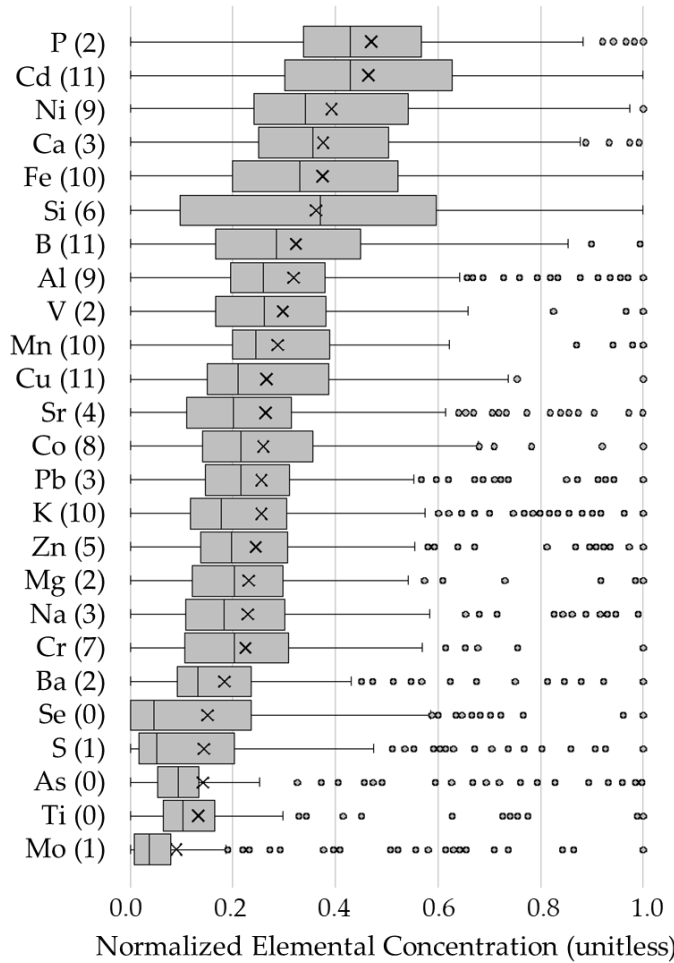


Figure 4.7. Min-max normalized distribution of elemental concentrations across all 10 core samples. The elements are listed in descending order by mean concentration, with the means represented by an X in each boxplot. The numbers in parentheses next to each element symbol indicate the number of strong correlations that element has with other ICP-detectable elements.

as well as a larger cluster encompassing most other elements. The MDS plot with Canberra distances ( $\rho = 0.874$ ) emphasizes this clustering pattern, further isolating Se while distancing the loose cluster of As, Mo, S, and Ti even more from the cluster of the remaining elements.

In summary, our analytical methods found a connection between elemental concentration and correlation frequency among most ICP-detectable elements in Utah Lake sediments, with higher normalized mean concentrations associated with a higher number of strong correlations with other elements, and vice versa. Elements can be clustered according to this pattern, with exceptions assigned to their own cluster. MDS plots support clustering As, Mo, S, and Ti (which collectively have low normalized mean concentrations and few correlations) as their own cluster, as well as isolating Se as a separate cluster.

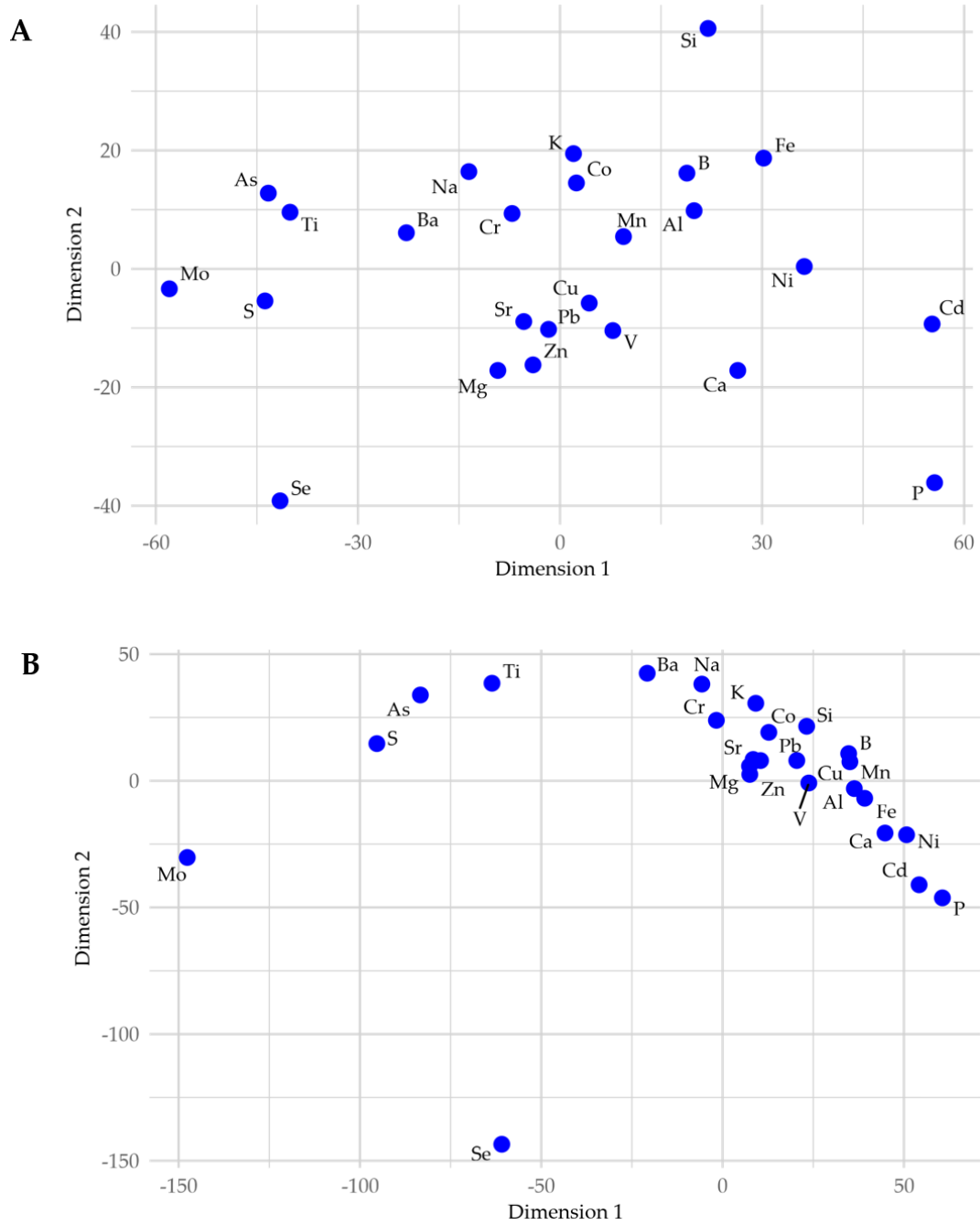


Figure 4.8. Multidimensional scaling results for ICP-detectable elements from all 10 sediment cores using Manhattan distances (panel A;  $\rho = 0.922$ ) and Canberra distances (panel B;  $\rho = 0.874$ ). Although Canberra distances have a slightly lower rank correlation ( $\rho$ ) than Euclidean distances, we chose to display them here because they better emphasize the clusters shown by the Manhattan distances, while Euclidean distances display a similar pattern to the Manhattan distances.

#### *4.3.2.3 Relationship with Sample Depth*

When assessed collectively, the Pearson Correlation between sample depths was very strong, with 89% of depth comparisons showing strong correlations. Clearer trends emerged when we assessed core samples individually, demonstrating the presence of localized effects across Utah Lake. When viewed in this manner, the elements most frequently correlating positively with depth (i.e., increased with depth) were Mn, Al, Fe, K, and V. The elements most frequently correlating negatively with depth (i.e., decreased with depth) were Ba, Cu, P, Pb, Sr, and Zn, while the elements that most frequently exhibited little-to-no correlation with depth were Se, Cr, Mo, Si, B, Cu, P, S, Ti, and Zn. Some elements, such as Cu and P, show up in more than one category, thus demonstrating different depositional patterns across Utah Lake sediments.

All the core samples exhibited trends across multiple elements. The cores with  $\geq 10$  elements with moderate to strong positive correlations with depth were the Benjamin, Goshen North, Lindon Marina, North Shore, and Powell Slough cores. On the other hand, the cores with  $\geq 10$  elements with moderate to strong negative correlations with depth were the Airport, Goshen South, and Provo Bay cores. The remaining sampling sites, Mosida and Saratoga Springs, were composed primarily of elements with little-to-no correlation with depth. Figure 4.9 displays the elemental trends in Benjamin and Provo Bay as examples of positive and negative correlations with depth.

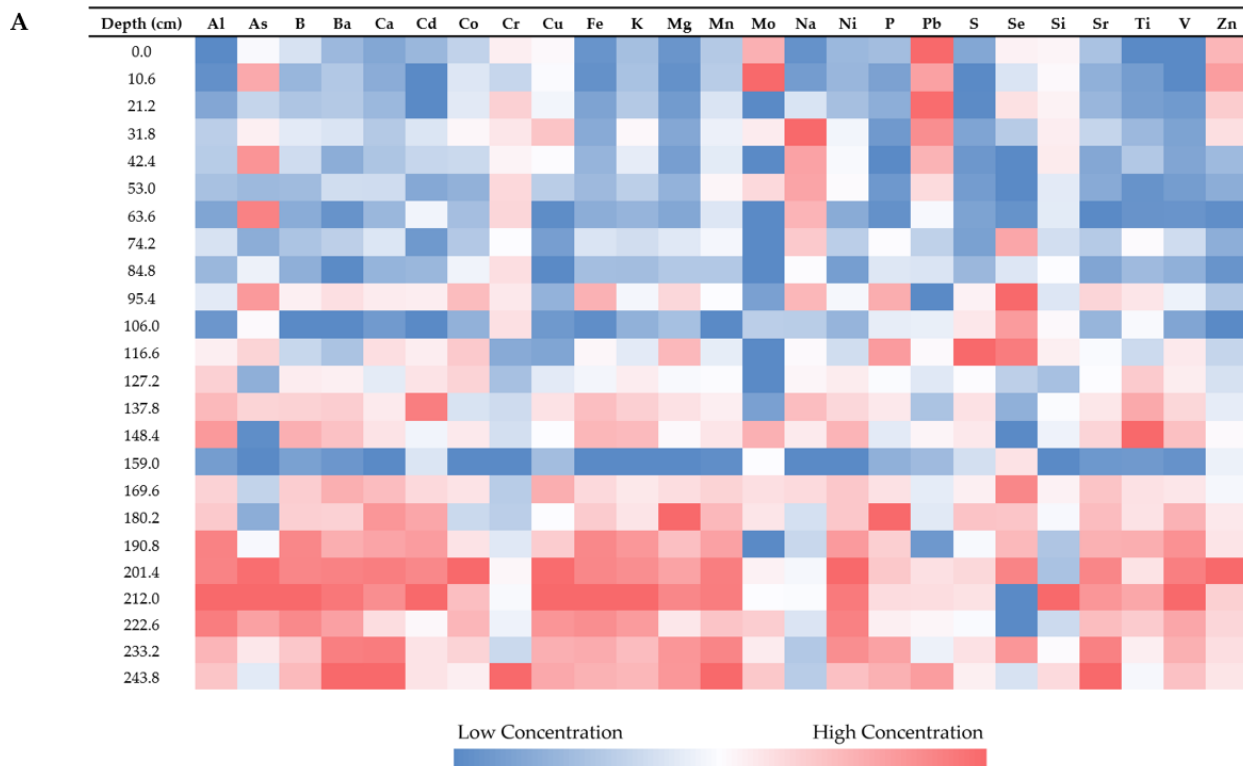
For the MDS analyses of sample depth, the Pearson Correlation and Spectral Angle distance metrics had the highest Spearman rank correlations, with  $\rho = 0.963$  and 0.925, respectively. The MDS plots for these and our other distance measures all display meandering patterns of sample points arranged in an approximately sequential order (Figure 4.10). This demonstrates a continuous transition between subsample concentrations, as would be expected for depth-related data. Large breaks in these patterns suggest a broad shift in elemental composition. While breaks occur at different points for different distance measures, perhaps the most interesting break occurs between 30-40 cm in the plots for both the Canberra and Manhattan distances ( $\rho = 0.916$  for both). Previous Utah Lake sediment core studies have identified the approximate depth coinciding with the arrival of European settlers at 30–40 cm deep (13-15). A gap at this position supports the notion that Utah Lake experienced significant geochemical changes following European settlement around the lake.

In summary, a variety of relationships exist between elemental concentration and sample depth. Mn, Al, Fe, K, and V often increase with depth whereas Ba, Cu, P, Pb, Sr, and Zn often decrease with depth. Se, Cr, Mo, Si, B, Cu, P, S, Ti, and Zn have also been found to remain consistent with depth. Broad trends in elemental concentration are often observed in

Utah Lake sediments, with most core samples exhibiting a general increase with depth although the opposite trend has been observed in some cores. Canberra and Manhattan distance metrics indicate that a geochemical shift occurs in Utah Lake sediments between 30-40 cm deep, coinciding with the arrival of European settlers [99-101].

#### *4.3.2.4 Relationship with Sample Location*

Pearson Correlation analysis of sample locations revealed that only 4% of location comparisons yielded a strong correlation. This included the Lindon Marina core strongly correlating with the North Shore core ( $r = 0.60$ ), and the Mosida core strongly correlating with the Saratoga Springs core ( $r = 0.54$ ). These correlations seem reasonable as the sites for these correlated samples share some geographic similarities. Both the Lindon Marina and North Shore cores were collected from the northern end of Utah Lake, and the Mosida and Saratoga Springs cores were collected as close as possible to the Lake Mountains before we encountered rocky sediment. While strong correlations between sampling sites weren't common, most showed moderate correlations with at least one other site with the exception of the Goshen North core, which did not correlate with any other locations.



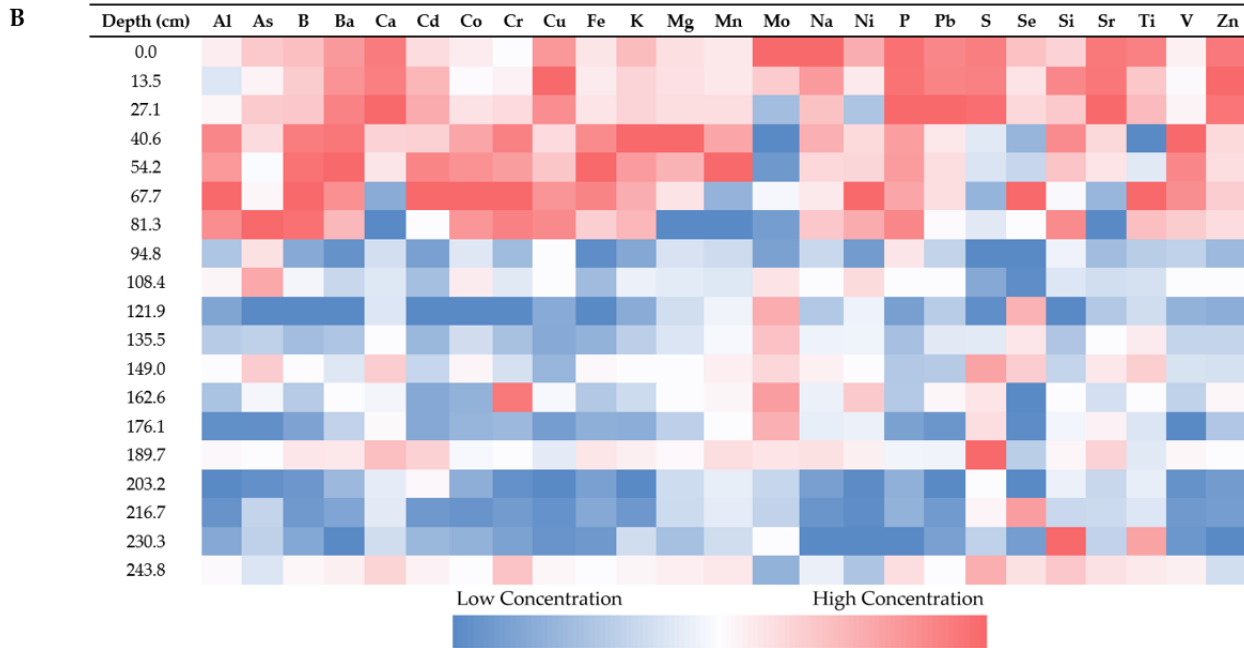


Figure 4.9. Min-max normalized elemental concentrations for the Benjamin (A) and Provo Bay (B) cores. The Benjamin core shows high elemental concentrations at greater depths while the Provo Bay core shows high concentrations near the surface, thus exhibiting opposite depth correlations. Chemostratigraphic variation is apparent in both cores as shown by the layer of low elemental concentration at 159.0 cm deep in the Benjamin core as well as the layer of moderate elemental concentration at 189.7 cm deep in the Provo Bay core. Notably, both sediment cores show high Pb concentrations near the surface, strongly indicating recent regional anthropogenic activity.

For the MDS analyses of sample locations, the Canberra and Euclidean distance metrics had the highest Spearman rank correlations, with  $\rho = 0.929$  and  $0.917$ , respectively. Each distance metric isolates different sampling locations (Figure 4.11), with the Canberra distances primarily isolating the Airport core while the Euclidean distances likewise isolates the Airport core in addition to the Goshen North, Saratoga Springs, and Provo Bay cores. The uniqueness of some of these cores is readily apparent, such as the large anthropogenic impact on Provo Bay or the sandiness of the Airport core. The uniqueness of the other isolated cores is less forthcoming.

Considering that we compared data from only 10 sampling sites, our analytical methods had limited capacity to detect extensive relationships or irregularities. However, we found that the Lindon Marina and North Shore cores were geochemically correlated, as were the Mosida and Saratoga Springs cores. In contrast, the Airport, Goshen North, and Provo Bay cores appeared to be the most geochemically distinct from the others.

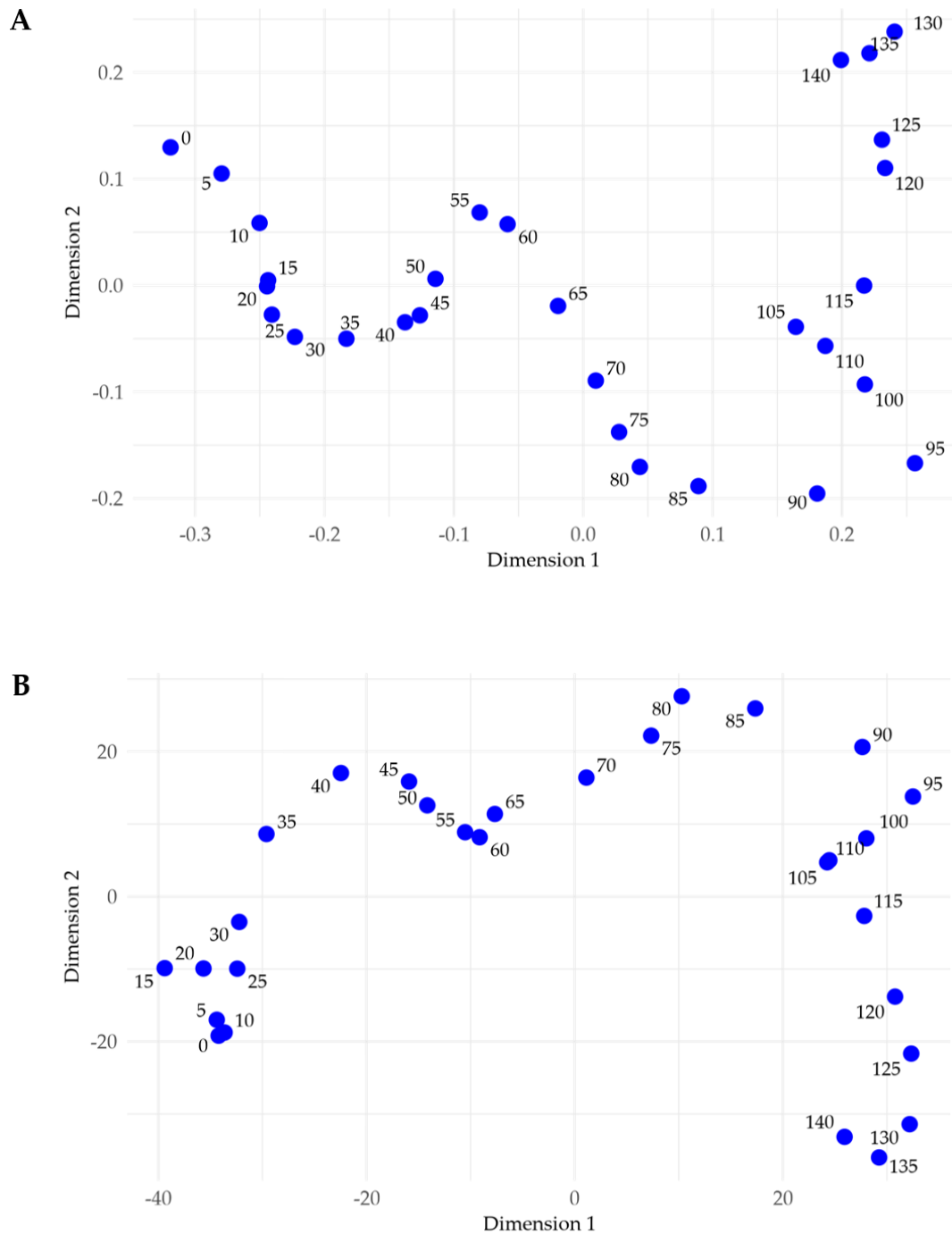


Figure 4.10. Multidimensional scaling results for sample depths 0-140 cm from all 10 sediment cores using Pearson Correlation distances (panel A;  $\rho = 96.3$ ) and Canberra distances (panel B;  $\rho = 0.916$ ). We show the MDS plot of Canberra distances rather than Spectral Angle distances ( $\rho = 0.925$ ) because the Canberra distances display a gap between 30-40 cm. This depth coincides with the arrival of European settlers and is therefore expected to be a point of shifting geochemical trends in Utah Lake sediments.

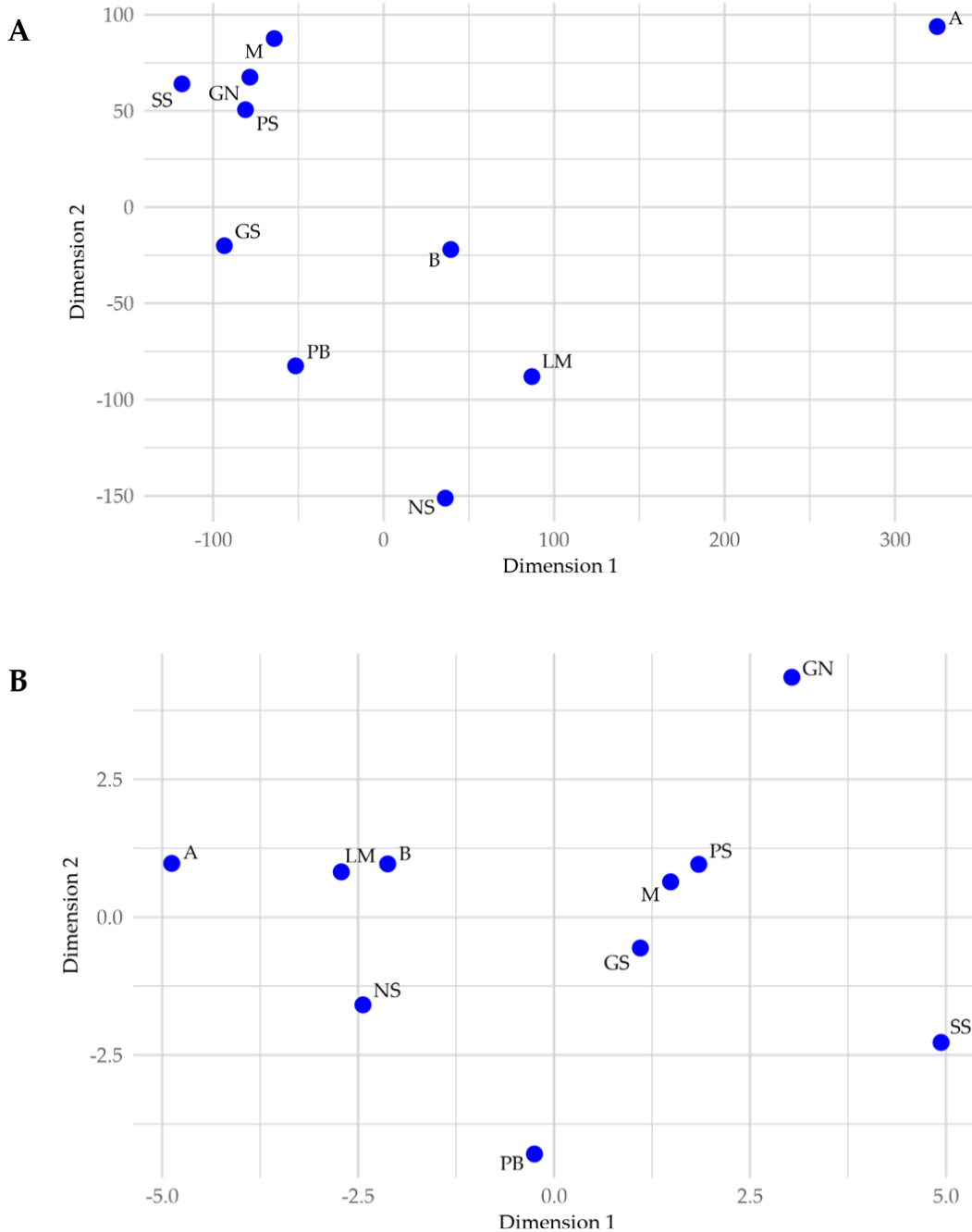


Figure 4.11. Multidimensional scaling results for all 10 sample locations using Canberra distances (panel A;  $\rho = 0.929$ ) and Euclidean distances (panel B;  $\rho = 0.917$ ). These plots appear to be better at identifying geochemically unique cores, such as the Airport core, rather than clustering similar cores together.

#### 4.3.3 Fractional Calcium Carbonate

We collected six subsamples from each sediment core for fractional  $\text{CaCO}_3$  analysis, totaling 60 samples (Figure 4.12). While there were no apparent  $\text{CaCO}_3$  trends with depth, the cores'  $\text{CaCO}_3$  content appears to be

associated with sediment texture, with siltier samples having moderate to high levels of  $\text{CaCO}_3$ , whereas sandy samples exhibited much lower levels of  $\text{CaCO}_3$ . The median  $\text{CaCO}_3$  content for all subsamples was 23 wt.%, with three quarters of the subsamples falling between 15-30 wt.%. Of the remaining subsamples, nearly a tenth exceeded 30 wt.% with the remainder falling below 15 wt.%. The samples above 30 wt.% included the topmost portions of the Powell Slough core (< 75 cm) and the deepest subsamples from the Mosida core (> 80). On the other hand, the samples below 15 wt.% included all samples from the Airport core, the topmost subsamples from the Saratoga Springs core (0 cm), and deeper subsamples from the Goshen North core (at 112 cm).

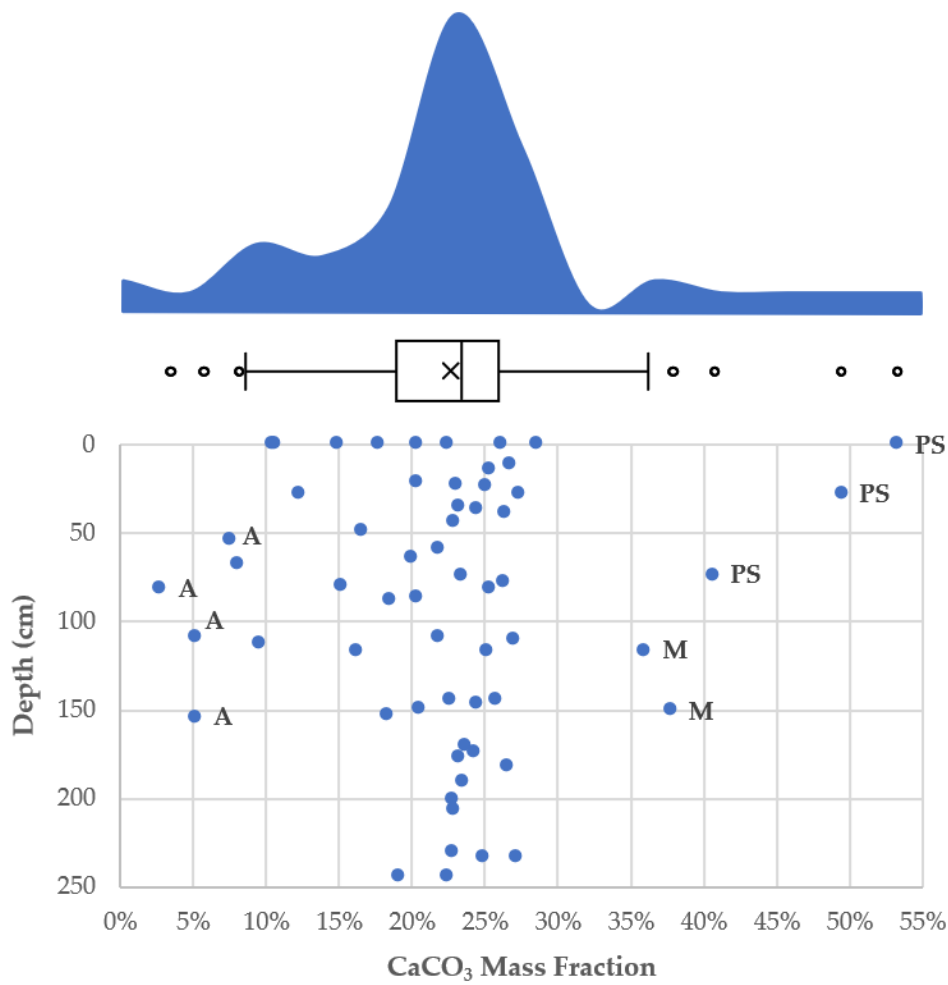


Figure 4.12. Fractional  $\text{CaCO}_3$  from near-shore core samples from Utah Lake.  $\text{CaCO}_3$  appears to be more closely associated with sediment texture than it is with depth, with non-silty sediments exhibiting lower levels of  $\text{CaCO}_3$ . Outliers are labeled by location.

#### 4.3.4 Fractional Organic Matter

Duplicate subsamples were collected from the same sediment layers sampled for fractional  $\text{CaCO}_3$  analysis, producing 60 samples for fractional OM analysis (Figure 4.13). The samples have a median OM value of 1.3 wt.%, with the majority of subsamples (90%) falling below 3.0 wt.%. The subsamples that exceed 3.0 wt.% came exclusively from the bays and were usually less than 1 m deep. These samples included most subsamples from the Provo Bay core (< 230 cm) and the topmost and bottommost subsamples from the Goshen South core (< 40 cm and at 234 cm, respectively).

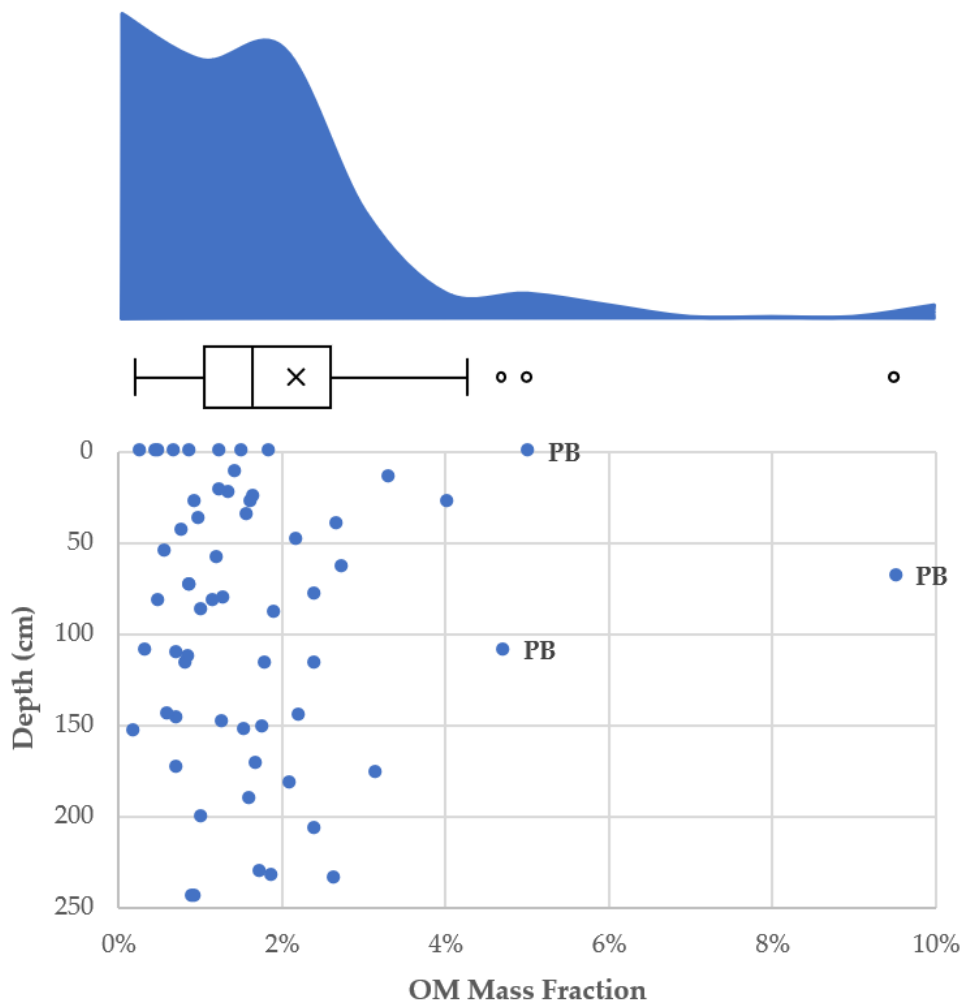


Figure 4.13. Fractional OM from near-shore core samples from Utah Lake. Elevated levels of OM tend to be associated with core samples collected from the bays, often less than 1 m deep. Outliers are labeled by location.

### 4.3.5 Sediment Phosphorus

#### 4.3.5.1 The Use of Sediment Phosphorus for Paleolimnological Studies

Because P is a key nutrient that helps regulate the productivity of water bodies, sediment core P has the potential to reveal historical trends in P loading and trophic status. This process, however, isn't always straightforward. Sediment profiles for total P (as measured in this study) are useful for determining the current trophic status of a lake [113], but the mobility of P in sediments, particularly P associated with redox-sensitive materials, causes total P to not necessarily reflect historical P loading to lakebed sediments [114].

The analysis of less-mobile P fractions through sequential extraction procedures is a promising alternative, but such methods must account for the unique chemical behavior of each water body and its sediments [88]. Researchers are developing a method to use P coprecipitated with  $\text{CaCO}_3$  to study historical P loading and trophic status of Utah Lake prior to the arrival of European settlers [98, 100]. While this method shows potential, further research is needed to determine whether  $\text{CaCO}_3\text{-P}$  extraction is more effective than Ca-P extraction and to determine how autogenic  $\text{CaCO}_3\text{-P}$  or the potential dissolution of  $\text{CaCO}_3\text{-P}$  might affect the reliability of a  $\text{CaCO}_3\text{-P}$  extraction method.

The sediment core data from this study cannot be used to determine Utah Lake's past trophic status or historical P loading. However, the key objective for this study was to enhance the representation of sediment core P across Utah Lake as a means of addressing the limitations of previous studies that relied on four or fewer core samples to characterize the lake. By collecting 10 lakebed cores from throughout Utah Lake and analyzing them for 25 ICP-detectable elements along with fractional  $\text{CaCO}_3$  and OM, we have created a dataset that provides deeper insights into P and its relationship with other chemical constituents in Utah Lake sediments.

#### 4.3.5.2 Phosphorus Concentration-Depth Profiles

Sediment core P from our 10 sediment cores ranges from 166-941 mg kg<sup>-1</sup>, with an interquartile range of 428-606 mg kg<sup>-1</sup>, a median concentration of 498 mg kg<sup>-1</sup>, and a mean concentration of 530 mg kg<sup>-1</sup>. This data is visualized in greater detail in Figure 4.14, Figure 4.15, and Figure 4.16, which respectively present a connected scatterplot, depth distributions, and a normalized heatmap of the data. These figures show that while P generally decreases with depth, as exhibited by the Goshen North, Goshen South, and Provo Bay cores, this trend is not ubiquitous throughout the lake. The Benjamin and Lindon Marina cores instead show P increasing with depth, while most other core samples show elevated levels of P at intermediate depths.

Carey and Rydin [113] explain that the mean sediment P profile within the top 30 cm of lakebed sediment corresponds to the trophic status of a lake. They found that sediment P decreases with depth in eutrophic lakes, while P remains consistent with depth in mesotrophic lakes, and P increases with depth in oligotrophic lakes. As shown in Figure 4.15A, among the highest mean sediment P is at the surface, with concentrations dipping slightly before returning to elevated levels, and then remaining consistent down to 30 cm deep. A profile such as this would suggest that Utah Lake is oligotrophic. However, when the profile is shown down to 140 cm deep, the overall trend is a gradual decrease of P with depth.

While Utah Lake is unquestionably eutrophic, the sediment P profiles of individual core samples do not always correspond with the sediment P profiles expected in a eutrophic lake (Figure 4.15B). This phenomenon may be unique to Utah Lake and other shallow lakes because their lakebed sediments are more susceptible to being reworked, thus obscuring sediment P within the topmost portions of the lakebed. Deeper lakes with a more stable lakebed likely don't require more than 30 cm to identify the lake's trophic status, but we hypothesize that shallow lakes require deeper sediment P profiles in order to accurately determine their trophic status. This phenomenon also underscores the importance of collecting numerous core samples to accurately represent large lakes, as variations in sediment composition across different areas may lead to misleading assessments of the lake's trophic status. A larger number of samples is therefore needed to ensure a more reliable measurement of the lake's sediment P content.

#### *4.3.5.3 Connection to Calcium and Iron*

Our analysis identified P as distinct among the ICP-detectable elements in Utah Lake sediments for the following reasons:

- P has a high normalized mean concentration but few strong correlations with other elements.
- P has variable depth trends, decreasing in concentration in some cores, remaining stable in others, and even increasing in some cases.
- P is geochemically isolated, as highlighted by Manhattan distances in a multidimensional scaling (MDS) plot of lake-wide elemental concentrations.

Despite its unique behavior, P has noteworthy relationships with Ca and Fe, which, like P, exhibit some of the highest normalized mean concentrations (Figure 4.7).

The primary link between P and Ca in Utah Lake sediments is through  $\text{CaCO}_3$ , which coprecipitates with P, making Ca-bound P one of the largest P fractions in the lakebed [40, 115, 116]. Despite this relationship, P shows only weak correlations with Ca and  $\text{CaCO}_3$  ( $r = 0.26$  and  $0.27$ , respectively),

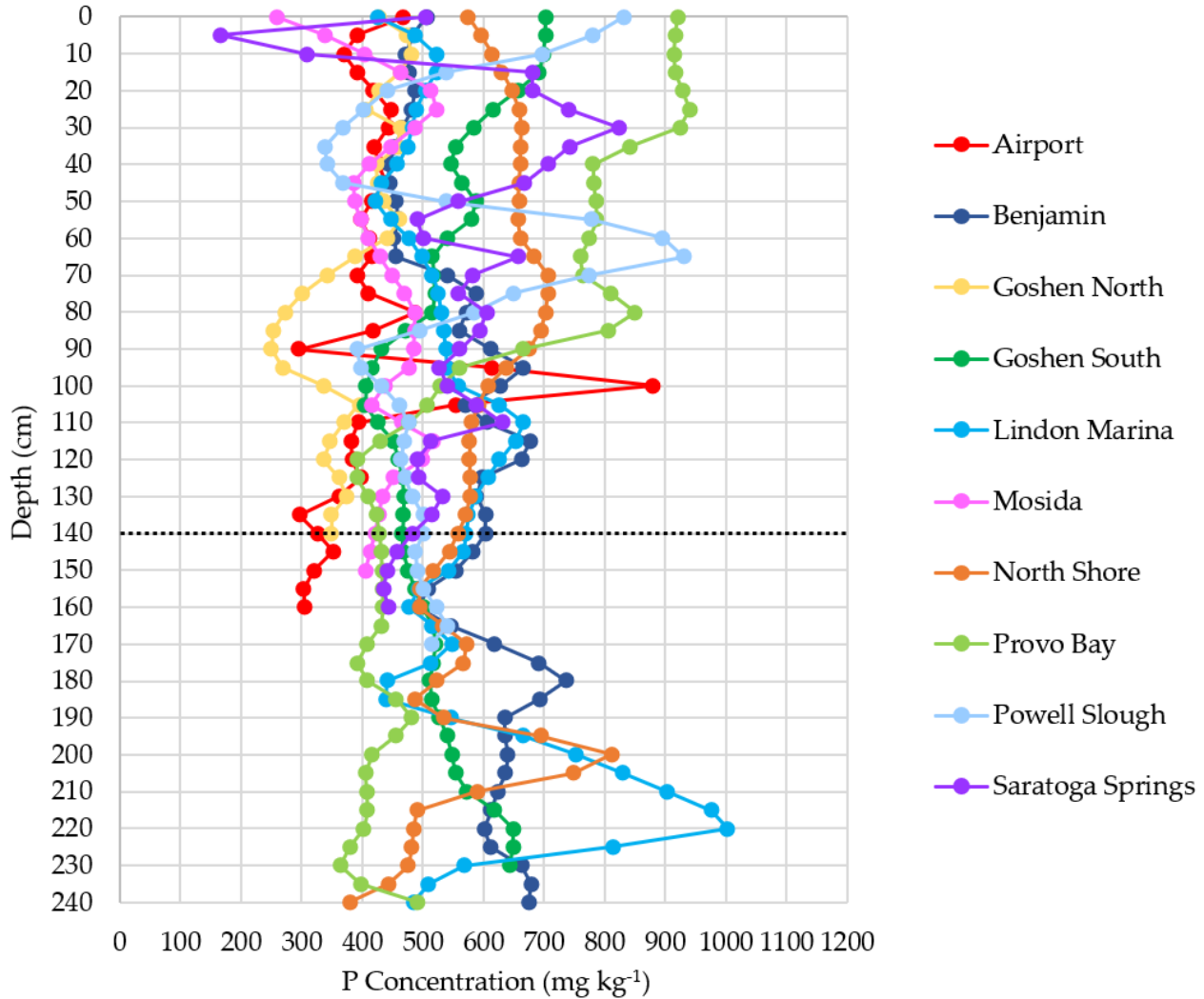


Figure 4.14. Interpolated P concentrations across all 10 sediment core samples. The dotted black line shows the depth of the shallowest core, marking the point reached by all sediment cores.

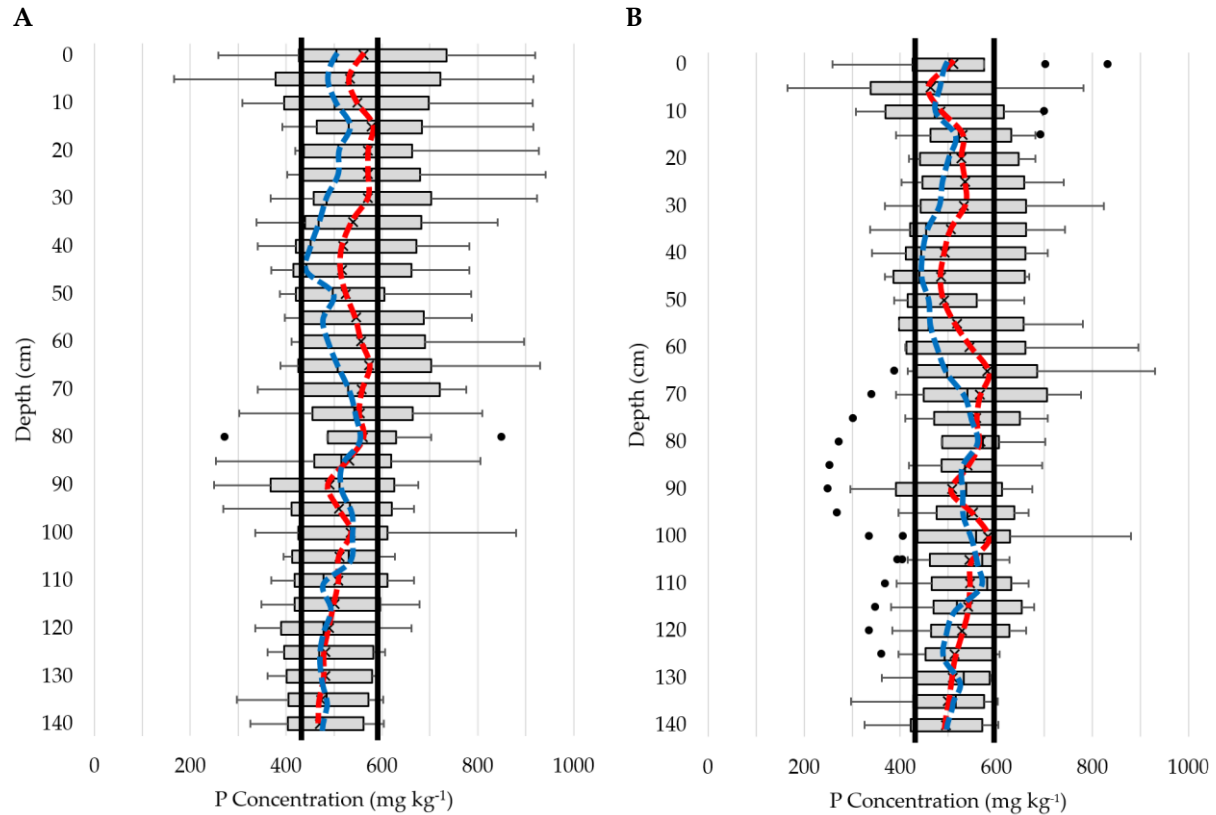


Figure 4.15. Distribution of sediment P down to 140 cm deep from all 10 core samples (panel A) and the non-bay core samples (excluding Goshen North, Goshen South, and Provo Bay; panel B). The red dashed line marks mean concentration while the blue dashed line marks median concentration. Black vertical lines are shown on either side of the means and medians to emphasize the trends with depth. The consistency shown in the top 30 cm of both plots resembles the sediment P profile of mesotrophic lakes. However, a look at the overall trend down to 140 cm is consistent with a eutrophic sediment P profile (decreasing with depth) in panel A, and an oligotrophic sediment P profile (increasing with depth) in panel B. Inclusion of the Goshen Bay and Provo Bay cores is critical for creating a lake-wide sediment P profile that aligns with Utah Lake's eutrophic status. Conversely, the exclusion of the Goshen Bay and Provo Bay cores indicates that sediments across most of Utah Lake are not significantly impacted by P.

Depth (cm)	A	B	GN	GS	LM	NS	M	PB	PS	SS
0	468	507	428	703	426	259	575	920	832	503
5	392	483	474	702	487	338	596	916	781	166
10	370	472	481	699	522	405	615	915	696	308
15	392	478	464	692	522	463	631	916	538	681
20	419	487	428	657	505	514	646	928	441	681
25	446	482	407	616	489	523	659	941	402	740
30	442	466	464	584	482	487	662	924	368	823
35	421	454	460	554	475	447	661	842	338	743
40	427	443	423	545	458	412	661	782	341	707
45	440	444	425	565	431	386	660	782	369	668
50	416	457	434	588	422	388	658	786	539	559
55	397	459	462	580	446	398	656	787	780	490
60	413	453	440	540	477	411	661	775	896	500
65	416	457	388	516	498	429	684	760	930	657
70	391	540	341	518	516	449	706	763	776	582
75	411	587	302	521	525	471	707	810	649	560
80	488	572	272	515	531	486	702	850	585	605
85	419	561	253	472	535	487	695	805	495	594
90	296	612	250	431	538	485	675	664	392	562
95	615	667	269	416	540	476	637	561	397	527
100	880	628	336	406	558	436	606	529	432	540
105	553	571	394	405	627	416	592	507	461	589
110	393	606	369	426	667	465	581	478	477	631
115	381	678	348	451	653	518	577	430	469	514
120	384	662	336	461	627	499	577	392	464	491
125	397	597	362	467	606	452	578	392	471	493
130	362	589	374	470	587	434	578	409	483	532
135	297	603	350	468	575	428	571	424	501	515
140	326	604	349	466	571	421	559	428	500	483



Figure 4.16. P concentrations for each of the 10 sediment cores, with the color scale of each core corresponding to that core's minimum and maximum concentrations. While P generally decreases with depth as shown by the Goshen North, Goshen South, Provo Bay cores, this trend doesn't occur universally across all core samples.

likely because Ca is relatively immobile in lakebed sediments, whereas certain forms of P, such as ion-exchangeable P and P bound to redox-sensitive materials, are more mobile and can diffuse upward through the sediment [114].

Similarly, P associates with Fe through coprecipitation with Fe-oxyhydroxides under aerobic conditions but can become mobilized under reducing conditions [40]. The weak correlation between P and Fe ( $r = 0.19$ ) may reflect ongoing mobilization of P bound to redox-sensitive Fe. Additionally, Fe appears to diffuse more fully through the sediment, while P concentrations remain elevated in the surface layers.

Sediment concentration data for P, Ca, and Fe as well as the other ICP-detectable elements for all 10 sediment cores are shown in the Appendix.

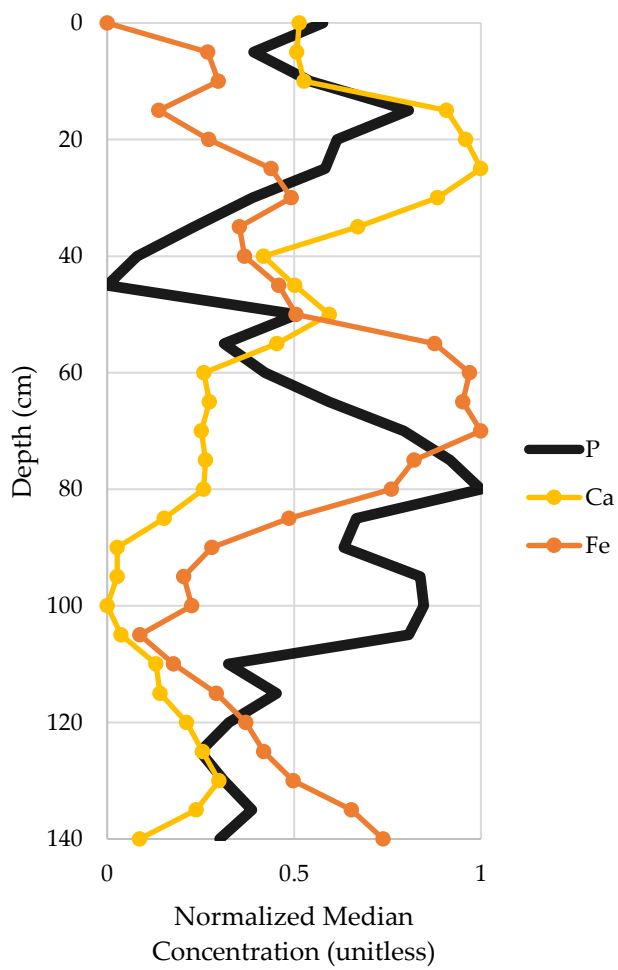


Figure 4.17. Median normalized concentration for P, Ca, and Fe across all 10 core samples.

#### 4.3.5.4 Connection to Immobile Pollutants

Across Utah Lake, our sediment core data reveal strong to moderate correlations between P and Zn, Cu, Pb, Cd, and Ni ( $r = 0.62, 0.50, 0.47, 0.47$ , and  $0.42$ , respectively). Trace metals such as these are generally considered immobile pollutants in lakebed sediments, as explained by Bertrand, et al. [117]. Previous studies, such as Williams, et al. [99], observed increases in Pb, Zn, and Cu concentrations near the surface of Utah Lake core samples, and attribute this to industrial emissions, urban runoff, and coal combustion aerosols over the last century. Our data (Figure 4.18) similarly show elevated levels of these metals above 40 cm depth, coinciding with post-European settlement, followed by declining levels below 20 cm with the exception of P and Pb. Elevated surface concentrations of P are likely the result of sediment-water interactions in a eutrophic water body, while elevated Pb levels may indicate ongoing pollution.

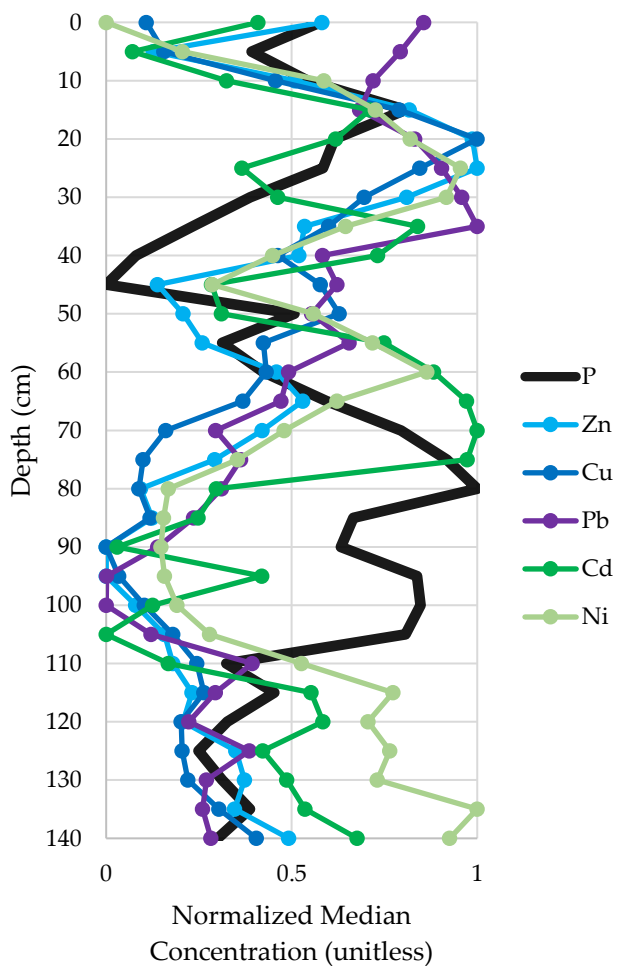


Figure 4.18. Median normalized concentrations for P and strong to moderately correlated immobile pollutants, including Zn, Cu, Pb, Cd, and Ni.

These elements are likewise correlated by location. P, Zn, Cu, Pb, Cd, and Ni all tend to be elevated in the Provo Bay, Goshen South, Powell Slough, and Saratoga Springs cores when compared to other portions of the lake. This correlation, alongside the tendency for P to be elevated in the upper portions of the Goshen North, Goshen South, and Provo Bay cores (Figure 4.16), suggests that Goshen Bay and Provo Bay have likely been impacted by anthropogenic P loading. Lower levels of trace metal pollutants found elsewhere throughout the lake and the non-eutrophic sediment P profile observed when excluding core samples from Goshen Bay and Provo Bay (Figure 4.15B) suggest that lakebed sediments in the main body Utah Lake are less impacted by anthropogenic P loading.

It is important to recognize that the correlation between P and trace metal pollutants does not necessarily imply that they originate from the same sources. While recent trends in these elements may be influenced by human activities following European settlement, the increase in phosphorus deposition in lakebed sediments is more likely attributed to urban and agricultural runoff, wastewater discharge, and heightened erosion than to heavy industrial pollution. Determining the exact cause of these elemental relationships will require further research.

Sediment concentration data for P, the aforementioned trace metal pollutants, and the other ICP-detectable elements for all 10 sediment cores are shown in the appendix.

## 4.4 Conclusion

### 4.4.1 Key Findings

Our analysis of Utah Lake sediments revealed that elements with higher normalized mean concentrations tend to have more strong correlations with other elements. Clustering patterns show that As, Mo, S, and Ti form a distinct group with low concentrations and few correlations, while Se is isolated as its own cluster.

Elemental depth trends show that Mn, Al, Fe, K, and V tend to be positively correlated with depth, while Ba, Cu, P, Pb, Sr, and Zn tend to be negatively correlated with depth, and Se, Cr, Mo, Si, B, Cu, P, S, Ti, and Zn often exhibit no depth correlation. Geochemical shifts identified by Canberra and Manhattan distance metrics at 30–40 cm deep support other studies which found that this depth corresponds to the onset of European settlement near Utah Lake.

$\text{CaCO}_3$  accounts for about 20 wt.% of lake-wide sediment, and is typically associated with fine-grained sediment layers, while OM averages 1.3 wt.%, peaking near the surface. Sediment core P indicates Utah Lake is eutrophic, though individual cores vary in their depositional behavior, highlighting the need for numerous core samples that extend deeper than

30 cm in order to accurately represent large, shallow lakes with reworked sediments.

Sediment P in Utah Lake is connected to several elements. It shares patterns with Ca (via  $\text{CaCO}_3$  coprecipitation) and with Fe (via redox-related coprecipitation) but is weakly correlated with the two likely because of differences in mobility. P is also strong to moderately correlated with several trace metal pollutants, including Zn, Cu, Pb, Cd, and Ni. Elevated P levels in the upper sections of the Goshen North, Goshen South, and Provo Bay cores, combined with high concentrations of immobile pollutants, indicate that Goshen Bay and Provo Bay have likely been more significantly impacted by anthropogenic P loading compared to other portions of the lake. The correlation between P and these metals likely reflects a shared connection to human activities rather than direct pollution. Elevated P levels are more likely driven by urban and agricultural runoff, wastewater discharge, and increased erosion rather than by heavy industrial pollution.

#### 4.4.2 Study Limitations and Suggestions for Future Research

This study involved collecting 10 near-shore lakebed cores from Utah Lake and analyzing them for ICP-detectable elements,  $\text{CaCO}_3$ , and OM. We assessed the relationships between chemical constituents, depth, and sample location while relying on the geochronological work of other studies to give us a historical reference point when evaluating our cores. Researchers who want to incorporate an age component into future sediment core studies will need to identify and analyze specific isotopic, radiometric, or stratigraphic markers to determine the age and historical timeline associated with their sediment cores.

Due to factors beyond our control, we were limited to collecting sediment cores that were near or on the shoreline of Utah Lake. Future sediment core studies on Utah Lake may want to consider collecting numerous cores from throughout the interior of the lake. We also suggest collecting core samples that are moderate in length ( $> 1 \text{ m}$ ) to better capture geochemical trends throughout the reworked sediment.

The dataset we assembled from our core samples represents a comprehensive collection of geochemical data from various locations around Utah Lake. While our initial analysis has provided valuable insights into the lake's sediment composition and depositional history, we recognize that there is still much to uncover. We encourage other researchers to delve into our dataset, apply different analytical techniques, and explore additional questions. We hope this will further enhance our collective understanding of the lake's geochemical processes and contribute to the broader scientific knowledge of sediment dynamics in shallow lakes.

While this study explored relationships between P and other elements in Utah Lake sediment cores, assessing historical P loading and the lake's previous trophic state using P was beyond its scope. As researchers examine the potential of  $\text{CaCO}_3$ -P extraction for such assessments, we encourage further investigation into whether  $\text{CaCO}_3$ -P extraction is more effective than Ca-P extraction. Additionally, we suggest evaluating how autogenic  $\text{CaCO}_3$ -P and the potential dissolution of  $\text{CaCO}_3$ -P could impact the reliability of this extraction method.

## 4.5 Appendix

Table 4.4. Airport Core Sample Results.

Length (cm)	Depth (cm)	Texture	Munsell Notation	Color Name	Color	LOI	CaCO <sub>3</sub>	Al	As	B	Ba	Ca	Cd	Co	Cr	Cu	Fe	K	Mg	Mn	Mo	Na	Ni	P	Pb	S	Se	Si	Sr	Ti	V	Zn
0	0.00	Sandy	2.5Y 6/1	Gray	0.48%	10.4%	1549	0.1	6.5	36.8	37050	0.3	2.1	14.8	1.4	4368	440	5730	228	0.0	199	2.9	468	3.3	233	0.0	166	126	96.4	16.3	22.0	
5	9.03	Silty Sand	2.5Y 7/1	Light Gray	1332	0.0	5.6	33.9	30550	0.3	1.3	12.5	1.3	3268	449	4660	165	0.1	180	3.1	369	1.2	142	1.4	141	128	87.3	15.6	12.0			
10	18.05	Silty	2.5Y 7/2	Light Gray	1874	11.6	8.1	48.4	39675	0.7	2.8	16.2	1.9	5245	650	6350	282	0.0	270	4.3	408	3.4	215	3.9	149	164	108.6	25.4	16.1			
15	27.08	Silty	2.5Y 7/2	Light Gray	0.94%	12.3%	2254	9.6	8.9	59.4	43850	0.6	2.9	17.9	2.1	5738	785	6685	257	0.0	319	6.3	450	3.6	235	0.0	156	176	108.3	27.6	19.3	
20	36.10	Silty	2.5Y 7/2	Light Gray	2068	9.1	8.6	47.3	35925	0.6	2.5	17.7	2.3	4805	708	5703	179	0.0	270	5.7	419	2.0	191	0.0	140	130	113.7	23.3	16.1			
25	45.13	Silty Sand	2.5Y 6/2	Light Brownish Gray	1430	12.4	7.2	24.9	22990	0.3	2.5	15.7	1.1	4373	443	5285	91	0.8	198	4.1	440	1.5	124	1.1	130	54	171.8	23.4	15.6			
30	54.15	Silty Sand	2.5Y 6/2	Light Brownish Gray	0.56%	7.48%	1488	10.8	6.4	30.6	25600	0.4	2.3	14.6	1.6	3818	494	5108	111	0.1	204	4.2	397	2.0	153	0.6	145	69	124.5	19.2	13.2	
35	63.18	Silty Sand	2.5Y 6/1	Gray	1828	1.2	5.7	34.1	30000	0.4	2.5	14.8	3.7	3253	608	5275	116	0.2	248	5.3	419	3.1	203	0.0	146	76	126.1	23.3	15.9			
40	72.20	Sandy	2.5Y 5/1	Gray	1168	1.6	4.5	16.9	11398	0.2	2.4	12.1	1.3	2282	356	3063	50	0.6	205	4.0	387	1.3	145	1.4	153	28	111.7	14.0	12.8			
45	81.23	Sandy	2.5Y 5/1	Gray	0.50%	2.72%	1022	3.9	4.0	13.5	8300	0.2	2.3	11.7	1.3	2219	279	2452	43	0.7	246	4.1	493	1.4	216	0.3	137	21	103.4	12.4	15.9	
50	90.25	Sandy	2.5Y 5/2	Grayish Brown	815	3.2	3.8	12.3	7833	0.3	2.4	22.5	1.4	1893	220	2216	37	0.9	180	5.1	296	0.8	163	1.0	132	19	92.9	11.7	12.1			
55	99.28	Sandy	2.5Y 6/2	Light Brownish Gray	1034	4.0	4.1	25.2	18248	0.2	2.6	21.3	1.1	2471	292	3255	67	0.6	189	2.6	889	1.8	132	0.0	208	44	120.7	14.1	12.9			
60	108.31	Sandy	2.5Y 6/2	Light Brownish Gray	0.32%	5.11%	1088	2.2	4.2	18.3	17075	0.2	2.3	11.8	1.5	2540	307	3640	59	0.8	176	2.5	399	1.5	108	0.0	136	37	109.8	14.5	12.3	
65	117.33	Sandy	2.5Y 6/2	Light Brownish Gray	1481	1.5	5.1	27.4	17330	0.4	1.6	12.7	1.7	3253	435	2898	60	0.9	231	3.2	380	2.1	232	3.7	142	52	115.2	11.1	13.0			
70	126.36	Sandy	2.5Y 6/2	Light Brownish Gray	1027	2.7	4.4	20.5	13655	0.4	1.3	16.2	0.6	2820	310	2362	49	0.9	195	2.1	398	0.3	218	0.6	135	38	78.6	9.7	10.2			
75	135.38	Sandy	2.5Y 6/2	Light Brownish Gray	632	4.3	3.7	14.0	11493	0.2	1.4	13.8	0.6	205	2128	38	1.0	180	1.3	297	0.4	242	3.2	111	27	65.1	7.8	7.4				
80	144.41	Sandy	2.5Y 6/2	Light Brownish Gray	597	6.2	3.9	11.2	13878	0.2	1.8	24.2	0.4	2187	198	2411	44	1.2	151	1.7	353	1.1	294	0.0	126	66.4	8.2	9.2				
85	153.43	Sandy	2.5Y 6/1	Gray	0.20%	5.13%	777	7.5	4.2	12.4	14058	0.4	1.8	11.3	0.4	2880	197	2346	56	1.0	172	2.7	304	1.1	730	0.0	102	31	77.5	8.9	8.3	
90	162.46	Sandy	2.5Y 6/1	Gray	732	3.8	3.8	17.0	14373	0.3	1.6	15.0	0.2	2553	219	2423	51	0.5	181	1.1	305	1.5	601	0.0	123	32	80.1	8.7	7.8			

Table 4.5. Benjianin Core Sample Results.

Length (cm)	Depth (cm)	Texture	Munsell Notation	Color Name	Color	LOI	CaCO <sub>3</sub>	Al	As	B	Ba	Ca	Cd	Co	Cr	Cu	Fe	K	Mg	Mn	Mo	Na	Ni	P	Pb	S	Se	Si	Sr	Ti	V	Zn
0	0.00	Silty	2.5Y 5/2	Grayish Brown	1.23%	17.8%	2131	4.5	9.5	58.0	58525	0.5	2.3	26.5	5.6	4890	767	5613	292	0.5	381	4.9	507	8.2	537	1.5	388	125	75.9	16.5	33.1	
5	10.60	Silty	10YR 6/2	Light Grayish Brown	1.24%	20.3%	2334	3.6	8.9	60.3	60725	0.4	2.5	34.3	5.4	5113	799	5695	312	0.0	476	5.0	488	8.1	299	1.8	395	121	84.2	17.3	31.1	
10	21.20	Silty	10YR 6/2	Light Grayish Brown	2615	4.7	9.7	63.7	62925	0.6	2.7	28.6	6.5	5208	968	5893	321	0.2	649	5.7	462	7.3	512	0.7	408	131	94.0	17.8	29.3			
15	31.81	Silty	10YR 6/2	Light Grayish Brown	2595	6.1	9.4	56.6	62350	0.5	2.4	25.2	5.5	5335	903	506	575	316	0.0	593	5.8	442	6.5	404	0.4	414	116	100.1	17.9	21.8		
20	42.41	Silty	10YR 6/2	Light Grayish Brown	2520	8.9	8.7	62.8	65400	0.5	2.1	32.2	4.5	5425	817	6060	334	0.3	591	5.8	460	6.5	445	0.0	336	117	79.6	17.5	20.9			
25	53.01	Silty	10YR 6/2	Light Grayish Brown	2221	4.6	7.5	52.0	56950	0.4	2.1	30.2	3.3	4813	724	6268	245	0.1	450	4.8	569	4.5	1554	3.2	377	121	119.2	17.9	18.3			
30	63.61	Silty	10YR 6/2	Light Grayish Brown	3055	5.1	9.3	59.4	73075	0.6	3.1	16.1	3.5	6450	900	6900	325	0.0	555	5.2	588	3.7	485	3.0	317	127	121.0	20.8	21.0			
35	74.21	Silty	10YR 6/2	Light Grayish Brown	2448	4.3	8.4	52.1	60175	0.5	2.6	30.6	2.9	5485	763	6395	291	0.0	505	4.5	561	4.2	680	1.0	367	116	94.9	18.5	19.1			
40	84.81	Silty	10YR 6/2	Light Grayish Brown	2810	6.0	10.5	73.7	71475	0.6	3.3	28.1	3.8	7435	937	7490	329	0.0	573	5.7	688	1.9	1414	4.2	330	167	128.3	22.0	22.8			
45	95.42	Silty	10YR 6/2	Light Grayish Brown	2221	4.6	7.5	52.0	56950	0.4	2.1	30.2	3.3	4813	724	6268	245	0.1	450	4.8	569	4.5	1554	3.2	377	121	119.2	17.9	18.3			
50	106.02	Silty	10YR 6/2	Light Grayish Brown	2266	1.8	8.1	53.7	54800	0.6	1.8	13.4	4.1	4748	605	5430	248	0.1	372	4.3	490	3.1	1016	1.8	177	112	82.1	16.9	25.8			
55	116.62	Silty	10YR 6/2	Light Grayish Brown	3288	3.5	11.5	84.8	77150	0.7	2.9	18.9	6.9	6868	1017	7445	361	0.3	538	6.8	644	4.4	1438	3.6	397	17.8	129.7	23.2	26.3			
60	127.22	Silty	10YR 6/2	Light Grayish Brown	3363	2.6	11.4	76.8	81750	0.8	2.4	19.1	5.5	7063	1026	8550	382	0.2	472	6.8	737	4.4	2031	2.4	359	183	129.4	24.9	28.5			
65	137.82	Silty	10YR 6/2	Light Grayish Brown	3955	4.4	13.5	85.1	80025	0.8	2.9	21.1	6.3	8023	1262	7678	400	0.0	462	7.6	634	2.2	1238	26.6	147.8	26.0	28.8					
70	148.42	Silty	10YR 6/2	Light Grayish Brown	3945	6.7	13.5	95.2	84650	0.9	4.0	24.5	8.0	8038	1291	7900	427	0.2	499	8.5	641	5.5	1758	3.7	271	217	129.2	26.6	40.1			
75	159.03	Silty	10YR 6/2	Light Grayish Brown	4160	6.8	14.3	98.0	82725	1.0	3.2	22.6	8.0	8460	1402	8118	428	0.1	503	8.2	620	5.6	1622	0.0	767	207	150.3	27.3	30.7			
80	169.63	Silty	10YR 6/2	Light Grayish Brown	3995	5.9	13.4	88.3	73150	0.6	3.3	22.0	7.3	7943	1252	7368	373	0.3	477	8.1	600	5.0	1247	0.0	310	183	137.5	25.3	30.1			
85	180.23	Silty	10YR 6/2	Light Grayish Brown	1.59%	23.4%	3955	4.4	13.5	85.1	80025	0.8	2.9	21.1	6.3	8023	1262	7678	400	0.0	462	7.6	634	2.2	1238	26.6	147.8	26.0	28.8			
90	190.83	Silty	10YR 6/2	Light Grayish Brown	4160	6.8	14.3	98.0	82725	1.0	3.2	22.6	8.0	8460	1402	8118	428	0.1	503	8.2	620	5.6	1622	0.0	767	207	1					

Table 4.6. Goshen North Core Sample Results.

Length (cm)	Depth (cm)	Texture	Munsell Notation	Color Name	Color	LOI	CaCO <sub>3</sub>	Al	B	Ba	Ca	Cd	Co	Cr	Cu	Fe	K	Mg	Mn	Mo	Na	Ni	P	Pb	S	Se	Si	Ti	V	Zn	
0	0.00	Silty Sand	2.5Y7/1	Light Gray	1.52%	28.5%	2258	52.9	9.8	106.4	102900	0.6	2.3	33.2	6.0	4808	1139	7330	290	1.4	459	5.7	428	8.8	682	0.0	382	406	103.8	19.8	21.5
5	8.02	Silty Sand	2.5Y6/2	Light Brownish Gray	2698	3.5	11.6	106.6	83575	0.7	2.3	51.2	3.6	6023	1509	8718	318	2.6	598	5.9	483	3.0	298	0.0	436	289	152.2	23.3	19.8		
10	16.04	Silty Sand	2.5Y7/2	Light Gray	2523	2.5	10.6	101.7	83550	0.2	1.8	29.9	4.4	5395	1394	8488	299	2.5	740	6.6	459	3.9	298	0.0	400	309	159.3	23.1	19.7		
15	24.06	Silty	2.5Y6/1	Gray	1.65%	24.9%	2720	7.5	11.8	106.7	88200	0.5	1.6	21.5	6.1	5918	1439	7988	338	1.1	823	6.8	404	5.0	393	0.0	377	347	177.2	23.9	20.0
20	32.08	Silty Sand	2.5Y6/2	Light Brownish Gray	3043	7.2	13.0	105.6	98100	0.5	2.3	22.5	6.5	6445	1615	8925	379	1.7	1154	7.6	476	4.7	461	0.2	446	362	149.7	25.4	23.6		
25	40.11	Silty Sand	2.5Y5/1	Gray	3518	0.3	15.8	85.6	74400	0.7	2.7	25.4	15.8	6775	1657	8140	304	1.8	1617	13.0	423	6.8	854	4.5	670	224	101.3	38.0	33.3		
30	48.13	Silty Sand	2.5Y6/1	Gray	2.16%	16.5%	3193	0.0	16.3	88.6	70675	0.6	3.0	37.4	9.9	7698	1525	7445	334	2.8	1190	8.6	428	8.7	1159	0.1	769	182	326.5	36.6	36.4
35	56.15	Silty	2.5Y5/1	Gray	4035	5.4	22.1	82.6	73200	0.8	3.2	29.7	17.4	8379	47	1818	11.7	464	9.4	3578	0.0	775	217	190.3	43.9	41.5					
40	64.17	Silty Sand	2.5Y5/1	Gray	3410	4.8	21.6	86.8	65500	0.8	4.1	30.8	10.8	7755	1616	7675	384	3.6	1745	8.8	396	9.1	3865	0.0	586	226	416.3	53.6	39.7		
45	72.19	Silty Sand	2.5Y6/1	Gray	2212	7.8	16.2	103.6	51225	1.0	5.2	33.1	3.6	11775	993	4645	436	15.5	940	6.4	323	6.8	9803	0.0	504	133	737.8	41.2	32.0		
50	80.21	Silty Sand	2.5Y5/1	Gray	1.28%	15.2%	1365	16.4	14.5	61.3	46925	0.9	4.2	36.2	3.1	10270	752	3190	353	21.0	780	5.5	271	4.5	8910	0.3	414	108	544.0	38.0	23.8
55	88.23	Sandy	2.5Y5/1	Gray	1508	20.1	13.0	59.0	45350	0.7	3.7	23.9	2.8	703	710	3013	367	15.5	686	5.8	248	4.7	7290	0.0	370	101	525.8	29.0	26.5		
60	96.25	Sandy	2.5Y5/1	Gray	2020	45.8	16.4	72.3	64625	0.8	4.1	47.6	2.7	10860	939	3898	545	13.3	898	5.9	276	6.8	8363	2.2	640	179	508.5	31.2	24.2		
65	104.27	Silty	2.5Y6/1	Gray	2843	20.0	13.9	55.2	58475	0.7	3.8	36.7	11.6	9025	1389	7543	439	3.0	1035	8.0	395	9.7	5733	0.2	449	138	124.2	28.1	27.6		
70	112.29	Sandy	2.5Y6/1	Gray	2780	36.0	15.0	46.8	35425	1.0	11.0	22.2	8.1	9018	1527	6655	352	2.4	794	12.0	358	10.1	5885	0.0	625	153	146.9	28.9	27.2		
75	120.32	Silty Sand	2.5Y7/1	Light Gray	6753	10.6	30.4	55.8	81025	0.7	3.0	32.7	11.5	8895	4255	25825	1105	1.1	1529	6.6	336	7.8	2421	1.8	705	756	146.3	73.0	29.0		
80	128.34	Silty Sand	2.5Y7/1	Light Gray	6820	11.9	33.6	17.8	87600	0.9	3.8	46.3	13.2	10913	4345	33175	129	1.7	1699	7.6	377	5.4	3590	0.0	766	993	170.1	85.9	30.1		
85	136.36	Silty Sand	2.5Y7/2	Light Gray	5900	8.8	27.9	99.0	79590	0.6	2.7	22.7	10.5	9438	3465	33950	1160	1.1	1558	5.9	347	6.0	2086	0.0	862	763	172.2	83.7	24.0		
90	144.38	Silty Sand	2.5Y7/1	Light Gray	2.19%	22.6%	5360	7.9	24.1	96.6	72225	0.7	2.8	23.9	10.0	8330	3070	32050	1033	0.5	15336	6.1	361	5.8	746	0.0	620	669	147.4	83.9	24.9

Table 4.7. Goshen South Core Sample Results.

Length (cm)	Depth (cm)	Texture	Munsell Notation	Color Name	Color	LOI	CaCO <sub>3</sub>	Al	B	Ba	Ca	Cd	Co	Cr	Cu	Fe	K	Mg	Mn	Mo	Na	Ni	P	Pb	S	Se	Si	Ti	V	Zn	
0	0.00	Silty	2.5Y7/1	Light Gray	4161	6.6	21.9	162.1	163245	1.2	3.2	26.5	19.8	8853	1803	11002	603	1.7	813	11.5	703	19.0	2138	0.0	706	669	71.8	31.1	58.6		
5	12.97	Silty	2.5Y7/1	Light Gray	3.31%	25.3%	4093	9.5	19.7	161.9	161033	1.0	3.5	32.3	17.7	8477	1768	596	0.9	714	10.3	697	18.3	2331	0.0	742	663	72.0	31.1	62.6	
10	25.94	Silty	2.5Y7/1	Light Gray	3903	7.9	17.8	144.5	148333	0.6	3.2	30.5	15.7	8787	1643	9951	544	1.3	615	8.8	610	14.8	3169	0.4	576	52	72.9	29.4	51.4		
15	38.91	Silty	2.5Y7/1	Light Gray	2.67%	26.3%	3437	10.4	15.9	135.9	140518	1.0	3.0	29.5	14.4	7229	1374	8811	50.9	541	82	544	18.3	3050	0.0	319	565	50.4	25.5	43.6	
20	51.88	Silty	2.5Y7/2	Light Gray	3550	3.1	15.1	141.6	142149	0.8	2.9	34.5	11.7	7638	8142	8980	50.2	0.5	688	9.0	591	11.0	853	0.7	630	527	74.8	25.7	32.1		
25	64.85	Silty	2.5Y7/2	Light Gray	3556	4.9	15.2	155.7	157973	0.7	3.2	37.3	8.7	8020	1397	9029	541	2.5	872	12.3	516	5.0	1241	0.0	448	523	53.5	25.4	37.5		
30	77.82	Silty	2.5Y7/1	Light Gray	2.39%	26.2%	3493	2.6	14.8	159.6	166193	0.9	3.4	45.3	8.9	7651	1375	930	536	1.4	934	12.6	521	5.9	4876	0.0	538	584	54.5	25.7	40.1
35	90.79	Silty	2.5Y7/1	Light Gray	2347	3.0	9.5	125.9	151886	0.4	2.1	26.5	4.3	4508	884	7744	382	1.2	651	7.6	428	4.8	7146	1.5	399	534	62.6	20.1	23.5		
40	103.76	Silty	2.5Y7/1	Light Gray	2184	1.7	9.6	126.2	142595	0.5	1.9	28.2	4.8	4248	874	7502	554	1.5	691	5.8	404	3.9	5860	0.0	313	501	66.0	19.5	20.5		
45	116.73	Silty	2.5Y7/1	Light Gray	3.78%	25.2%	2805	0.6	11.4	148.3	165768	0.4	2.7	29.5	5.9	5425	1145	8982	432	1.2	840	9.0	455	4.0	3783	0.0	551	604	75.9	23.5	23.6
50	129.70	Silty	2.5Y7/1	Light Gray	2993	7.4	12.7	151.8	158224	0.6	2.5	37.2	6.5	6496	1301	9026	445	1.0	801	7.8	470	4.3	1581	0.0	330	588	78.5	23.8	24.4		
55	142.67	Silty	2.5Y7/1	Light Gray	3642	0.7	14.6	192.0	195793	0.7	4.1	61.6	7.3	7288	1745	10868	579	4.0	1287	13.8	466	3.8	4276	0.0	534	743	94.8	28.8	34.9		
60	155.64	Silty	2.5Y7/1	Light Gray	3720	0.4	15.1	177.7	172199	0.9	3.3	43.4	8.0	7301	1774	9954	547	1.6	1000	9.1	488	4.7	3569	0.0	628	633	89.3	27.3	30.0		
65	168.61	Silty	2.5Y7/1	Light Gray	3118	2.9	13.6	169.5	153508	0.5	2.3	34.9	7.7	6065	1497	9685	457	0.8	967	7.6	522	3.8	2782	0.0	466	619	91.2	25.5	25.2		
70	181.58	Silty	2.5Y7/1	Light Gray	2.08%	26.5%	3077	0.0	13.5	152.9	137075	0.5	2.4	30.2	7.1	5541	1455	9202	403	1.1	980	7.2	511	5.8	2775	1.7	510	580	93.8	24.7	23.9
75	194.55	Silty	2.5Y6/1	Gray	3300	1.8	16.8	165.3	135575	0.5	2.3	30.0	8.0	6355	1677	10243	403	1.2	1223	8.3	539	4.6	2727	0.1	500	594	90.7	26.3	28.4		
80	207.52	Silty	2.5Y6/1	Gray	3367	4.3	17.5	153.0	122294	0.6	2.2	26.3	9.0	6353	1637	10022	373	1.5	1150	8.9	560	5.2	1791	0.0	654	566	112.2	26.7	27.5		
85	220.49	Silty	2.5Y6/1	Gray	3367	3.8	17.9	165.6	124844	0.5	2.7	33.2	8.6	6846	1794	10672	390	1.0	1201	7.6	650	5.6	1660	0.8	600	588	107.1	28.0	29.6		
90	233.46	Silty	2.5Y6/1	Gray	2.66%	24.9%	3592	2.5	17.7	167.0	138326	0.6	3.3	26.0	8.6	6797	1687	10377	406	0.8											

Table 4.8 Lindon Marina Core Sample Results.

Length (cm)	Depth (cm)	Texture	Munsell Notation	Color Name	Color	LOI	CaCO <sub>3</sub>	Al	As	B	Ba	Ca	Cd	Cr	Cu	Fe	K	Mg	Mn	Mo	Na	Ni	P	Pb	S	Se	Si	Ti	V	Zn	
0	0.00	Silty Sand	2.5Y 6/1	Gray	0.67%	14.9%	1606	1.9	7.5	33.8	40325	0.5	3.0	13.6	4.6	4220	559	5568	161	0.1	170	4.5	426	9.2	393	0.0	168	118	52.2	14.8	33.1
5	12.19	Silty Sand	2.5Y 7/1	Light Gray	1209	2.1	5.5	29.6	55200	0.4	2.1	11.6	1.8	3183	431	9850	189	0.0	204	3.3	526	2.7	236	0.0	178	131	65.5	22.8	12.7		
10	24.38	Silty	2.5Y 7/1	Light Gray	3413	1.1	11.0	1080	84925	0.6	2.4	18.9	7.8	6093	1145	9863	307	0.2	369	6.2	491	4.7	506	0.0	210	285	65.2	25.6	23.5		
15	36.58	Silty	2.5Y 6/1	Gray	0.99%	24.3%	2280	3.2	6.7	68.6	82175	0.5	1.8	13.7	4.9	3570	712	12538	289	0.4	281	4.9	472	2.0	394	2.2	189	235	83.3	28.8	22.1
20	48.77	Salty	2.5Y 7/1	Light Gray	2900	0.2	8.8	99.2	102900	0.4	2.1	37.0	7.8	4710	918	9720	328	0.5	330	5.8	421	3.6	546	0.0	215	332	84.7	25.5	27.1		
25	60.96	Salty	2.5Y 7/1	Light Gray	2017	1.3	6.6	65.7	89000	0.4	1.8	18.2	4.1	3675	638	12593	285	0.0	275	5.3	481	1.8	445	0.7	193	250	71.1	27.8	20.9		
30	73.15	Salty	2.5Y 7/1	Light Gray	0.87%	23.3%	2228	4.1	7.1	65.7	84575	0.5	1.8	17.5	4.5	3730	737	12930	280	0.0	271	4.7	523	3.2	392	1.8	182	238	83.4	29.1	23.0
35	85.34	Salty	2.5Y 7/1	Light Gray	2580	8.4	7.5	81.6	101925	0.5	2.2	15.5	5.7	4463	785	13155	321	0.3	325	5.8	535	2.2	532	0.0	158	303	82.4	30.4	25.7		
40	97.54	Salty	2.5Y 7/1	Light Gray	2291	0.8	6.9	79.1	103450	0.5	1.7	14.8	6.0	3920	752	14510	324	0.0	295	5.0	543	1.4	489	0.0	138	309	69.0	32.8	25.2		
45	109.73	Salty	2.5Y 6/1	Gray	2413	1.6	7.3	50.8	101950	0.6	1.7	15.4	6.8	4298	677	21500	334	0.4	298	7.4	667	6.5	495	1.1	184	217	73.4	46.0	36.6		
50	121.92	Salty	2.5Y 6/1	Gray	2883	0.8	8.9	78.2	123300	0.8	2.4	26.1	8.4	5188	848	17978	402	0.3	363	8.6	619	8.3	663	0.1	178	365	73.7	40.0	41.7		
55	134.11	Salty	2.5Y 7/1	Light Gray	3050	1.1	9.9	94.7	129500	0.7	3.3	20.2	7.4	6488	957	15895	419	0.0	358	8.7	576	4.2	623	0.0	154	387	77.4	36.6	39.0		
60	146.30	Salty	2.5Y 7/1	Light Gray	1.68%	23.7%	2883	1.0	9.2	95.9	12375	0.8	2.6	17.7	8.5	4820	946	16153	381	0.4	383	8.4	565	5.8	700	3.5	166	384	85.7	37.4	40.5
65	158.50	Salty	2.5Y 7/1	Light Gray	3168	2.0	9.2	110.4	132650	0.8	2.3	18.1	9.1	4883	1034	12963	392	0.1	381	7.7	475	5.6	794	0.9	120	454	74.9	31.1	37.0		
70	170.69	Salty	2.5Y 7/1	Light Gray	2918	4.4	10.5	1531	164750	0.7	2.7	18.5	5.8	5828	1059	13818	467	0.0	415	7.4	549	5.8	803	0.0	170	582	69.5	32.2	29.0		
75	182.88	Salty	2.5Y 7/1	Light Gray	3068	0.0	9.8	160.3	181825	0.4	2.2	23.2	6.9	5145	10198	481	0.0	389	6.8	424	2.3	933	1.6	121	642	55.4	25.1	27.1			
80	195.07	Salty	2.5Y 6/1	Gray	4370	16.5	14.0	100.1	82800	2.0	5.5	27.1	7.5	10160	1214	14583	652	1.0	338	14.1	668	18.8	412	0.0	127	221	281	38.3	66.0		
85	207.26	Salty	2.5Y 7/3	Pale Yellow	2.39%	22.9%	4798	59.1	28.6	83.9	75950	3.0	9.8	46.5	9.5	26375	1314	11595	958	7.5	328	27.5	862	19.6	449	2.1	122	175	24.4	39.0	89.1
90	219.46	Salty	2.5Y 6/1	Gray	7195	14.8	18.9	93.1	9955	1.3	9.4	40.5	11.7	15575	2023	8620	152	1.5	401	26.9	1006	20.5	308	0.0	138	56	34.4	32.1	92.4		
95	231.65	Salty	2.5Y 7/1	Light Gray	2530	3.4	10.2	80.1	118400	1.1	2.8	20.8	6.1	7370	751	16310	1135	0.5	277	7.7	535	7.1	499	1.1	141	296	41.5	39.9	36.9		
100	243.84	Salty	2.5Y 6/1	Gray	0.91%	22.4%	2570	5.0	8.2	71.1	101075	0.8	3.4	17.7	6.3	6003	721	16720	717	0.4	213	9.2	478	6.9	406	0.0	117	228	43.9	40.9	35.0

Table 4.9 Mosida Core Sample Results.

Length (cm)	Depth (cm)	Texture	Munsell Notation	Color Name	Color	LOI	CaCO <sub>3</sub>	Al	As	B	Ba	Ca	Cd	Co	Cr	Cu	Fe	K	Mg	Mn	Mo	Na	Ni	P	Pb	S	Se	Si	Ti	V	Zn		
0	0.00	Sandy	2.5Y 6/1	Gray	0.50%	20.3%	1293	7.6	7.3	41.4	92562	0.3	24	13.0	2.3	3711	614	2229	178	0.7	220	2.5	259	5.6	604	0.0	404	130	181.6	11.6	14.2		
5	11.60	Sandy Silt	10YR 7/2	Light Gray	1.43%	26.7%	4214	5.1	14.7	143.0	130167	0.7	4.4	25.4	10.0	7845	1935	8505	441	0.5	490	10.4	424	10.6	382	1.5	641	285	101.0	30.4	33.9		
10	23.19	Silty	10YR 8/2	Very Pale Brown	6885	4.1	21.3	264.3	122350	1.4	5.5	34.8	14.3	10933	3075	11958	599	0.9	586	14.3	526	14.0	247	0.7	766	241	125.9	41.9	49.9				
15	34.79	Silty	10YR 7/2	Light Gray	1.58%	23.1%	5090	5.3	17.6	157.0	75667	1.0	4.0	31.1	8.6	9593	2315	8202	296	0.6	473	9.8	448	9.9	130	0.0	549	129	127.0	35.1	37.4		
20	46.38	Silty	10YR 7/2	Light Gray	5133	7.0	17.1	72.8	77500	0.6	3.7	40.1	5.1	9830	2109	7709	228	0.9	434	7.0	385	7.4	98	0.6	438	104	179.7	38.9	24.9				
25	57.98	Silty	10YR 7/2	Light Gray	4724	14.6	16.4	102.7	78310	0.8	4.7	25.3	4.7	8136	1978	7695	241	1.1	1013	6.4	405	7.1	107	0.6	611	107	138.0	31.3	22.3				
30	69.57	Silty	10YR 7/3	Very Pale Brown	5582	22.4	19.5	260.4	77624	0.9	4.0	28.0	5.9	11369	2156	8629	272	0.6	465	7.5	447	5.7	150	0.0	425	11.0	162.7	39.8	25.7				
35	81.17	Silty Gravel	10YR 7/2	Light Gray	3288	24.5	12.8	183.5	79736	0.6	3.2	26.7	4.6	7743	1281	5385	270	0.9	351	5.5	487	5.9	108	0.2	419	7.5	127.3	27.5	19.3				
40	92.77	Sandy Gravel	10YR 6/2	Light Brownish Gray	2295	47.1	13.0	53.8	126203	0.8	3.3	32.9	4.7	9233	890	3262	332	0.5	287	5.5	484	4.7	89	0.0	386	65	232.3	27.2	20.2				
45	104.36	Sandy Gravel	10YR 7/3	Very Pale Brown	3963	35.4	15.2	50.5	127770	0.5	5.8	27.3	5.4	8380	1477	6142	660	0.4	377	6.4	415	9.3	132	0.0	514	100	107.6	27.7	19.8				
50	115.96	Silty Gravel	10YR 7/2	Light Gray	4793	48.1	17.2	58.2	93125	0.6	4.7	40.8	5.3	8943	2040	7805	531	3.2	631	13.1	447	4.7	204.1	27.1	19.9	0.0	414	0.0	661	118	115.9	31.3	29.9
55	127.55	Silty	10YR 7/2	Light Gray	6843	49.3	22.0	233.3	105980	0.6	5.2	49.8	7.0	10703	2620	10150	791	1.8	552	9.6	423	6.2	240	0.0	644	177	138.1	36.3	28.8				
60	139.15	Silty	10YR 7/2	Light Gray	5.76%	37.7%	5436	43.5	18.3	10538	123048	0.4	7.5	5.8	8355	2186	8895	779	2.0	500	8.7	405	6.0	414	0.0	682	212	84.5	31.2	25.3			

Table 4.10. North Shore Core Sample Results.

Length (cm)	Depth (cm)	Texture	Munsell Notation	Color Name	Color	LOI	CaCO <sub>3</sub>	Al	As	B	Ba	Ca	Cd	Co	Cr	Cu	Fe	K	Mg	Mn	Mo	Na	Ni	P	Pb	S	Se	Si	St	Ti	V	Zn
0	0.00	Silty Sand	2.5Y 6/1	Gray	0.28%	26.0%	1312	2.0	6.0	34.0	961/75	1.0	11.0	4.0	3035	362	14580	243	0.0	188	3.0	575	5.0	393	1.0	137	217	34.0	43.0	34.0		
5	14.34	Silty Sand	2.5Y 6/1	Gray	0.76%	22.9%	2513	9.0	12.0	65.0	111100	1.0	2.0	13.0	9.0	50590	842	15110	295	0.0	309	6.0	629	14.0	1335	5.0	149	30.6	65.0	49.0	71.0	
10	28.69	Silty	2.5Y 7/1	Light Gray	0.76%	22.9%	3610	10.0	16.0	106.0	129950	1.0	3.0	23.0	17.0	66533	1254	12880	352	0.0	521	10.0	662	25.0	5993	3.0	158	462	62.0	48.0	112.0	
15	43.03	Silty	2.5Y 5/1	Gray	0.101%	20.3%	2090	4.0	7.0	57.0	88125	1.0	1.0	14.0	4.0	3703	798	19053	328	0.0	298	4.0	660	4.0	1938	2.0	160	209	79.0	59.0	25.0	
20	57.37	Silty	2.5Y 5/1	Gray	0.60%	25.7%	3228	4.0	9.0	114.0	111625	1.0	2.0	18.0	6.0	4425	1114	16968	329	1.0	367	7.0	656	8.0	2240	4.0	134	285	84.0	56.0	29.0	
25	71.72	Silty	2.5Y 5/1	Gray	0.94%	19.1%	3423	3.0	9.0	124.0	97775	1.0	2.0	21.0	5.0	4353	1130	18053	284	0.0	362	7.0	708	5.0	2565	3.0	128	222	83.0	58.0	29.0	
30	86.06	Silty	2.5Y 5/1	Gray	0.94%	19.1%	2433	2.0	7.0	88.0	77775	0.0	1.0	24.0	4.0	3405	827	18818	240	0.0	329	6.0	693	6.0	604	3.0	136	153	69.0	59.0	23.0	
35	100.40	Silty	2.5Y 5/1	Gray	0.94%	19.1%	2608	2.0	7.0	80.0	88125	1.0	2.0	16.0	5.0	3490	824	18025	272	0.0	375	6.0	605	3.0	635	2.0	136	190	85.0	57.0	24.0	
40	114.75	Silty	2.5Y 5/2	Grayish Brown	0.94%	19.1%	2778	2.0	7.0	70.0	81450	1.0	2.0	13.0	5.0	3873	810	16065	246	0.0	362	8.0	577	4.0	565	0.0	96	17	69.0	51.0	27.0	
45	129.09	Silty	2.5Y 6/2	Light Brownish Gray	0.94%	19.1%	3608	3.0	10.0	67.0	95375	1.0	2.0	29.0	3.0	4993	944	15610	259	1.0	414	7.0	578	6.0	934	1.0	161	238	116.0	55.0	36.0	
50	143.44	Silty	2.5Y 5/2	Grayish Brown	0.94%	19.1%	3785	2.0	10.0	82.0	60950	1.0	2.0	22.0	9.0	5023	959	14193	185	0.0	402	8.0	549	6.0	1051	3.0	103	140	65.0	50.0	32.0	
55	157.78	Silty	2.5Y 6/1	Gray	0.94%	19.1%	1374	2.0	4.0	44.0	81400	0.0	0.0	9.0	3.0	1935	467	15518	262	0.0	327	2.0	489	1.0	566	4.0	138	179	65.0	48.0	15.0	
60	172.12	Silty	2.5Y 5/1	Gray	0.94%	19.1%	1617	0.0	5.0	51.0	87100	0.0	1.0	11.0	3.0	2282	571	17435	294	14.0	360	3.0	577	3.0	660	3.0	165	190	70.0	55.0	18.0	
65	186.47	Silty	2.5Y 5/1	Gray	0.94%	19.1%	3618	6.0	10.0	140.0	160150	1.0	2.0	20.0	11.0	4500	1128	10910	346	21.0	720	10.0	484	7.0	1930	5.0	149	57.0	83.0	41.0	32.0	
70	200.81	Silty	2.5Y 7/1	Light Gray	0.94%	19.1%	6118	5.0	14.0	71.0	79125	1.0	3.0	25.0	10.0	7640	2081	16773	287	0.0	579	11.0	814	20.0	1818	2.0	181	180	30.0	64.0	73.0	
75	215.15	Silty	2.5Y 5/1	Gray	0.94%	19.1%	4485	11.0	15.0	162.0	144125	1.0	4.0	47.0	16.0	7773	1192	9598	448	0.0	855	16.0	490	8.0	2347	1.0	161	546	77.0	39.0	47.0	
80	229.50	Silty	2.5Y 7/1	Light Gray	0.94%	19.1%	4085	8.0	13.0	100.0	130350	1.0	3.0	16.0	4.0	8098	1368	14218	639	0.0	613	8.0	477	12.0	1164	0.0	146	361	30.0	53.0	46.0	
85	243.84	Silty	2.5Y 7/1	Light Gray	0.94%	19.1%	2127	9.0	10.0	124.0	212900	1.0	2.0	12.0	3.0	6098	735	13415	687	1.0	683	6.0	320	4.0	2087	0.0	145	879	49.0	46.0	29.0	

Table 4.11. Powell Slough Core Sample Results.

Length (cm)	Depth (cm)	Texture	Munsell Notation	Color Name	Color	LOI	CaCO <sub>3</sub>	Al	As	B	Ba	Ca	Cd	Co	Cr	Cu	Fe	K	Mg	Mn	Mo	Na	Ni	P	Pb	S	Se	Si	St	Ti	V	Zn
0	0.00	Silty	2.5Y 7/1	Light Gray	1.84%	53.2%	3785	6.4	15.6	162.9	141800	0.7	3.5	17.6	10.4	6370	1090	7278	358	0.7	531	9.5	832	6.8	965	0.0	609	601	181.2	209	29.6	
5	9.14	Silty	2.5Y 7/1	Light Gray	3485	4.4	15.7	205.6	165725	0.3	3.7	22.7	13.5	5785	1017	7930	503	1.2	611	9.3	714	4.1	1116	0.0	609	734	170.3	20.0	22.0			
10	18.29	Silty	2.5Y 7/1	Light Gray	2963	5.7	14.3	319.8	187700	0.3	3.9	11.6	12.5	4978	1026	7955	573	1.5	601	10.2	460	3.7	1193	0.2	585	816	152.6	19.9	18.7			
15	27.43	Silty	2.5Y 7/1	Light Gray	1.62%	49.4%	2933	4.8	12.6	499.5	206775	0.2	4.3	13.1	8.2	5353	1012	10540	688	2.1	745	10.1	387	4.3	1669	0.6	760	1007	154.8	24.1	19.8	
20	36.58	Silty	2.5Y 6/1	Gray	1759	2.9	10.4	445.8	222350	0.4	2.3	9.8	8.2	3418	801	7890	545	2.0	889	6.8	335	4.9	1225	0.0	637	1007	95.5	17.3	17.1			
25	45.72	Silty	2.5Y 7/1	Light Gray	1486	2.7	11.5	374.3	226600	0.4	2.3	11.2	13.5	3005	693	8125	773	1.4	667	5.3	374	4.6	1254	2.0	707	92	84.9	18.5	13.7			
30	54.86	Silty	2.5Y 6/1	Gray	3590	5.0	21.1	225.9	159250	0.5	2.3	27.4	7613	1725	10900	553	1.0	901	12.2	776	5.7	1041	0.0	687	754	149.5	26.1	26.7				
35	64.01	Silty	2.5Y 6/1	Gray	4280	0.7	21.1	565.0	140900	1.1	5.7	22.4	13.4	10900	2565	13410	644	1.5	1098	12.3	937	6.6	1060	0.0	614	705	152.5	34.2	35.6			
40	73.15	Silty	2.5Y 7/1	Light Gray	3425	0.8	14.5	346.0	109650	0.5	4.5	16.8	7.0	7268	1861	11893	646	1.8	828	9.3	680	6.7	669	0.4	597	431	132.7	32.3	30.0			
45	82.30	Silty	2.5Y 7/1	Light Gray	3240	0.6	13.9	233.5	93300	0.6	4.3	16.8	7.0	7220	1698	11820	619	1.7	722	9.4	552	5.3	537	0.0	573	340	118.6	30.9	28.9			
50	91.44	Silty	2.5Y 8/1	White	3270	2.4	10.3	155.1	71750	0.7	3.4	15.9	3.3	6035	1699	9963	493	1.0	556	6.8	384	6.5	260	0.0	542	218	86.1	27.6	21.4			
55	100.58	Silty	2.5Y 8/1	White	4935	2.8	13.0	174.9	60350	0.8	4.4	20.6	4.2	7803	2335	10920	440	1.2	652	10.4	435	6.6	246	0.0	563	180	123.6	32.7	28.0			
60	109.73	Silty	2.5Y 8/1	White	0.72%	26.9%	4448	2.7	12.7	190.5	76475	0.8	4.5	19.7	7.5	7070	2148	11790	583	0.9	661	9.6	477	7.1	281	0.0	552	229	100.2	39.9	27.4	
65	118.87	Silty	2.5Y 8/2	Pale Yellow	4638	2.6	13.3	176.6	78275	0.9	5.4	20.5	6.7	7728	2335	11958	738	2.1	703	11.5	464	5.4	328	0.0	600	225	102.4	37.1	32.2			
70	128.016	Silty	2.5Y 8/2	Pale Yellow	4425	3.0	12.7	124.0	74925	0.6	5.1	20.5	10.3	7425	2132	11565	674	1.6	696	12.3	478	8.7	313	0.0	616	211	118.1	34.6	32.4			
75	137.16	Silty	2.5Y 7/2	Light Gray	4933	3.3	14.9	73.7	60175	1.2	4.8	23.7	9.5	10310	2474	11718	602	0.9	813	11.4	504	7.6	212	0.0	604	150	98.5	33.5	34.0			
80	146.304	Silty	2.5Y 7/2	Light Gray	0.72%	24.4%	4933	3.6	15.7	105.2	63550	1.1	4.5	18.3	8.6	10588	2437	11593	1.7	792	12.3	487	9.1	232	0.0	592	104.9	34.6	34.3	34.0		
85	155.448	Silty	2.5Y 7/2	Light Gray	4873	6.1	14.2	113.1	9325	1.0	4.5	22.9	12.1	9365	2415	10850	580	1.3	775	12.2	501	8.2	262	0.0	600	148	104.3	32.8	35.7			
90	164.592	Silty	2.5Y 7/2	Light Gray	5825	6.2	19.4	124.5	73400	1.0	5.1	36.6	19.5	124.6	104.5	124.6	859	2.														

Table 4.12. Provo Bay Core Sample Results.

Length (cm)	Depth (cm)	Texture	Munsell Notation	Color Name	Color	LOI	$\text{CaCO}_3$	Al	As	Ba	Ca	Cd	Co	Cr	Cu	Fe	K	Mg	Mn	Mo	Na	Ni	P	Pb	S	Se	Si	Sr	Ti	V	Zn
0	0.00	Silty	2.5Y 6/1	Gray	5.03%	22.4%	3455	5.8	15.3	136.6	128525	0.9	2.8	22.5	14.3	7995	12.0	7365	398	17.7	561	15.7	920	22.1	5798	4.1	195	541	105.1	21.2	96.4
5	13.55	Silty	2.5Y 6/1	Gray	2.948	4.6	14.5	139.4	12730	1.1	2.6	23.5	17.0	7770	1.132	7285	400	11.7	495	12.4	915	22.5	5730	3.1	21.9	544	88.7	20.2	103.4		
10	27.09	Silty	2.5Y 5/1	Gray	4.03%	27.2%	3253	5.7	14.7	147.8	134050	1.2	3.0	25.8	14.9	8005	1.132	7405	429	5.5	441	9.5	943	26.2	6135	3.4	19.8	576	91.6	20.9	97.8
15	40.64	Silty	2.5Y 6/1	Gray	5733	5.3	19.5	153.0	100850	1.0	4.0	34.5	10.3	10950	1.140	12985	595	3.0	465	13.2	781	8.4	2670	0.9	218	303	42.6	37.2	51.0		
20	54.19	Silty	2.5Y 5/1	Gray	5355	4.3	20.2	159.3	95100	1.3	4.3	31.8	11.5	12063	1.1450	9458	774	3.7	410	13.4	788	9.9	2578	1.6	200	272	70.8	33.6	48.7		
25	67.73	Silty	2.5Y 4/1	Dark Gray	9.53%	8.0%	6380	4.5	20.8	140.8	3340	1.5	5.0	36.8	14.4	11193	1.1354	7140	19.6	8.4	387	19.4	756	9.6	1723	6.8	181	134	110.5	32.9	56.3
30	81.28	Silty	2.5Y 4/1	Dark Gray	5598	8.3	20.3	122.1	10758	0.8	4.2	34.5	15.1	8730	1.1295	4220	11.5	3.9	433	15.8	853	5.7	2680	2.3	218	85	90.7	25.6	49.2		
35	94.83	Silty	2.5Y 5/1	Gray	2695	5.1	8.7	66.3	68600	0.5	2.4	17.9	8.3	4405	700	5553	273	4.1	336	8.2	562	4.1	977	0.0	178	141	62.5	18.3	25.9		
40	108.37	Silty	2.5Y 5/1	Gray	4.73%	21.9%	3285	6.6	11.1	81.4	73900	0.6	2.8	21.2	8.2	5573	873	5675	296	10.1	360	13.2	490	5.4	1523	0.1	172	179	68.2	19.8	34.8
45	121.92	Silty	2.5Y 6/1	Gray	2454	4.4	7.6	64.5	73400	0.4	1.7	14.4	5.5	4318	710	5483	320	13.6	324	11.0	388	3.9	105	4.6	130	155	67.2	17.2	24.4		
50	135.47	Silty	2.5Y 6/1	Gray	2745	2.9	9.3	77.3	87875	0.6	2.3	18.4	5.5	5343	796	5593	329	12.3	354	11.0	425	4.8	2658	3.0	157	212	80.3	18.4	29.1		
55	149.01	Silty	2.5Y 6/1	Gray	3108	5.7	11.3	84.8	102800	0.7	2.6	20.6	5.9	7380	901	5930	379	10.9	113	433	3.9	4980	3.8	164	263	87.2	18.9	30.7			
60	162.56	Silty	2.5Y 6/1	Gray	2680	4.2	9.8	89.3	83625	0.5	2.0	35.4	8.1	5905	924	5958	359	14.5	353	14.2	434	6.2	3545	0.0	182	181	76.2	18.3	37.2		
65	176.11	Silty	2.5Y 6/1	Gray	3.14%	23.2%	2290	0.6	8.5	80.3	89125	0.5	2.0	17.8	5.0	5258	713	5283	336	13.3	351	10.9	390	2.3	3698	0.1	179	238	69.5	15.9	27.5
70	189.65	Silty	2.5Y 6/1	Gray	3223	4.4	12.8	99.4	107450	1.0	2.5	22.5	7.7	7965	977	6123	428	10.1	398	12.0	482	5.1	6240	14	184	317	70.7	20.6	34.1		
75	203.20	Silty	2.5Y 6/1	Gray	2250	0.6	8.1	74.6	77700	0.8	1.9	15.0	4.4	4898	629	5453	309	6.7	296	7.7	406	1.9	3000	0.0	177	172	72.1	16.2	22.2		
80	216.75	Silty	2.5Y 6/1	Gray	2325	3.0	8.1	70.3	76050	0.5	1.7	15.7	4.7	5098	663	5443	306	6.6	288	7.7	409	2.4	3185	5.2	166	175	69.9	16.4	24.4		
85	230.29	Silty	2.5Y 6/1	Gray	1.73%	22.7%	2483	2.9	8.6	64.5	66925	0.6	2.0	16.1	4.7	4705	827	5033	277	8.6	281	7.6	364	2.6	2263	0.4	228	166	97.1	16.3	20.0
90	243.84	Silty	2.5Y 6/1	Gray	3183	3.6	11.8	95.5	100725	0.8	2.5	28.1	8.6	7205	944	6638	399	4.9	352	9.5	587	5.6	4730	3.2	199	281	80.9	21.3	30.4		

Table 4.13. Saratoga Springs Core Sample Results.

Length (cm)	Depth (cm)	Texture	Munsell Notation	Color Name	Color	LOI	$\text{CaCO}_3$	Al	As	Ba	Ca	Cd	Co	Cr	Cu	Fe	K	Mg	Mn	Mo	Na	Ni	P	Pb	S	Se	Si	Sr	Ti	V	Zn
0.00	0.00	Silty Sand	2.5Y 6/1	Gray	0.88%	10.6%	2630	5.4	11.4	311.5	40225	0.8	3.6	21.9	3.4	5660	1337	3623	167	0.5	286	6.4	503	7.6	753	0.0	243	143	190.3	181	35.4
5.00	7.27	Silty Sand	2.5Y 6/2	Light Brownish Gray	5600	2.8	19.5	147.0	5860	0.7	4.0	38.8	5.7	9660	2865	4155	168	0.0	363	8.2	136	8.0	1860	0.0	392	93	233.3	27.3	25.9		
10.00	14.55	Silty	10YR 8/2	Very Pale Brown	7445	6.0	22.3	102.2	116150	1.0	5.4	49.1	12.9	11868	4045	11170	547	0.4	437	14.0	681	6.9	681	0.0	443	332	157.9	57.6	47.1		
15.00	21.82	Silty	10YR 7/2	Light Gray	7880	3.5	25.3	69.2	112550	1.4	6.0	44.5	12.3	12575	4418	11180	614	0.5	458	14.3	681	7.7	298	0.0	432	275	123.8	44.6	48.6		
20.00	29.09	Silty	10YR 7/2	Light Gray	8298	9.2	27.4	75.3	129400	1.5	7.8	47.1	14.1	13820	4855	12833	697	0.7	511	18.1	827	8.9	628	0.0	535	321	142.1	46.7	55.3		
25.00	36.37	Silty	10YR 7/2	Light Gray	7965	8.2	24.8	70.5	129525	1.3	6.6	56.0	13.1	12983	4320	12425	703	0.2	476	16.0	727	10.6	278	2.6	648	306	139.2	43.0	52.6		
30.00	43.64	Silty	10YR 7/2	Light Gray	7468	7.0	22.4	78.8	112625	1.3	5.1	58.7	11.1	11325	4035	11313	605	0.6	434	13.8	686	9.3	289	1.1	580	269	176.7	42.4	46.7		
35.00	50.92	Silty	10YR 7/2	Light Gray	7378	4.1	21.9	62.6	102375	1.0	4.8	42.4	10.6	11458	3690	9725	536	0.7	388	13.6	545	8.7	229	0.0	220	245	81.0	36.6	44.3		
40.00	58.19	Silty	10YR 7/2	Light Gray	6075	6.0	18.4	47.9	81850	0.8	4.3	36.1	8.5	9400	3173	8208	416	0.2	329	11.1	471	5.8	163	0.0	600	201	124.0	30.3	36.1		
45.00	65.46	Silty	10YR 7/2	Light Gray	8920	4.7	26.8	79.1	102125	1.4	7.1	42.3	14.2	13640	5280	12755	580	0.7	505	17.0	659	8.3	236	0.0	687	270	160.6	46.2	54.0		
50.00	72.74	Silty	10YR 7/2	Light Gray	7972	10.0	23.7	66.6	96700	1.4	5.1	44.8	11.1	12410	4168	10818	507	0.0	418	14.1	507	7.0	207	0.0	645	245	150.3	38.6	46.0		
55.00	80.01	Silty	10YR 7/2	Light Gray	8240	6.4	24.2	98.6	85050	1.3	5.8	37.7	13.1	13153	4468	10538	533	0.0	478	14.6	605	9.9	234	0.0	642	250	158.4	39.1	46.0		
60.00	87.28	Silty	10YR 7/2	Light Gray	9235	6.7	25.5	96.1	49625	1.2	6.1	39.7	13.7	1425	4463	8650	444	0.0	499	14.2	527	12.0	225	0.0	465	230	170.2	39.6	49.2		
65.00	94.56	Silty	10YR 7/2	Light Gray	8630	1.3	24.8	92.0	50000	1.1	5.1	38.8	12.3	13435	4220	8700	387	0.5	459	12.7	549	9.7	221	0.0	428	180	160.1	36.4	43.4		
70.00	101.83	Silty	10YR 7/2	Light Gray	8198	5.3	24.5	119.2	65275	1.3	5.5	36.1	12.6	13400	4465	9260	443	0.3	532	13.2	637	11.6	282	1.6	539	234	173.0	36.4	46.2		
75.00	109.10	Silty	10YR 7/2	Light Gray	9723	5.9	27.7	126.0	61600	0.9	6.4	40.2	15.1	15143	5115	10158	510	0.0	524	15.9	499	10.2	233	0.0	563	229	122.3	39.2	51.2		
80.00	116.38	Silty	10YR 7/2	Light Gray	10023	5.0	27.8	116.8	53450	1.4	6.2	88.1	14.8	15278	5088	9843	492	0.6	526	16.2	489	10.6	229	0.0	641	225	138.7	39.0	50.8		
85.00	123.65	Silty	10YR 7/2	Light Gray	6018	1.7	16.9	97.4	51475	0.9	3.6	28.7	8.1	9990	3018	6775	330	5.1	396	12.3	534	7.6	208	0.0	436	180	204.2	28.5	35.0		
90.00	130.93	Silty	10YR 7/2	Light Gray	7498	3.3	21.4	130.0	29025	0.8																					

## 5 Conclusions

The combined findings from these three studies provide a multifaceted understanding of phosphorus dynamics in Utah Lake, with broader implications for nutrient management in similar shallow lakes. The development of the phosphorus microfractionation (P-MF) method represents a new step towards analyzing phosphorus fractions in small samples of suspended solids and sediments. This method is particularly valuable for assessing nutrient dynamics in suspended solids, which have been shown to contain a significantly higher phosphorus content in comparison to lakebed sediments. While the method needs refinement, the ability to accurately measure phosphorus fractions in small samples is crucial for understanding the role of suspended solids in eutrophic water bodies.

The historical analysis of phosphorus mass and concentrations in Utah Lake reveals that the lake's dissolved phosphorus concentrations have remained stable over time despite significant changes in lake volume and internal phosphorus mass. This stability is attributed to sorption processes, which dominate the phosphorus dynamics in the lake. The study's findings suggest that reducing or eliminating external phosphorus loads will have minimal impact on water column phosphorus concentrations in Utah Lake. This has important implications for nutrient load management in Utah Lake as well as in other sorption-dominated shallow lakes where similar processes may be at play.

The geochemical analysis of near-shore sediment cores provides further insights into the complex interactions between phosphorus and other elements in Utah Lake sediments. The study found significant chemostratigraphic variability across the lake, with elements such as manganese, aluminum, iron, potassium, and vanadium showing positive correlations with depth, while barium, copper, phosphorus, lead, strontium, and zinc showing negative correlations with depth. The findings highlight the influence of both natural processes and human activities on elemental distribution in lakebed sediments. The study underscores the need for comprehensive sampling and analysis to accurately represent large, shallow lakes with reworked sediments.

Overall, these studies highlight the importance of considering both suspended solids and lakebed sediments in phosphorus management strategies for eutrophic water bodies. The development of accurate methods for phosphorus fractionation in small samples, combined with a comprehensive understanding of historical phosphorus dynamics and geochemical variability in lakebed sediments, provides a robust framework to help inform the development of effective nutrient management in Utah Lake. Future research should continue to refine these methods and explore their applicability to other water bodies with similar characteristics, ultimately contributing to the broader scientific knowledge of sediment dynamics and nutrient cycling in aquatic systems.

## 6 References

- [1] C. Lü *et al.*, "Responses of Organic Phosphorus Fractionation to Environmental Conditions and Lake Evolution," *Environmental Science & Technology*, vol. 50, no. 10, pp. 4893-5422, 2016, doi: 10.1021/acs.est.5b05057.
- [2] J. L. Kovar and G. M. Pierzynski, *Methods of Phosphorus Analysis for Soils, Sediments, Residuals, and Waters*, Second Edition ed. (Southern Cooperative Series Bulletin, no. No. 408). Raleigh, North Carolina, USA: North Carolina State University Raleigh, 2009.
- [3] P. J. A. Kleinman *et al.*, "Interlaboratory comparison of soil phosphorus extracted by various soil test methods," *Communications in soil science and plant analysis*, vol. 32, no. 15-16, pp. 2325-2345, 2001 2001, doi: 10.1081/CSS-120000376.
- [4] J. Liu, Y. Hu, J. Yang, D. Abdi, and B. J. Cade-Menun, "Investigation of soil legacy phosphorus transformation in long-term agricultural fields using sequential fractionation, P K-edge XANES and solution P NMR spectroscopy," *Environmental Science & Technology*, vol. 49, no. 1, pp. 168-176, 2015, doi: 10.1021/es504420n.
- [5] B. L. Turner and A. B. Leytem, "Phosphorus compounds in sequential extracts of animal manures: chemical speciation and a novel fractionation procedure," *Environmental Science & Technology*, vol. 38, no. 22, pp. 6101-6108, 2004, doi: 10.1021/es0493042.
- [6] H. Y. Abu-Hmeidan, G. P. Williams, and A. W. Miller, "Characterizing total phosphorus in current and geologic utah lake sediments: Implications for water quality management issues," *Hydrology*, vol. 5, no. 1, p. 8, 2018, doi: 10.3390/hydrology5010008.
- [7] R. A. Dorich, D. W. Nelson, and L. E. Sommers, "Algal availability of sediment phosphorus in drainage water of the Black Creek Watershed," *Journal of Environmental Quality*, vol. 9, no. 4, pp. 557-563, 1980/10// 1980, doi: 10.2134/jeq1980.00472425000900040004x.

- [8] R. A. Dorich, D. W. Nelson, and L. E. Sommers, "Estimating algal available phosphorus in suspended sediments by chemical extraction," *Journal of Environmental Quality*, vol. 14, no. 3, pp. 400-405, 1985/07// 1985, doi: 10.2134/jeq1985.00472425001400030018x.
- [9] M. C. Randall *et al.*, "Sediment potentially controls in-lake phosphorus cycling and harmful cyanobacteria in shallow, eutrophic Utah Lake," *PLOS ONE*, vol. 14, no. 2, 2019/02/14/ 2019, doi: 10.1371/journal.pone.0212238.
- [10] M. Hupfer, D. Zak, R. Roßberg, C. Herzog, and R. Pöthig, "Evaluation of a well-established sequential phosphorus fractionation technique for use in calcite-rich lake sediments: identification and prevention of artifacts due to apatite formation," *Limnology and Oceanography: Methods*, vol. 7, pp. 399-410, 2009 2009, doi: 10.4319/lom.2009.7.399.
- [11] W. Casbeer, G. P. Williams, and M. B. Borup, "Phosphorus Distribution in Delta Sediments: A Unique Data Set from Deer Creek Reservoir," *Hydrology*, vol. 5, no. 4, p. 58, 2018, doi: 10.3390/hydrology5040058.
- [12] Y. Zhu *et al.*, "Characterization of organic phosphorus in lake sediments by sequential fractionation and enzymatic hydrolysis," *Environmental Science & Technology*, vol. 47, no. 14, pp. 7679-7687, 2013, doi: 10.1021/es305277g.
- [13] G. W. Petersen and R. B. Corey, "A modified Chang and Jackson procedure for routine fractionation of inorganic soil phosphates," *Soil Science Society of America Journal*, vol. 30, no. 5, pp. 563-565, 1966 1966, doi: 10.2136/sssaj1966.03615995003000050012x.
- [14] H. Tiessen, J. W. B. Stewart, and C. V. Cole, "Pathways of phosphorus transformations in soils of differing pedogenesis," *Soil Science Society of America Journal*, vol. 48, no. 4, pp. 853-858, 1984/03/01/ 1984, doi: 10.2136/sssaj1984.03615995004800040031x.
- [15] G. Pan *et al.*, "Impact of Suspended Inorganic Particles on Phosphorus Cycling in the Yellow River (China)," *Environmental Science & Technology*, vol. 47, no. 17, pp. 9559-10094, 2013, doi: 10.1021/es4005619.
- [16] X. Li, Z. Zhang, Q. Xie, R. Yang, T. Guan, and D. Wu, "Immobilization and Release Behavior of Phosphorus on Phoslock-Inactivated Sediment under Conditions Simulating the Photic Zone in Eutrophic Shallow Lakes," *Environmental Science & Technology*, vol. 53, no. 21, pp. 12151-12960, 2019, doi: 10.1021/acs.est.9b04093.
- [17] K. J. Wilkinson and J. R. Lead, *Environmental Colloids and Particles Behaviour, Separation and Characterisation* (IUPAC Series on

- Analytical and Physical Chemistry of Environmental Systems). Chichester, West Sussex, England: John Wiley & Sons Ltd, 2007.
- [18] P. M. Kauppila. "Sequential extraction procedure." mineclosure gtk fi. <https://mineclosure.gtk.fi/sequential-extraction-procedure/> (accessed 4/26/2022).
- [19] G. J. Chakrapani and V. Subramanian, "Fractionation Of Heavy Metals And Phosphorus In Suspended Sediments Of The Yamuna River, India," *Environmental Monitoring and Assessment*, vol. 43, pp. 117-124, 1996 1996, doi: 10.1007/BF00398602.
- [20] C. A. Ellison, B. E. Savage, and G. D. Johnson, "Suspended-sediment concentrations, loads, total suspended solids, turbidity, and particle-size fractions for selected rivers in Minnesota, 2007 through 2011," US Geological Survey, 2328-0328, 2014.
- [21] F. Shen, W. Verhoef, Y. Zhou, M. S. Salama, and X. Liu, "Satellite estimates of wide-range suspended sediment concentrations in Changjiang (Yangtze) estuary using MERIS data," *Estuaries and Coasts*, vol. 33, pp. 1420-1429, 2010, doi: 10.1007/s12237-010-9313-2.
- [22] M. Meybeck, L. Laroche, H. Dürr, and J. Syvitski, "Global variability of daily total suspended solids and their fluxes in rivers," *Global and planetary change*, vol. 39, no. 1-2, pp. 65-93, 2003, doi: 10.1016/S0921-8181(03)00018-3.
- [23] W. C. Casbeer, "Phosphorus Fractionation and Distribution across Delta of Deer Creek Reservoir," Master's Thesis, Brigham Young University, Provo, Utah, USA, 2009.
- [24] P. A. Domenico and F. W. Schwartz, *Physical and Chemical Hydrogeology*. Hoboken, New Jersey, USA: John Wiley & Sons, 1997.
- [25] J. B. Taggart *et al.*, "Historical Phosphorus Mass and Concentrations in Utah Lake: A Case Study with Implications for Nutrient Load Management in a Sorption-Dominated Shallow Lake," *Water*, vol. 16, no. 7, 2024, doi: 10.3390/w16070933.
- [26] F. J. Millero, W. Yao, and J. Aicher, "The speciation of Fe(II) and Fe(III) in natural waters," *Marine Chemistry*, vol. 50, no. 1, pp. 21-39, 1995/08/01/ 1995, doi: 10.1016/0304-4203(95)00024-L.
- [27] J. Kopáček, J. Borovec, J. Hejzlar, K.-U. Ulrich, S. A. Norton, and A. Amirbahman, "Aluminum Control of Phosphorus Sorption by Lake Sediments," *Environmental Science & Technology*, vol. 39, no. 22, pp. 8784-8789, 2005, doi: 10.1021/es050916b.
- [28] M. C. Randall, "Characterizing the Fate and Mobility of Phosphorus in Utah Lake Sediments," Master's Thesis, Brigham Young University, Provo, Utah, USA, 2017.
- [29] R. A. Valek *et al.*, "Regulated Inductively Coupled Plasma–Optical Emission Spectrometry Detectable Elements in Utah Lake:

- Characterization and Discussion," *Water*, vol. 16, no. 15, p. 2170, 2024, doi: 10.3390/w16152170.
- [30] K. B. Tanner, A. C. Cardall, and G. P. Williams, "A spatial long-term trend analysis of estimated chlorophyll-a concentrations in Utah Lake using Earth observation data," *Remote Sensing*, vol. 14, no. 15, p. 3664, 2022, doi: 10.3390/rs14153664.
- [31] DWQ, "Utah Lake Water Quality Study Stakeholder Process, Version 10 - Approved May 12, 2017," Utah Department of Environmental Quality Water Quality, Salt Lake City, UT, USA, May 12, 2017 2017.
- [32] DWQ. "Study Phases: Utah Lake Water Quality Study." Utah Department of Environmental Quality Water Quality. <https://deq.utah.gov/water-quality/study-phases-utah-lake> (accessed 2/6/2024, 2024).
- [33] DEQ, "Utah Lake Water Quality Study Phase 1 Report, Final - December 7, 2018," Utah Department of Environmental Quality, Salt Lake City, UT, USA, December 7, 2018 2018.
- [34] M. Brett, "Quantification of nutrient inputs, sediment storage and release, and long-term recovery in Utah Lake," Utah Lake Science Panel, Presentation, Summer, 2023.
- [35] M. M. Brown *et al.*, "Nutrient Loadings to Utah Lake from Precipitation-Related Atmospheric Deposition," *Hydrology*, vol. 10, no. 10, p. 200, 2023, doi: 10.3390/hydrology10100200.
- [36] S. M. Barrus *et al.*, "Nutrient Atmospheric Deposition on Utah Lake: A Comparison of Sampling and Analytical Methods," *Hydrology*, vol. 8, no. 3, p. 123, 2021, doi: 10.3390/hydrology8030123.
- [37] J. M. Olsen, G. P. Williams, A. W. Miller, and L. Merritt, "Measuring and Calculating Current Atmospheric Phosphorous and Nitrogen Loadings to Utah Lake Using Field Samples and Geostatistical Analysis," *Hydrology*, vol. 5, no. 3, p. 45, 2018, doi: 10.3390/hydrology5030045.
- [38] J. T. Telfer *et al.*, "Source Attribution of Atmospheric Dust Deposition to Utah Lake," *Hydrology*, vol. 10, no. 11, p. 210, 2023, doi: 10.3390/hydrology10110210.
- [39] M. Hogsett, H. Li, and R. Goel, "The Role of Internal Nutrient Cycling in a Freshwater Shallow Alkaline Lake," *Environmental Engineering Science*, vol. 36, no. 5, pp. 551-563, 2019, doi: 10.1089/ees.2018.0422.
- [40] M. C. Randall *et al.*, "Sediment potentially controls in-lake phosphorus cycling and harmful cyanobacteria in shallow, eutrophic Utah Lake," *Plos One*, vol. 14, no. 2, p. e0212238, 2019, doi: 10.1371/journal.pone.0212238.

- [41] PSOMAS, "Utah Lake TMDL: Pollutant Loading Assessment & Designated Beneficial Use Impairment Assessment," PSOMAS, Salt Lake City, UT, USA, 2007. [Online]. Available: [https://deq.utah.gov/legacy/programs/water-quality/watersheds/docs/2009/02Feb/Final\\_Draft\\_Task2\\_Task3\\_Memo%20\\_08-01-07.pdf](https://deq.utah.gov/legacy/programs/water-quality/watersheds/docs/2009/02Feb/Final_Draft_Task2_Task3_Memo%20_08-01-07.pdf)
- [42] L. W. Hooton Jr., "Utah Lake & Jordan River Water Rights & Management Plan," The Salt Lake City Department of Public Utilities, Salt Lake City, UT, USA, 1989.
- [43] F. W. S. United States, "Reclassification of the Endangered June Sucker to Threatened With a Section 4(d) Rule; Final Rule," Fish and Wildlife Service, 2021, vol. 86(1). [Online]. Available: <https://fws.gov/federal-register-file/reclassification-endangered-june-sucker-threatened-section-4d-rule-final-rule>
- [44] URMCC. "Utah Reclamation Mitigation and Conservation Commission - Utah Lake Wetland Preserve." [https://www.mitigationcommission.gov/wetlands/wetlands\\_ulwp.html](https://www.mitigationcommission.gov/wetlands/wetlands_ulwp.html) (accessed 11/10/2023, 2023).
- [45] A. Zanazzi, W. Wang, H. Peterson, and S. H. Emerman, "Using Stable Isotopes to Determine the Water Balance of Utah Lake (Utah, USA)," *Hydrology*, vol. 7, no. 4, p. 88, 2020, doi: 10.3390/hydrology7040088.
- [46] D. W. Q. State of Utah, "Text of the Final TBPEL Rule (R317-1-3.3)," Division of Water Quality, Salt Lake City, UT, USA, 2015. [Online]. Available: [https://deq.utah.gov/legacy/pollutants/n/nutrients/docs/2014/12Dec/R317\\_1\\_3Final.pdf](https://deq.utah.gov/legacy/pollutants/n/nutrients/docs/2014/12Dec/R317_1_3Final.pdf)
- [47] D. L. Clark, S. M. Kirby, and C. G. Oviatt, "Geologic Map of the Rush Valley 30' x 60' Quadrangle, Tooele, Utah, and Salt Lake Counties, Utah," ed. Salt Lake City, UT, USA: Utah Geological Survey, 2023.
- [48] K. N. Constenius, D. L. Clark, J. K. King, and J. B. Ehler, "Interim Geologic Map of the Provo 30' x 60' Quadrangle, Utah, Wasatch, and Salt Lake Counties, Utah," ed. Salt Lake City, UT, USA: Utah Geological Survey, 2011.
- [49] E. H. Pampeyan, "Geological Map of the Lynndyl 30' x 60' Quadrangle, West-Central Utah," ed. Salt Lake City, UT, USA: Utah Geological Survey, 2005.
- [50] I. J. Witkind and M. P. Weiss, "Geologic Map of the Nephi 30' x 60' Quadrangle, Carbon, Emery, Juab, Sanpete, Utah, and Wasatch Counties, Utah," ed. Salt Lake City, UT, USA: Utah Geological Survey, 1991.

- [51] A. Rupke. (2015, May 2015) Today's (And Tomorrow's?) Phosphate. *Survey Notes*. 6-7.
- [52] P. W. Jewell, N. J. Silberling, and K. M. Nichols, "Geochemistry of the Mississippian Delle Phosphatic Event, Eastern Great Basin, U.S.A.," *Journal of Sedimentary Research*, vol. 70, no. 5, pp. 1222-1233, 2000, doi: 10.1306/030800701222.
- [53] E. E. Hiatt and D. A. Budd, "Sedimentary phosphate formation in warm shallow waters: new insights into the paleoceanography of the Permian Phosphoria Sea from analysis of phosphate oxygen isotopes," *Sedimentary Geology* vol. 145, pp. 119-133, 2001, doi: 10.1016/S0037-0738(01)00127-0.
- [54] E. K. Maughan, "Phosphoria Formation (Permian) And Its Resource Significance In The Western Interior, U.S.A.," *Pangea: Global Environments And Resources*, vol. Memoir 17, pp. 479-495, 1994.
- [55] L. F. Hintze and B. J. Kowallis, *Geologic History of Utah: A Field Guide to Utah's Rocks*, Special Publications 9 ed. Provo, UT, USA: Department of Geological Sciences, Brigham Young University, 2009.
- [56] R. A. Vollenweider, "Possibilities and limits of elementary models concerning budget of substances in lakes," *Archiv fur Hydrobiologie*, vol. 66, no. 1, pp. 1-&, 1969.
- [57] D. K. Mueller, "Mass Balance Model Estimation Of Phosphorus Concentrations In Reservoirs 1," *JAWRA Journal of the American Water Resources Association*, vol. 18, no. 3, pp. 377-382, 1982, doi: 10.1111/j.1752-1688.1982.tb00003.x.
- [58] J. R. Jones and R. W. Bachmann, "Prediction of Phosphorus and Chlorophyll Levels in Lakes," *Water Pollution Control Federation*, pp. 2176-2182, 1976.
- [59] A. C. Bryhn and L. Håkanson, "A Comparison of Predictive Phosphorus Load-Concentration Models for Lakes," *Ecosystems*, vol. 10, pp. 1084-1099, 2007, doi: 10.1007/s10021-007-9078-z.
- [60] S. C. Chapra, "Total Phosphorus Model for the Great Lakes," *Journal of the environmental engineering division*, vol. 103, no. 2, pp. 147-161, 1977, doi: 10.1061/JEEGAV.0000609.
- [61] S. C. Chapra, *Surface Water-Quality Modeling*. Long Grove, IL, USA: Waveland Press, Inc., 2008.
- [62] S. C. Chapra and D. M. Dolan, "Great Lakes total phosphorus revisited: 2. Mass balance modeling," *Journal of Great Lakes Research*, vol. 38, no. 4, pp. 741-754, 2012, doi: 10.1016/j.jglr.2012.10.002.
- [63] P. J. Dillon and F. H. Rigler, "A Test of a Simple Nutrient Budget Model Predicting the Phosphorus Concentration in Lake Water,"

- Journal of the Fisheries Board of Canada*, vol. 31, no. 11, pp. 1771-1778, 1974, doi: 10.1139/f74-225.
- [64] W. R. Boynton, J. H. Garber, R. Summers, and W. M. Kemp, "Inputs, Transformations, and Transport of Nitrogen and Phosphorus in Chesapeake Bay and Selected Tributaries," *Estuaries*, vol. 18, no. 1B, pp. 285-314, 1995, doi: 10.2307/1352640.
- [65] E. Anagnostou, A. Gianni, and I. Zacharias, "Ecological modeling and eutrophication—a review," *Natural Resource Modeling*, vol. 30, no. 3, p. e12130, 2017, doi: 10.1111/nrm.12130.
- [66] B. Bhagowati and K. U. Ahamad, "A review on lake eutrophication dynamics and recent developments in lake modeling," *Ecohydrology & Hydrobiology*, vol. 19, no. 1, pp. 155-166, 2019, doi: 10.1016/j.ecohyd.2018.03.002.
- [67] J. V. Klump, D. N. Edgington, P. E. Sager, and A. Robertson, "Sedimentary phosphorus cycling and a phosphorus mass balance for the Green Bay (Lake Michigan) ecosystem," *Canadian Journal of Fisheries and Aquatic Sciences*, vol. 54, pp. 10-26, 1997, doi: 10.1139/f96-247.
- [68] A. Van Heyst, A. Sinclair, and R. Jamieson, "Application of phosphorus loading models to understand drivers of eutrophication in a complex rural lake-watershed system," *Journal of Environmental Management*, vol. 302, p. 114010, 2022, doi: 10.1016/j.jenvman.2021.114010.
- [69] P. Noges, "Water and nutrient mass balance of the partly meromictic temperate Lake Verevi," *Lake Verevi, Estonia—A Highly Stratified Hypertrophic Lake*, pp. 21-31, 2005, doi: 10.1007/1-4020-4363-5\_2.
- [70] K. E. Havens and R. T. James, "The Phosphorus Mass Balance of Lake Okeechobee, Florida: Implications for Eutrophication Management," *Lake and Reservoir Management*, vol. 21, no. 2, pp. 139-148, 2005, doi: 10.1080/07438140509354423.
- [71] C. D. Pollman and R. T. James, "A simple model of internal loading of phosphorus in Lake Okeechobee," *Lake and Reservoir Management*, vol. 27, no. 1, pp. 15-27, 2011/03/15 2011, doi: 10.1080/07438141.2010.542877.
- [72] P. Kelderman, Z. Wei, and M. Maessen, "Water and mass budgets for estimating phosphorus sediment–water exchange in Lake Taihu (China P. R.)," *Hydrobiologia*, vol. 544, pp. 167-175, 2005, doi: 10.1007/s10750-005-0542-5.
- [73] M. Søndergaard, R. Bjerring, and E. Jeppesen, "Persistent internal phosphorus loading during summer in shallow eutrophic lakes," *Hydrobiologia*, vol. 710, pp. 95-107, 2013, doi: 10.1007/s10750-012-1091-3.

- [74] C. van der Salm, J. Kros, and W. de Vries, "Evaluation of different approaches to describe the sorption and desorption of phosphorus in soils on experimental data," *Science of the Total Environment*, vol. 571, pp. 292-306, 2016, doi: 10.1016/j.scitotenv.2016.07.004.
- [75] H. Wang, A. Appan, and J. S. Gulliver, "Modeling of phosphorus dynamics in aquatic sediments: I—model development," *Water Research*, vol. 37, no. 16, pp. 3928-3938, 2003, doi: 10.1016/S0043-1354(03)00304-X.
- [76] B. Spears, L. Carvalho, and D. Paterson, "Phosphorus partitioning in a shallow lake: implications for water quality management," *Water and Environment Journal*, vol. 21, no. 1, pp. 47-53, 2007, doi: 10.1111/j.1747-6593.2006.00045.x.
- [77] C. W. Fetter, *Applied Hydrogeology*, 4th Edition ed. Long Grove, IL, USA: Waveland Press, Inc., 2001.
- [78] B. O. R. United States. "Historic Data | Water Operations | UC Region | Bureau of Reclamation." <https://www.usbr.gov/rsrvWater/HistoricalApp.html> (accessed 10/23/2023, 2023).
- [79] DWR. "Document Listing for Folder: DSYS059REPORT." Utah Division of Water Rights. <https://www.waterrights.utah.gov/cgi-bin/docview.exe?Folder=DSYS059REPORT&Key=Sort%20by%20Date> (accessed 10/23/2023, 2023).
- [80] C. Y. Kramer, "Extension of multiple range tests to group means with unequal numbers of replications," *Biometrics*, vol. 12, no. 3, pp. 307-310, 1956.
- [81] J. W. Tukey, "The problem of multiple comparisons," *Multiple comparisons*, 1953.
- [82] W. McKinney, "Data structures for statistical computing in python," in *Proceedings of the 9th Python in Science Conference*, 2010, vol. 445, no. 1: Austin, TX, USA, pp. 51-56.
- [83] D. L. Sparks, *Environmental Soil Chemistry*, 3rd ed. San Diego, CA, USA: Academic Press, 2003.
- [84] P. L. Brezonik and W. A. Arnold, *Water Chemistry: An Introduction to the Chemistry of Natural and Engineered Aquatic Systems*. New York City, NY, USA: Oxford University Press, Inc., 2011, p. 782.
- [85] A. C. Cardall, R. C. Hales, K. B. Tanner, G. P. Williams, and K. N. Markert, "LASSO (L1) Regularization for Development of Sparse Remote-Sensing Models with Applications in Optically Complex Waters Using GEE Tools," *Remote Sensing*, vol. 15, no. 6, p. 1670, 2023.
- [86] G. Sposito, *The Surface Chemistry of Soils*. Oxford, England: Oxford University Press, 1984.

- [87] W. M. Last and J. P. Smol, *Tracking Environmental Change Using Lake Sediments: Volume 1: Basin Analysis, Coring, and Chronological Techniques*. Springer Science & Business Media, 2002.
- [88] W. M. Last and J. P. Smol, *Tracking Environmental Change Using Lake Sediments: Volume 2: Physical and Geochemical Methods*. Springer Science & Business Media, 2002.
- [89] H. J. Bissell, "Preliminary study of the bottom sediments of Utah Lake, Utah," *Report of the Committee on Sedimentation. National Research Council, Division of Geologic and Geography Annual Report*, vol. 1941, pp. 62-69, 1940.
- [90] C. C. Bingham, "Recent Sedimentation Trends in Utah Lake," Master of Science Thesis, Department of Geology, Brigham Young University, Provo, UT, USA, 1974.
- [91] R. F. Bolland, "Paleoecological interpretation of the diatom succession in the recent sediments of Utah Lake, Utah," Doctor of Philosophy Dissertation, Department of Biology, The University of Utah, Salt Lake City, Utah, USA, 1974.
- [92] W. H. Brimhall, I. G. Bassett, and L. B. Merritt, "Reconnaissance study of deep-water springs and strata of Utah Lake:," Eyring Research Institute, Provo, UT, USA, January 1976 1976.
- [93] J. R. Bushman, "The Rate of Sedimentation in Utah Lake and the Use of Pollen as an Indicator of Time in the Sediments," *Brigham Young University Geology Studies*, vol. 27, 3, pp. 35-43, December 1980 1980.
- [94] W. H. Brimhall and L. B. Merritt, "Geology of Utah Lake: Implications for resource management," *Great Basin Naturalist Memoirs*, vol. 5, pp. 24-42, 1981. [Online]. Available: <https://www.jstor.org/stable/23376545>.
- [95] A. N. Macharia, "Reconstructing paleoenvironments using a mass-energy flux framework," Doctor of Philosophy Dissertation, Department of Geography, The University of Utah, Salt Lake City, Utah, USA, 3546858, 2012.
- [96] S. Brothers, L. King, A. Klein, and J. Brahney, "Final Report to the Utah Division of Water Quality: Littoral-Benthic Primary Production in Utah Lake," Department of Watershed Sciences and Ecology Center, Utah State University, Logan, UT, USA, 2021.
- [97] R. R. R. Williams, "Determining the anthropogenic effects on eutrophication of Utah Lake since European settlement using multiple geochemical approaches," Master of Science Thesis, Department of Geological Sciences, Brigham Young University, Provo, Utah, USA, 2021.
- [98] M. R. Devey, "Comparing Multiple Approaches to Reconstructing the Phosphorus History of Marl Lakes: A Utah Lake Case Study,"

- Master of Science Thesis, Department of Watershed Sciences, Utah State University, Logan, Utah, USA, 29067526, 2022. [Online]. Available: <https://www.proquest.com/dissertations-theses/comparing-multiple-approaches-reconstructing/docview/2650274496/se-2?accountid=4488>
- [99] R. Williams *et al.*, "Human-Driven Trophic Changes in a Large, Shallow Urban Lake: Changes in Utah Lake, Utah from Pre-European Settlement to the Present," *Water, Air, & Soil Pollution*, vol. 234, no. 4, p. 218, 2023, doi: 10.1007/s11270-023-06228-5.
- [100] J. Brahney, Powers, M., King, L., Devey, M., Carter, M., Carling, G., Brothers, S., Provard, A., Young, B., West, R., "Utah Lake Paleoecology Study Report to DEQ, April 2024," Watershed Sciences Faculty Publications, 2024, vol. Paper 1163.
- [101] L. King, M. Devey, P. R. Leavitt, M. J. Power, S. Brothers, and J. Brahney, "Anthropogenic forcing leads to an abrupt shift to phytoplankton dominance in a shallow eutrophic lake," *Freshwater Biology*, vol. 69, no. 3, pp. 335-350, 2024, doi: 10.1111/fwb.14214.
- [102] B. W. Abbott *et al.*, "Getting to know the Utah Lake ecosystem," Brigham Young University, Provo, Utah, 2021. [Online]. Available: [https://www.researchgate.net/publication/353830822\\_Getting\\_to\\_know\\_the\\_Utah\\_Lake\\_Ecosystem](https://www.researchgate.net/publication/353830822_Getting_to_know_the_Utah_Lake_Ecosystem)
- [103] J. B. Taggart *et al.*, "Historical Phosphorus Mass and Concentrations in Utah Lake: A Case Study with Implications for Nutrient Load Management in a Sorption-Dominated Shallow Lake," *Water*, vol. 16, no. 7, p. 933, 2024, doi: 10.3390/w16070933.
- [104] A. W. Miller, "Utah Lake Area Lookup Table - October 1963 ", J. B. Taggart, Ed., ed. Provo, Utah, USA, 2024.
- [105] W. F. Wrath, "Contamination and compaction in core sampling," *Science*, vol. 84, no. 2189, pp. 537-538, 1936, doi: 10.1126/science.84.2189.537.b.
- [106] EPA, *Method 3051A (SW-846): Microwave Assisted Acid Digestion of Sediments, Sludges, and Oils*. Washington, DC, USA, 2007.
- [107] R. Gavlak, D. Horneck, R. O. Miller, and J. Kotuby-Amacher, *Soil, plant and water reference methods for the western region*, 3rd Edition ed. (WCC-103 Publication ). Fort Collins, CO, USA, 2003, pp. 1-207.
- [108] Munsell, *Munsell Soil Color Charts*. New Windsor, New York, USA: Munsell Color, 2000.
- [109] D. Hongve and A. H. Erlandsen, "Shortening of Surface Sediment Cores During Sampling," *Hydrobiologia*, vol. 65, 3, pp. 283-287, 1979.

- [110] R. A. Morton and W. A. White, "Characteristics of and Corrections for Core Shortening in Unconsolidated Sediments," *Journal of Coastal Research*, vol. 13, no. Summer, 1997, 3, pp. 761-769, 1997.
- [111] G. Zheng, B. Takano, M. Matsuo, and Y. Tanaka, "Compaction of modern soft sediments during core sampling—An in situ investigation at an estuary site," *Environmental Geosciences*, vol. 9, no. 3, pp. 109-114, 2002, doi: 10.1046/j.1526-0984.2002.93004.x.
- [112] D. Olsen, "Discussion Regarding The Original Provo River Delta," J. Taggart, Ed., ed. Provo, Utah, USA, 2024.
- [113] C. C. Carey and E. Rydin, "Lake trophic status can be determined by the depth distribution of sediment phosphorus," *Limnology and oceanography*, vol. 56, no. 6, pp. 2051-2063, 2011, doi: 10.4319/lo.2011.56.6.2051.
- [114] R. Carignan and R. Flett, "Postdepositional mobility of phosphorus in lake sediments," *Limnology and Oceanography*, vol. 26, no. 2, pp. 361-366, 1981, doi: 10.4319/lo.1981.26.2.0361.
- [115] J. Taggart, T. Miller, A. Navarre-Sitchler, and G. Carling, "Mineral Precipitation In Utah Lake And Its Effluent Mixing Zones," in 2022 *Intermountain Engineering, Technology and Computing (IETC)*, 2022: IEEE, pp. 1-5, doi: 10.1109/IETC54973.2022.9796662.
- [116] J. B. Taggart, "Inorganic Phosphorus Chemistry of Utah Lake's Effluent Mixing Zones," Master of Science, Department of Civil and Environmental Engineering, Colorado School of Mines, Golden, Colorado, USA, 2560073160, 2021.
- [117] S. Bertrand *et al.*, "Inorganic geochemistry of lake sediments: A review of analytical techniques and guidelines for data interpretation," *Earth-Science Reviews*, p. 104639, 2023, doi: 10.1016/j.earscirev.2023.104639.